Nonshivering Thermogenesis: Responses to Acute Mild Cold Exposure in Obese Males

by

Andrew Cameron McMillan

B.Sc. (Biology), Acadia University, 2012

Thesis Submitted In Partial Fulfillment of the
Requirements for the Degree of
Master of Science

in the
Department of Biomedical Physiology and Kinesiology
Faculty of Science

SIMON FRASER UNIVERSITY

Summer 2015

Approval

Name:	**Andrew Cameron McMillan**
Degree:	**Master of Science (Biomedical Physiology and Kinesiology)**
Title of Thesis:	***Nonshivering Thermogenesis: Responses to Acute Cold Exposure in Obese Males***
Examining Committee:	**Chair: David Clarke, Ph.D** **Assistant Professor**

Matthew D. White, Ph.D
Senior Supervisor
Associate Professor

Mike A. Walsh, Ph.D
Supervisor
Senior Lecturer

François Haman, Ph.D
Supervisor
Associate Professor

John Halliwill, Ph.D
External Examiner
Professor
Department of Human Physiology
University of Oregon

Date Defended: 13 May 2015

Partial Copyright Licence

Ethics Statement

The author, whose name appears on the title page of this work, has obtained, for the research described in this work, either:

a. human research ethics approval from the Simon Fraser University Office of Research Ethics,

or

b. advance approval of the animal care protocol from the University Animal Care Committee of Simon Fraser University;

or has conducted the research

c. as a co-investigator, collaborator or research assistant in a research project approved in advance,

or

d. as a member of a course approved in advance for minimal risk human research, by the Office of Research Ethics.

A copy of the approval letter has been filed at the Theses Office of the University Library at the time of submission of this thesis or project.

The original application for approval and letter of approval are filed with the relevant offices. Inquiries may be directed to those authorities.

Simon Fraser University Library
Burnaby, British Columbia, Canada

update Spring 2010

Abstract

The studies in this thesis were to assess whether obese relative to non-obese individuals have blunted metabolic and non-shivering thermogenic responses in acute mild cold exposure, possibly established by a higher capacity to activate brown adipose tissue in the non-obese, resulting in greater energy expenditure. It was hypothesised that the obese would demonstrate a reduced non-shivering thermogenesis during acute mild cold exposure despite having lower skin temperatures and the same core temperature. The first study resulted in obese individuals having lower mean rate of oxygen consumption ($p < 0.05$), lower mean skin temperatures ($p < 0.05$), and lower mean heat flux ($p < 0.05$) during a 19°C exposure. There was no difference, however, in carbohydrate ($p = 0.14$) or lipid ($p = 0.46$) oxidation rates. The second study resulted in obese having lower mean supraclavicular skin temperatures ($p < 0.001$), lower mean supraclavicular heat flux ($p < 0.05$), lower mean surface temperatures from FLIR thermography ($p < 0.05$) and a lower mean metabolic response ($p < 0.05$). Non-shivering thermogenesis was achieved as there was minimal and no significantly different skeletal muscle activity between the two groups ($p = 0.94$). In conclusion, during acute mild cold exposure, obese individuals displayed a significantly lower non-shivering thermogenesis despite having lower skin temperatures and the same core temperatures relative to non-obese individuals. This possibly originates from a decreased capacity to activate brown adipose tissue depots in the obese that contributes to their lower energy expenditure in these conditions.

Keywords: brown adipose tissue; energy expenditure; non-shivering thermogenesis; obese

Dedication

I would like to dedicate this thesis to my family and friends. A special appreciation must be given to my loving parents, Peter and Lew, whose words of encouragement never wore thin. To my sister, Christina, whose energetic character provided me with continuous motivation, and to Nicole, whose continuous support went above and beyond everyday. This thesis could not have been completed without you all.

Acknowledgements

I would like to take this opportunity to acknowledge the many people who made this thesis possible. I would like to thank my supervisor, Dr. Matthew White, along with my co-supervisors, Dr. Mike Walsh and Dr. François Haman; for providing me with their experience and guidance, I am forever grateful. I would also like to thank my lab mates, Kate Henderson, Assaf Yogev, Dora Hsaio, and Mike Rogers for their continuing support. I must also recognise those around the department who have helped me in any capacity throughout this process, including Susie Nugent, Joel Blok, King Chao, Joe Wang, Sherri Ferguson, Dr. Parveen Bawa, Craig Asmundson, Dr. James Wakeling and Ollie Blake. From outside the department, I would like to thank Dr. Denis Blondin for his insight and knowledge. Finally, I would like to thank all those that took the time to help me with my data collection including Cindy Zhang, Alex Liu, Jingkai Pang, Alex Ngo, Mike Hosseini and Angelina Marinkovic.

Table of Contents

List of Tables

List of Figures

List of Acronyms

ANOVA	Analysis of Variance
ATP	Adenosine Triphosphate
BAT	Brown Adipose Tissue
BMI	Body Mass Index
cAMP	Cyclic Adenosine Monophosphate
CHO	Carbohydrate
CRE	cAMP Response Element
CREB	CRE-binding Protein
CT	Computed Tomography
EMG	Electromyography
FAT	Lipid
FFA	Free Fatty Acid
FLIR	Forward Looking Infrared Camera
HSL	Hormone-Sensitive Lipase
ICER	Inducible cAMP early
MVC	Maximal Voluntary Contraction
NE	Norepinephrine
PET	Positron Emission Tomography
$P_{ET}O_2$	End-tidal Partial Pressure of O_2
$P_{ET}CO_2$	End-tidal Partial Pressure of CO_2
PKA	Protein Kinase-A
RER	Non-protein respiratory exchange ratio
TG	Triglyceride
TRP	Transient Receptor Potentials
UCP-1	Uncoupling Protein-1
VCO_2	Rate of carbon dioxide production
V_E	Rate of pulmonary Ventilation
VO_2	Rate of oxygen consumption

Glossary

Anapyrexia	When the core temperature set-point or null-zone shifts and a mammal defends a new lower core temperature, or set of core temperatures.
BRL-37344	A β_3-agonist used to mimic the physiological effects of norepinephrine on brown adipose tissue stimulation. At higher concentrations it is also a β_2-agonist.
Brown Adipose Tissue	One of two types of fat, or adipose tissue, found in the body. Its primary function is related to the release of heat. It is especially abundant in hibernating animals and newborns.
cAMP	Cyclic adenosine monophosphate is a messenger molecules, derived from ATP, used in the cellular signalling process of thermogenesis in brown adipose tissue
Cholecystokinin	A peptide hormone secreted by the small intestine and is responsible for stimulating the digestion of fat and protein.
CGP-12177	A β_3-agonist used to analyse the physiological effects of norepinephrine on brown adipose tissue stimulation. It couples as a β_1/ β_2-agonist.
CL-316243	A β_3-agonist used to analyse the physiological effects of norepinephrine on brown adipose tissue stimulation. It is considered to be the most selective agonist for $ß_3$- with little effect on $ß_1$- or $ß_2$- adrenoreceptors.
Enterostatin	A pentapeptide released in the gastrointestinal tract. It functions to reduce fat intake by signalling the hypothalamus and may aid in signalling brown adipose tissue activation while feeding.
^{18}F-fluorodeoxyglucose	A radiopharmaceutical used in medical imaging, such as PET, as a glucose analog.
G Protein Binding Masks	A process hypothesised to take place in hibernation arousal whereby G Protein binding sites in the brown adipocyte become unmasked, allowing the cell to engage in the thermogenic process.
G_i Protein	A membrane-associated protein subunit found on the cell membrane of a mature brown adipocyte. It functions to inhibit the synthesis of cAMP from ATP.
G_s Protein	A membrane-associated protein subunit found on the cell membrane of a mature brown adipocyte. It aids in activating the cAMP-dependent pathway leading to thermogenesis.
Hyperphagia	Abnormally increased appetite and consumption of food.

Metabolic Efficiency	The body's ability to store food as energy. A decreased metabolic efficiency means there is a lower fraction of food energy being stored in the form of fat. BAT activation aids in decreasing of metabolic efficiency.
Nonshivering Thermogenesis	Heat release in humans exposed to cold temperatures. Associated with physical responses other than shivering, like brown adipose tissue activation.
Nuclear-Related Protein	A protein found in the cell nucleus. As opposed to cytosolic proteins found in the cytosole.
Null-zone	A neutral temperature zone between core thresholds for shivering thermogenesis and sweating.
Peripilin	Also known as a lipid droplet-associated protein that when phosphorylated, aids in the mobilisation of fats in adipose tissue.
Set-point	Single point at which the body attempts to regulate its core temperature.
Thermogenin	The previous name given to uncoupling protein 1. Found in the mitochondria of brown adipose tissue and used in non-shivering thermogenesis.
Uncoupling Protein	A mitochondrial membrane protein that dissipates the proton gradient before it is used to provide energy for oxidative phosphorylation. There are five known variants ranging from UCP-1-UCP-5.
Uncoupling Protein 1	Also known as thermogenin; a mitochondrial membrane protein found in brown adipose tissue. It is an integral part in the cellular signalling pathway leading to the thermogenic effects of BAT.

Executive Summary

This thesis assessed non-shivering thermogenesis and metabolic responses in the obese versus non-obese in response to acute mild cold exposure. The first chapter includes a literature review on human thermogenesis in response to ambient cold exposure. It focuses on the two methods of heat production in the human body: shivering and non-shivering thermogenesis. The second chapter includes a study of the metabolic and substrate oxidation responses corresponding to mean skin temperatures and heat flux between the obese and non-obese, while the third chapter includes a study of the supraclavicular fossae skin temperatures and heat flux corresponding to changes in non-shivering thermogenesis between the obese and non-obese.

It was hypothesised that during acute mild cold exposure at 19°C, the obese relative to the non-obese would demonstrate a blunted non-shivering thermogenic metabolic response and lower mean heat flux despite having lower mean skin temperatures and the same core temperatures. It was also hypothesised that this response would be coupled with no difference in substrate oxidation rates.

Due to the paradoxical cooler skin temperatures seen in the obese in previous studies, it was hypothesised that relative to the non-obese, the obese would demonstrate a reduced brown adipose tissue non-shivering thermogenesis at the supraclavicular fossae. This would correspond to, it was hypothesised, to lower mean skin temperatures and heat flux over these supraclavicular fossae in the obese when exposed to mild cold. It was hypothesised that this would be in concert with similar and minimal skeletal muscle activation as assessed by surface EMG.

If the above hypotheses were supported by the data, it was postulated that the obese relative to non-obese would have a reduced capacity to activate brown adipose tissue stores in response to acute mild cold exposure, possibly contributing to a positive energy balance and obesity.

Chapter 1.

Introduction

Exposure to cold environments and the survival in mild to extreme temperatures has long been a challenge for the furless, somewhat ill-equipped human. As homeotherms, originating from the warmer equatorial regions of the planet, humans evolved excellent mechanisms for dissipating heat such as cutaneous vasodilation, and superficial eccrine sweating (Shibasaki, Wilson et al. 2006). The ability to retain heat in cooler climates has been somewhat more challenging from an evolutionary standpoint (Blondin, Labbe et al. 2015). Nonetheless, millions of humans live in the more temperate and arctic environments and our physiology has been pushed to counter this behaviour by evolving a number of responses to the cold.

The thermoregulatory system of the body is able to coordinate defences against the cold in order to regulate its core temperature at a set-point (Hammel, Jackson et al. 1963, Cabanac 2006) or within a small, ideal range of 37.0 ± 1.0°C known as the null or inter-threshold zone (Mekjavic, Sundberg et al. 1991, Bligh 2006). Most physiological, chemical, and metabolic responses of the body operate within this small temperature range. The human body quickly initiates defence responses, such as shivering or sweating, as core temperatures drop or increase from the normothermic core temperature set-point or null-zone (Cabanac and Massonnet 1977, Mekjavic, Sundberg et al. 1991, Bligh 2006). The physiological responses to the cold are intricate and are controlled by a vast network of autonomic nervous tissue that elicit thermoregulatory responses. These include shivering thermogenesis (ST), observed by increases in skeletal muscle activity and indirectly by metabolic variables such as the rate of oxygen consumption (VO_2) and rate of carbon dioxide production (VCO_2). In the last decade, there has been a re-emergence of research focused on non-shivering thermogenesis (NST) fuelled by brown adipose tissue (BAT) activation during mild cold exposure

(Cannon and Nedergaard 2004, Nedergaard, Bengtsson et al. 2007, Virtanen, Lidell et al. 2009, van Marken Lichtenbelt 2012). The following sections will outline some of the primary physiological responses to the cold in relation to human energy expenditure including BAT thermogenesis.

1.1. Literature Review

1.1.1. Shivering Thermogenesis

Before discussing the implications of NST on energy balance, it would be prudent to first take a look at the most crucial adaptation of humans to the cold, our ability to shiver. This also has the greatest implications to cold-induced energy expenditure; skeletal muscle during ST is the main tissue that oxidises macronutrients resulting in heat release from macronutrients throughout the body and is mainly an involuntary response to cold exposure. The control of shivering has been detailed in several papers (Benzinger, Pratt et al. 1961, Haman, Legault et al. 2004, Morrison 2011). Briefly, afferent signals are continually received by the central nervous system (CNS) from cold receptors in the skin and core. These peripheral and central afferent signals travel through myelinated afferent A fibres, specifically group III delta fibres to the dorsal root ganglion (Guyton 2006). The dorsomedial hypothalamus is then stimulated in the brain which signals alpha and gamma motor neurons that project to the skeletal muscle (Hemingway 1963). Initially, the control system for shivering was thought only to include a negative feedback loop with proportional control of skeletal muscle thermogenesis. That is, the afferent input from decreased skin and core temperatures gave proportional increases in shivering thermogenesis (Benzinger, Pratt et al. 1961). Subsequently, a feedback control was identified as it was shown that progressive increases in ST was evident with incremental skin cooling prior to any core cooling (Morrison 2011).

Quantification of Shivering Thermogenesis and Substrate Oxidation

Shivering can be quantified by a number of methods. While early shivering protocols relied on visual assessment of the increase in muscle contractions (Hemingway 1963), there has since been an introduction of more reliable methods to

quantify this heat transfer. These include assessing increases in metabolic rate by indirect or direct calorimetry and increases in muscle contractions with electromyography (EMG) (Hemingway 1963). Specifically, measuring the rate of oxygen consumption with indirect calorimetry quantifies metabolic responses during cold exposure. Shivering is an asynchronous rhythmic progression of muscle contractions and metabolic responses given by increased VO_2 and VCO_2 similar to that of light exercise (Hemingway 1963, Tikuisis, Bell et al. 1991). Several studies give predictive formulas for metabolic responses in response to shivering (Buskirk 1963, Tikuisis, Bell et al. 1991). These equations are based on shivering onset and intensity of particular muscle groups, as well as body composition (Buskirk 1963, Timbal, Boutelier et al. 1976). Differences in metabolic responses and shivering are evident with differences in body composition as it has been shown that leaner individuals have a greater metabolic response to cold relative to obese who had the same core temperatures and, paradoxically, lower skin temperatures, even when normalised to body weight (White and LeBlanc 1993). This suggests those who tend to gain weight have a lower relative rate of energy expenditure when exposed to mild cold than those who tend to be exempt from gaining weight or gain less weight (Tikuisis, Bell et al. 1991). Some studies have proposed various predictive formulas for ST and have based their formulae on anthropometric measurements as well as core and skin temperatures (Hilliges, Wang et al. 1995, Peier, Moqrich et al. 2002, Lee, Ho et al. 2011).

Indirect calorimetry, Substrate Oxidation and Fuel Selection

The mechanism of fuel selection to sustain ST has received a lot of attention and it was suggested that fuel selection may be modified in a number of ways (Haman, Peronnet et al. 2002, Haman 2006). These include the following: the ability to recruit different metabolic pathways within the same muscle fibres, by recruiting specific sub groups of fibres within a muscle, or by recruiting muscles that vary in their fibre composition (Haman, Legault et al. 2004). Such differences in muscle fibre recruitment, and therefore shivering pattern, may be linked to carbohydrate (CHO) availability during cold exposure (Haman, Peronnet et al. 2004). Carbohydrate reserves are acutely affected by changes in diet and supplies the largest percentage of substrate needed to sustain energy expenditure during cold exposure (Benzinger, Pratt et al. 1961). Since skeletal muscle fibre recruitment during shivering has been linked to CHO availability,

there has been a heightened interest in fuel selection and its relation to energy expenditure during cold exposure (Haman 2006). In studies that limited the amounts of CHO available, a noticeable shift was seen from lipid (FAT) to CHO use depending on the extent of muscle glycogen loading (Haman, Legault et al. 2004). Some studies revealed that altering glycogen storage did not alter the thermoregulatory responses (Young, Sawka et al. 1989, Peier, Moqrich et al. 2002) with either glycogen loading or depletion of skeletal muscle and it was long suggested that limited glycogen reserves would limit the amount of heat released in an individual through ST (Wang 1980, 1981). In 2004, the contributions of plasma glucose, muscle glycogen, proteins, CHO and FAT were quantified for total heat transfer in humans (Haman, Peronnet et al. 2004). They found that the size of the CHO reserves had no effect on heat transfer, but had a major influence on fuel selection. Low glycogen stores corresponded to substrate oxidation rates that were 53% FAT, 28% CHO, and 19% proteins. Conversely, a high CHO diet corresponded to oxidation rates that were 23% FAT, 65% CHO, and 12% proteins. It was concluded that there is a remarkable flexibility in human oxidative fuel selection during ST and that all three macronutrients, CHO, FAT, and proteins, can play an important role in fuelling heat transfer (Haman, Legault et al. 2004, Haman, Peronnet et al. 2004).

Quantification of Shivering Utilising Electromyography

Electromyography provides another method for quantifying ST. Electromyography analysis on skeletal muscle shivering has indicated two distinct patterns: 1) a continuous, low-intensity shivering with skeletal muscle contractions at 4-8 Hz, and 2) high-intensity burst shivering at a lower frequency with skeletal muscle contractions at 0.1-0.2 Hz (Petajan and Williams 1972, Israel and Pozos 1989). Continuous, low-intensity shivering utilises more type I, slow-oxidative fatigue-resistant fibres, while burst-shivering transitions to rely more on type II, fast-glycolytic, more fatigable fibres (Petajan and Williams 1972, Israel and Pozos 1989).

Electromyography analysis has enabled a different perspective on metabolic responses in relation to shivering and several interindividual differences have been observed (Hemingway 1963, Haman 2006). Muscle shivering activity can differ between low-intensity, lipid-fuelled, type-I muscle specific shivering and high-intensity burst, CHO-

fuelled, type-II muscle specific shivering. Depending on the type of shivering, fuel supply could range from 20-60% from either CHO or FAT (Haman 2006). Previous observations (Martineau and Jacobs 1989) suggested that burst-shivering, being more CHO-fuelled, may be significantly affected by glycogen reserves. Haman *et al.* (2004) however, demonstrated that this was not the case. Despite differences in glycogen reserves, both types of shivering responses, assessed by EMG, and therefore both types of muscle fibres, were unaffected by changes in CHO and FAT reserves.

Sympathetic Nervous Control

In order for humans to maintain homeostasis around a tightly regulated core temperature set-point or null-zone, energy must be expended in response to the fluctuating environmental conditions. The neural mechanisms that control thermogenic and heat conservation responses are integral to the understanding of energy balance and weight control in humans (Morrison 2011).

Early studies recognised the possibility that mammalian neural responses may be altered when they live in cold environments. The explanation of these alterations or adaptations to cold were assessed in studies of catecholamine responses (Buskirk 1963) and previous cold exposure studies (Keatinge 1960) in humans. LeBlanc *et al.* (1975) demonstrated autonomic nervous system adaptations via parasympathetic and sympathetic responses using Inuit, arctic expeditionary soldiers and non-adapted Caucasian controls. Subtle variations in several physiological variables were observed including cutaneous vasoconstriction, heart rate, and systolic blood pressure were seen when comparing these cold adapted individuals to the non-adapted Caucasians. A lower mean heart rate of 10 beats/min and a lower mean systolic blood pressure of 15 mm Hg was observed when comparing these cold-adapted groups to non-acclimated Caucasian controls (LeBlanc, Dulac et al. 1975). These differences were attributed to adaptations in the neural control mechanisms of these responses to cold stresses (LeBlanc, Dulac et al. 1975).

Further demystifying of the neuronal contributions and the exact pathway for the control of thermogenesis in the cold came through studies focusing at the cellular level (Hammel, Hardy et al. 1960, Hammel, Jackson et al. 1963). Early studies found that the

preoptic area and anterior hypothalamus were important anatomical areas of the brainstem in the CNS for integration of temperature information that is received from peripheral and central temperature sensitive neurons (Hammel, Hardy et al. 1960).

More recently, changes in transient receptor potentials (TRP) by TRP channels in cold sensitive afferent neurons were identified as the receptors detecting the changes in surface temperatures (Caterina 2007). Thermo-sensitive TRP channels are expressed in free nerve endings found in the epidermis and dermis (Hilliges, Wang et al. 1995), as well as keratinocytes (Peier, Moqrich et al. 2002). Differing TRP channels are thought to be either warm or cold sensitive; for example, temperatures above 30^{o}C may activate TRPV1 channels, while TRPV8 channels are thought to activate between 5-25^{o}C. These studies have demonstrated that TRP channels have a part in thermosensory functions during temperature regulation, however, the specific contributions of TRPV1 to thermoregulation in particular are still of some debate (Caterina 2007).

As discussed above, the temperature signal is relayed through the dorsal root ganglia of the vertebral column to the integrative areas of the hypothalamus in the brainstem (Hammel, Hardy et al. 1960, Caterina 2007, Morrison 2011). Both warm and cold temperatures are sensed by CNS neurons that integrate this information in the hypothalamus to regulate core temperature. Hammel (1965) demonstrated his hypothesis of warm-sensitive (W) and temperature insensitive (I) neurons and their interactions resulting in increased energy expenditure to produce heat. Boulant (2006) gives a schematic of a modified version this model (Figure 1.1). Temperature insensitive neurons display little to no change in their firing rates (FR) during hypothalamic cooling or warming. Firing rat refers to the frequency of action potentials generated, and around 20% of neurons were found to strongly change their FR during hypothalamic warming and were labelled as W neurons. Through a reciprocal cross-inhibition mechanism, displayed in the FR graphs, W and I neurons are able to coordinate the body's response to external temperature changes. The result is either a gain or loss of heat (Boulant and Dean 1986, Boulant 2006).

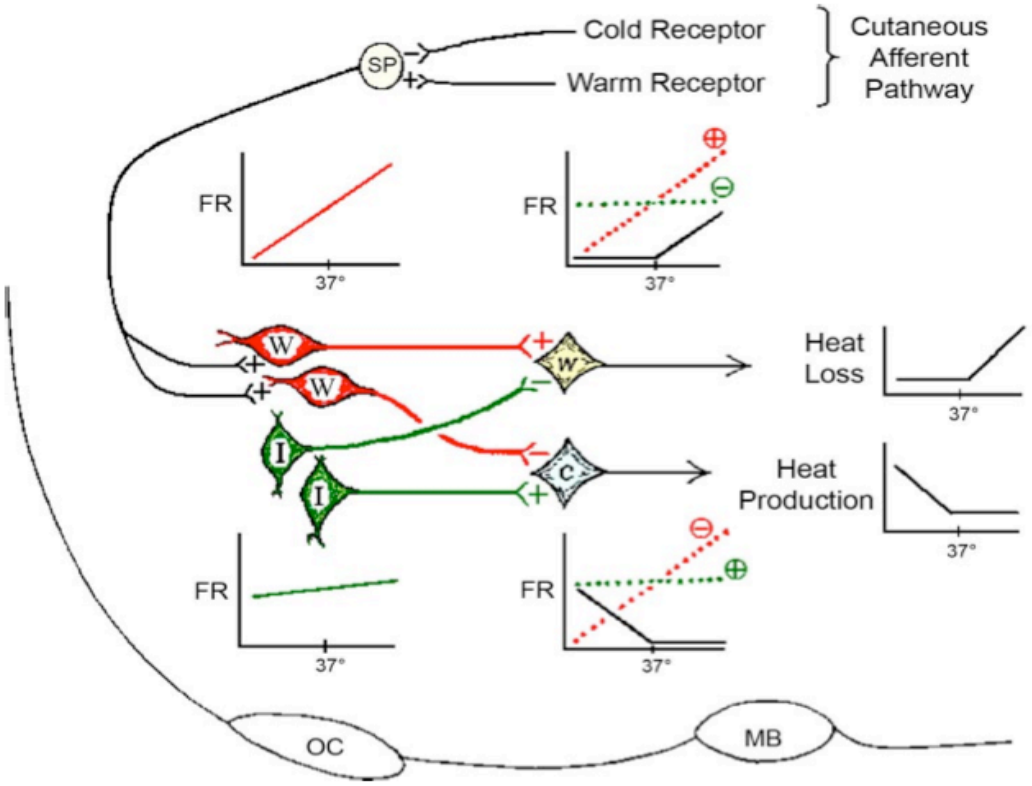

Figure 1.1. A modified neuronal model originally proposed by H. T. Hammel (1965) giving the set-point model for regulation of core temperature. W, warm-sensitive neuron; I, temperature-insensitive neuron; w, heat loss effector neuron derived from warm-sensitivity; c, heat production effector neuron derived from cold-sensitivity; SP, dorsal horn spinal neuron; OC, optic chiasm; MB, mammilary body. Graphs show the firing rates (FR) of each group of neurons as well as thermoregulatory effector responses to changing hypothalamic temperatures (right). Dotted lines indicate the frequency of excitatory (+) and inhibitory (-) synaptic inputs (Boulant 2006).

Obese Adaptations During Cold Exposure

When exposed to similar cold stresses, individuals with greater subcutaneous fat have been shown to elicit lower skin temperatures with limited to no ST (Leblanc 1954). As ambient temperatures decrease, the difference between individuals of normal weight and those with increased adiposity seems to increase as higher subcutaneous fat elicit cooler skin temperatures (Leblanc 1954). This was further investigated in following studies that found obese individuals, despite having lower skin temperatures and the same core temperatures, demonstrated no heightened metabolic response to the cold

(Wyndham, Williams et al. 1968, White and LeBlanc 1993). While it would seem logical to increase metabolic rate to increase heat release with decreasing skin temperatures, the obese seem to have a blunted response to cold exposure and some have suggested they share similar properties to those that are cold acclimatised (Young 1988, White, Ross et al. 1992, White and LeBlanc 1993).

Non-adapted humans respond to the cold with increased ST, elevated metabolic response and heat release, as well as cutaneous vasoconstriction (Young 1988). Those who are acclimatised demonstrate a number of adaptations, the first is known as the *metabolic adaptation* whereby less metabolic output is evident in response to cold exposure. The second adaption is known as the *hypothermic adaptation* and is hypothesised to include a lower set-point or null-zone being defended, corresponding to a lower core temperature (Young 1988). Less heat release, and therefore less energy is required to be expended to defend core temperatures. The final adaptation has been extensively observed in previous mentioned studies and is known as the *insulative adaptation*. Cold-adapted and obese individuals exhibit lower skin temperatures. This corresponds to less thermal conductivity and less heat exchange with the surrounding environment (Young 1988).

While it is unresolved whether obese individuals exhibit all of these cold adaptations it is clear that, to a certain extent, the obese exhibit a type of 'insulative-trap' whereby their afferent cold receptor inputs do not seem to initiate the same heat liberation and metabolic responses as observed in leaner individuals. These adaptations certainly reduce the need for ST in larger individuals, but it is unknown if this response is causal or consequential of the ability to activate the second type of heat release in the body known as NST.

1.1.2. Non-Shivering Thermogenesis

Brown Adipose Tissue

Along with various other physiological adaptations to uniquely evolve in mammals, BAT is thought to have been one of the earliest to develop (Cannon and Nedergaard 2004). The functional significance of this distinctly mammalian tissue is of

great interest due to its suggested tie to increased energy expenditure (Rothwell and Stock 1997, Cannon and Nedergaard 2004). It has been linked to a number of important responses including our ability to survive during long exposure to cold temperatures, to survive the cooling stress to the neonate at childbirth, and possibly to initiate a greater and more sustained basal metabolic rate in adults.

Although observed for decades, BAT is relatively new in terms of its proposed physiological significance for human energy expenditure. Earliest discussions on what is believed to be BAT were given by Swiss zoologist, Conrad Gessner, in his 1551 revolutionary five-volume Historiae animalium as cited by Cannon and Nedergaard (2004). Over the past century, many mammals have been shown to possess BAT, most notably hibernating bears as well as mice and rats studied in laboratory settings. The theories of BAT thermogenic applications, however, have developed in the past 50 years (Carlson and Cottle 1956, Smith 1964). Most recently, BAT has been linked to a variety of metabolic inefficiencies and this tissue has been postulated by different groups to make a significant contribution to human energy balance (Rothwell and Stock 1979, Bartelt, Bruns et al. 2011).

Overview of Brown Adipose Tissue

The brown adipocyte (Figure 1.2) is the functional, cellular unit of the tissue (Guyton 2006) and is said to arise from the myoblastic cell lineage rather than the previously hypothesised preadipocytes (Lee, Ho et al. 2011). While the brown adipocyte may be the powerhouse cell of the tissue, a larger proportion of the tissue is comprised of endothelial cells within interlaying capillaries. This allows for a greater availability of oxygen and substrates from the rest of the body via the circulatory system (Geloen, Collet et al. 1990) and provides the easy transfer of heat from the tissue to the circulating blood (Sacks and Symonds 2013). Under conditions of increased recruitment of the tissue, such as chronic cold exposure, these BAT progenitor cells function to divide and differentiate into new brown adipocytes (Boeuf, Klingenspor et al. 2001). Brown adipose tissue receives information on the body's temperature, lipid reserves and current feeding status from the ventromedial hypothalamic nucleus in the brain (Guyton 2006). If any of the aforementioned physiological states are altered from their homeostatic zones, for example, if there is reason to increase the rate of food oxidation

or increase the rate of heat release, signals are transmitted via the sympathetic nervous system to the brown adipocytes (Trayhurn and Wusteman 1987). Therefore, the proper functioning of BAT relies on the initial input from an extensive network of catecholamine-driven sympathetic nerve fibres along with sufficient supply of oxygen and substrate from the capillary system.

The adequate stimulation from the sympathetic nervous system, coupled with the appropriate fuel sources, allows the brown adipocyte to breakdown available triglycerides that have been taken up from the blood. Intracellular sympathetic signalling, discussed in greater detail in following sections, propel the release of the triglycerides into free fatty acids (FFA) that are thought to be involved in the activation of the brown fat-specific uncoupling protein-1 (UCP-1) (Benzinger, Pratt et al. 1961). The FFA are used as the acute substrate in thermogenesis (McCormack 1982). Fatty acid oxidation happens during beta-oxidation of the mitochondria resulting in the expulsion of an H^+ ion and the release of energy (Cannon and Nedergaard 2004, Kajimura and Saito 2014). The outcome of this FFA oxidation is that there is an increase in the amount of food and energy reserves available in the blood that are taken up by the tissue and combusted, leading to increased heat release (Figure 1.2).

In smaller mammals living in more temperate climates, the participation of BAT in heat release may be responsible for almost half of their total energy expenditure (Cannon and Nedergaard 2004). It may also be the predominant thermogenic tissue in those smaller mammals living in cooler climates. Brown adipose tissue capacity in all mammals therefore varies depending on size and exposure to certain environments: it may atrophy when unused after continual non-exposure to the cold, and may proliferate when cold exposure is chronic (Cannon and Nedergaard 2004).

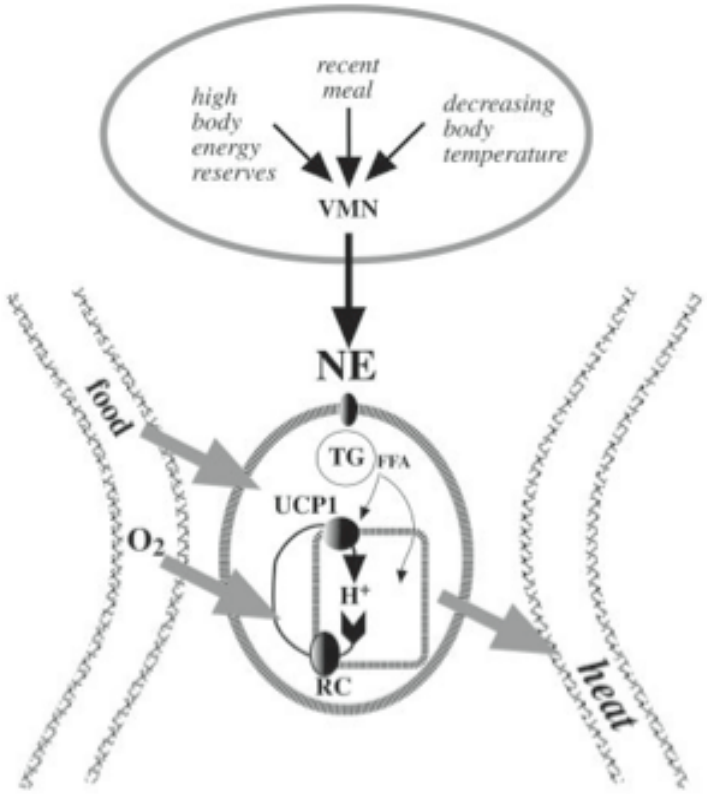

Figure 1.2. An overview of the acute control of brown adipose tissue activity including the initiation of sympathetic nervous tissue from ß3-adrenoreceptors, to the uptake of oxygen and fuel in the form of food, resulting in the transfer of energy to give heat. VMN, ventromedial hypothalamic nucleus; NE, norepinephrine; TG, triglycerides; FFA, free fatty acids; UCP-1, uncoupling protein-1; H^+, hydrogen ion; O_2, oxygen molecule; RC, respiratory chain (Cannon and Nedergaard 2004).

Adrenergic Control of Brown Adipose Tissue

To understand the thermogenic properties of BAT, it is necessary to understand how its activity is controlled and what regulates its release of heat. The brown adipocyte is under sympathetic nervous control via norepinephrine signalling (Trayhurn and Wusteman 1987). Norepinephrine is responsible for initiating the brown adipocyte's most important thermogenic effects, as well as cell proliferation, maturation, and apoptosis (Trayhurn and Wusteman 1987).

Norepinephrine Signalling

Norepinephrine release is heightened after increases in food intake, energy reserves, or cold exposure. It is released by the ventromedial hypothalamic nucleus and medulla in the adrenal glands as well as by postganglionic neurons of the sympathetic nervous system (Guyton 2006). Although able to initiate signalling with the mature brown adipocyte via all three types of known adrenoreceptors including ß, α_1, and α_2, the most significant pathway is provided through ß-adrenergic stimulation (Preitner, Muzzin et al. 1998, Bronnikov, Bengtsson et al. 1999).

Upon reaching the brown adipocyte (Figure 1.3), norepinephrine binds primarily to $ß_3$-adrenoreceptors (Cannon and Nedergaard 2004). Of the three main subgroups of ß-adrenoreceptors, $ß_3$-adrenorecptors are the most significant in mature adipocytes. $ß_1$-adrenoreceptors are also expressed in the mature adipocyte but are not coupled in the signalling process to any significant degree (Bronnikov, Bengtsson et al. 1999). $ß_2$-adrenoreceptors, not shown in Figure 1.3, couple with cyclic adenosine monophosphate (cAMP), a derivative of ATP, are thought to be more associated with the signalling process involved with preadipocytes (Bronnikov, Bengtsson et al. 1999). Recently it has been shown that $ß_2$-adrenoreceptors are not found on the surface of the brown adipocyte, but rather in the surrounding vascular tissue (Bengtsson, Cannon et al. 2000). A fourth $ß_4$-adrenoreceptor, with similar properties to $ß_3$-adrenoreceptors, has also been described (Preitner, Muzzin et al. 1998), although no gene expression for it has been found and its function is not fully understood.

Examination of the physiological effects of norepinephrine on the brown adipocyte can be simulated with various agonists including BRL-37344, CGP-12177 and CL-316243 (Preitner, Muzzin et al. 1998). These agonists help quantify and characterise the actual brown adipocyte response to cold exposure or high-energy reserves from increased food intake. This is because $ß_3$-adrenoreceptors are primarily located on the surface of brown adipocytes and are seldom found elsewhere in the body (Cannon and Nedergaard 2004).

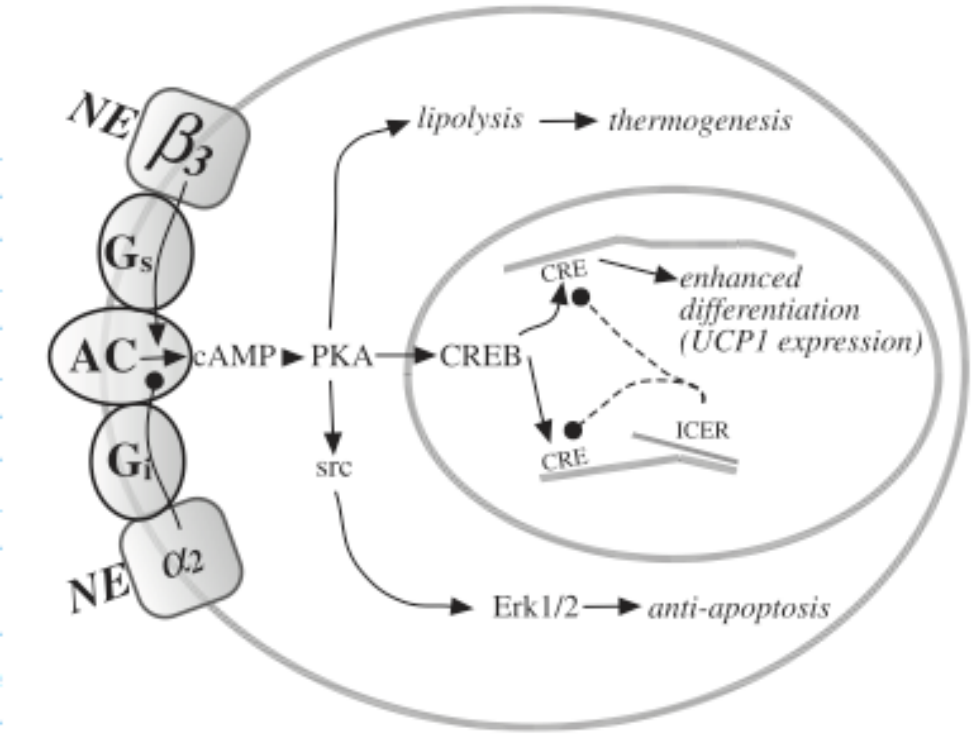

Figure 1.3. ß$_3$-adrenergic signaling pathway in mature brown adipocytes. NE, norepinephrine; ß3, ß3-adrenoreceptor; G_s, stimulatory G protein; G_i, inhibitory G protein; α_2, α_2-adrenoreceptor, AC, adenylyl cyclase; cAMP, cyclic adenosine monophosphate; PKA, protein kinase A; CREB, CRE-binding protein; CRE, cAMP response element; ICER, inducible cAMP early repressor; Erk 1/2, anti-apoptosis protein kinase (Cannon and Nedergaard 2004).

G protein, cAMP, and Protein Kinase A Mediation

Following the stimulation of the brown adipocyte via ß$_3$-adrenoreceptors, the signal passes through stimulatory G_s proteins (Figure 1.3). The stimulatory G_s protein aids in bringing the signal through the membrane to the inside of the cell (Neves, Ram et al. 2002). It has been suggested that the brown adipocyte may be linked with inhibitory G_i proteins (Figure 1.3) as well (Chaudhry, MacKenzie et al. 1994). This would serve as a possible "self-limiting" pathway, inhibiting cAMP formation and possible downstream thermogenic properties of the brown adipocyte (Williams and Matthews 1974).

Continuing along the ß-adrenergic signalling pathway (Figure 1.3), further activation of the brown adipocyte proceeds with the norepinephrine-induced formation of

cAMP from adenylyl cyclase (AC), an enzyme that helps convert ATP to cAMP (Williams and Matthews 1974). Throughout the body, cAMP initiates activation of other proteins through cation channels, such as Ca^{2+} and K^{+} channels; the brown adipocyte is no different, current research shows that cAMP continues the signalling progress through activation of protein kinase A (Williams and Matthews 1974).

The adrenergic pathway continues with a group of phosphorylating enzymes (Figure 1.3), both in the nuclear and cytosolic areas of the cell (Thonberg, Fredriksson et al. 2002). Protein kinase A phosphorylation with nuclear-related proteins are able to promote a cascade of transcription factors (CREB, CRE, ICER), thought to aid in the expression of genes that account for UCP-1 synthesis; this will be discussed in a later section (Nedergaard, Matthias et al. 1999). Paralleling the phosphorylation of nuclear proteins, protein kinase A also stimulates cytosolic protein phosphorylation (Thonberg, Fredriksson et al. 2002). Most importantly, these cytosolic proteins move to initiate the lipolytic pathway as is described below. This leads to thermogenesis in the brown adipocyte and this contributes to the heat release from the tissue as a whole.

Initiation of Non-shivering Thermogenesis in BAT

The thermogenic effect of BAT was initially described some 50 years ago (Smith 1964), and since then, a variety of molecular mechanisms that signal the brown adipocyte have been postulated on how it is able to liberate heat from the oxidative phosphorylation in mitochondria (Lindberg, de Pierre et al. 1967, Prusiner, Cannon et al. 1968). Some earlier proposed mechanisms described an ATP-dependent system that lead to the formation of ADP and the subsequent stimulation of substrate oxidation and thermogenesis in the mitochondria (Prusiner, Cannon et al. 1968). Later observations that ATP synthase inhibition only partly reduced the thermogenic effect (Hilliges, Wang et al. 1995), and that BAT mitochondria generally have a low capacity for ATP synthase activity (Lindberg, de Pierre et al. 1967) effectively disproved this idea. Using an ATP synthase inhibitor called oligomycin, Prusiner *et al.* (1968) demonstrated only a partially reduced effect of norepinephrine on the thermogenic response of BAT. This collectively established an understanding that the thermogenesis via BAT was aided by some other mechanism, and it is not primarily ATP-controlled.

Another theory on the exact activation mechanism of thermogenesis in BAT came through in the form of an uncoupling process (Lindberg, de Pierre et al. 1967). This was described as an oxidative process not coupled to ATP synthesis (Klingenberg and Huang 1999, Cannon and Nedergaard 2004). Uncoupling protein-1, first known as thermogenin, was found to be, at least to some extent, the missing mechanism in the mitochondrial thermogenic process. Other uncoupling proteins, including UCP-2 and UCP-3, have also been identified, resulting in some scrutiny as to UCP-1's importance to thermogenesis. A recent study, however, demonstrated (Figure 1.4) through the use of normally functioning mice compared with UCP-1-ablated mice that thermogenesis, via its norepinephrine signalling process, is completely UCP-1-dependent (Matthias, Ohlson et al. 2000). The study demonstrates that no NST takes place once UCP-1 is removed from the brown adipocyte (Matthias, Ohlson et al. 2000). Currently, there is little evidence to suggest there are other mechanisms that aid in the initiation of BAT thermogenesis.

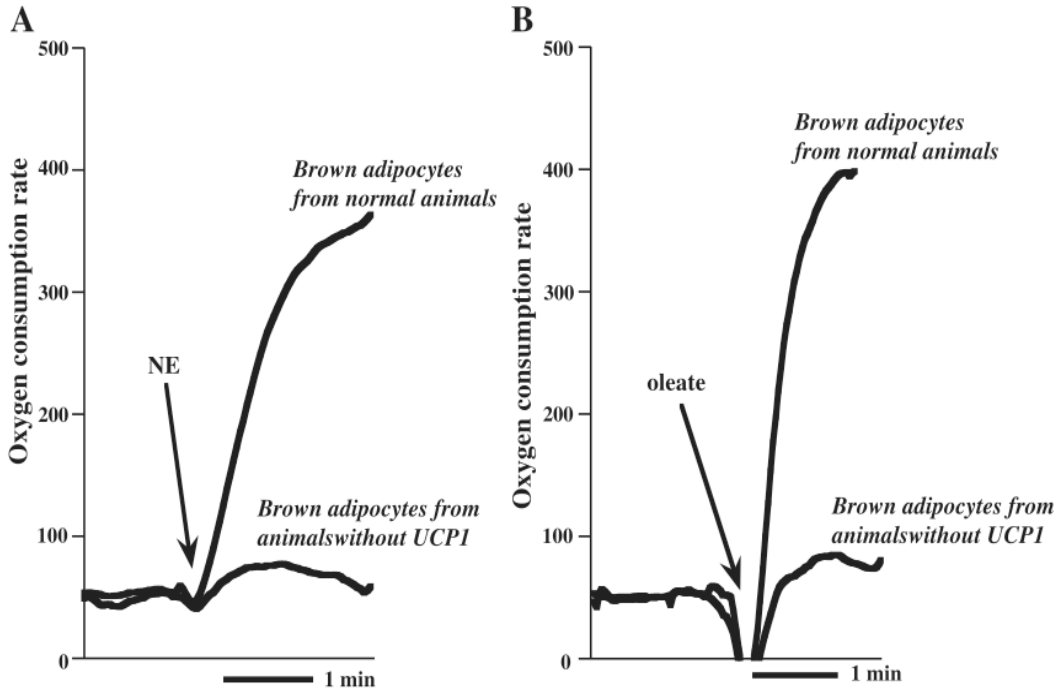

Figure 1.4. Brown adipocytes from normal and UCP-1 ablated mice were exposed to A) norepinephrine (NE), or B) fatty acid (oleate, ^{18}Carbon) to assess whether UCP-1 is essential for thermogenesis. The almost 10-fold increase in oxygen consumption (fmol O_2•min^{-1}•$cell^{-1}$) (fmol = femtomole; SI unit for 10^{-15} moles) represents the thermogenic response and its reliance on UCP-1 (Cannon and Nedergaard 2004).

Stimulation of Lipolysis and BAT Thermogenesis

As triglycerides (TG), glycerols, or FFAs accumulate within the brown adipocytes of the body (Figure 1.5), norepinephrine may be released which initiates the lipolysis or breakdown of the fat molecules (Cannon and Nedergaard 2004). Although not fully resolved, the process begins downstream of protein kinase A. The cascade continues in the cell through the phosphorylation of hormone-sensitive lipase (HSL), which acts in effectively breaking the TG molecules into glycerol and smaller FFA. Peripilin has been found to act as a balancing molecule with HSL as it surrounds the TG and protects it from degradation (Chaudhry, MacKenzie et al. 1994, Bartelt, Bruns et al. 2011). In mice studies where peripilin has been artificially ablated, mice have been shown to have higher basal metabolic rates. Conversely, studies with HSL-deficient mice have been shown to have an increased adiposity. While some FFA may be expelled from the brown adipocyte, most are channelled towards the mitochondria and used as the substrate for NST (Prusiner, Cannon et al. 1968).

The thermogenic effect in BAT (Figure 1.4B), while dependent on UCP-1 presence in the mitochondria (Matthias, Ohlson et al. 2000), can be simulated by the addition of FFAs such as oleate into the cell (Prusiner, Cannon et al. 1968). Employment of these factors that induce lipolysis in brown adipocytes subsequently initiate NST, and no NST is observed without lipolysis (Matthias, Ohlson et al. 2000).

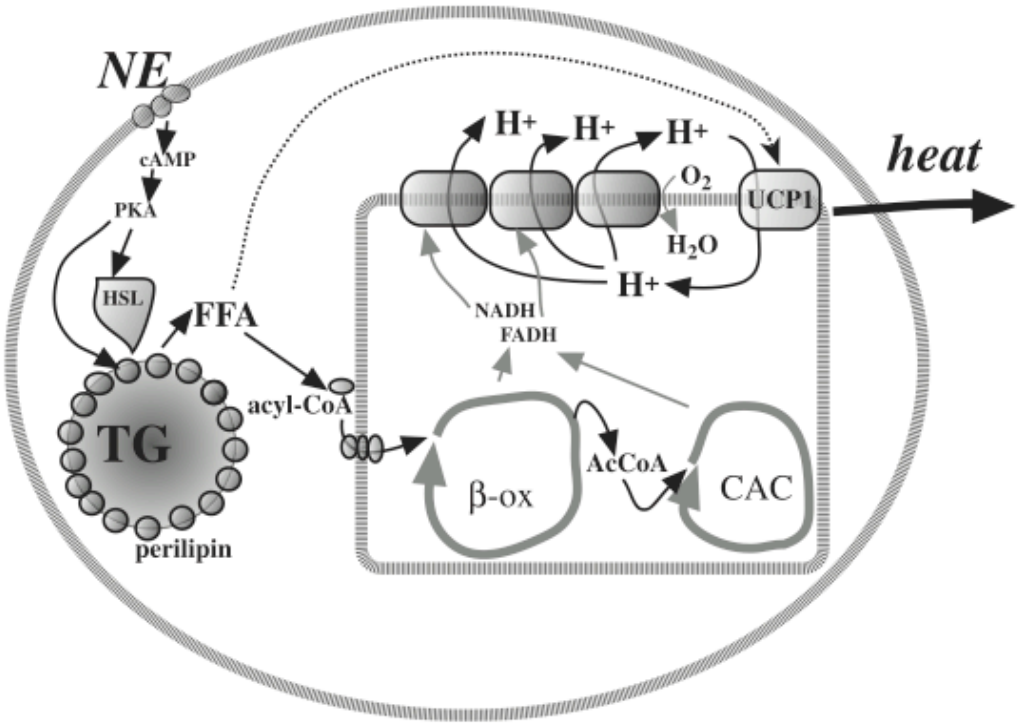

Figure 1.5. Events downstream of protein kinase A in the norepinephrine-induced stimulation of thermogenesis in the brown adipocyte. NE, norepinephrine; cAMP, cyclic adenosine monophosphate; PKA, protein kinase-A; HSL, hormone-sensitive lipase; TG, triglyceride; FFA, free fatty acid; NADH, nicotinamide adenine dinucleotide; FADH, flavin adenine dinucleotide; H_2O, water molecule; O_2, oxygen molecule; H+, hydrogen ion; UCP-1, uncoupling protein-1; ß-ox, ß-oxidation; AcCoA, acetyl CoA; CAC, citric acid cycle (Cannon and Nedergaard 2004).

The UCP-1 protein has been studied extensively, yet a full understanding of how it is incorporated into the mitochondrial wall is one of the most intriguing mysteries of BAT and its thermogenic effects. Three models have been proposed on how UCP-1 is incorporated into the mitochondrial wall. In the allosteric model, a FFA interacts with a site directly on UCP-1, initiating its activation (Rial and Gonzalez-Barroso 2001). In the cofactor model, FFAs bind to sites within the proton channel of UCP-1 and act as stepping-stones for protons as they pass through the membrane (Winkler and Klingenberg 1994). In the proton shuttle model, protons with a dissociated FFA move through the mitochondria and exit in its anionic form carried by UCP-1 (Garlid, Jaburek et al. 2000). These models have been extensively reviewed elsewhere (Nedergaard, Matthias et al. 1999).

Diet-Induced Thermogenesis

Thermogenesis is the liberation of chemical energy from ingested food into heat. Brown adipose tissue completes this transfer without the need to store much energy. This means that a smaller proportion of the total food energy consumed from a meal is stored in the form of FAT, CHO, proteins and ATP, when BAT is active (Trayhurn, Thurlby et al. 1977). This was first observed in the late 1970's in mice and several theories were advocated on the linkage between metabolic efficiency and BAT (Trayhurn, Thurlby et al. 1977).

Single Meal Thermic Effects on BAT Thermogenesis

Thermic effects of eating are marked by increases in the metabolic rate above that of normal basal rates for 5 to 6 h in postprandial period. A single meal has been shown to increase BAT activity in mice through increased oxygen consumption within this tissue (Glick, Teague et al. 1983), as well as an increase in blood flow to the area surround BAT depots (Glick, Wickler et al. 1984). There have also been reports on possible systemic increases in norepinephrine concentration and overall weight increases in BAT after consumption of a single meal (Glick, Teague et al. 1983). The thermic effects of a single meal are evidently initiated by sympathetic effector systems, but the actual mechanism underlying the response is unknown.

Leptin, a protein hormone fundamental in the regulation of energy expenditure including appetite, hunger, and metabolism, is thought to act too slowly in single meal-induced thermogenesis and its involvement in diet-induced thermogenesis is unlikely. Rather, increased release of glucose from muscle and liver glycogen stores, insulin from the pancreas, cholecystokinin released from the stomach during a meal, and enterostatin, a pentapeptide released upon pancreatic lipase activation by lipase, have each been suggested as possible molecules involved in the control of BAT NST. All these are blood-borne substances that could interact with the centres in the brain responsible for BAT control and have been discussed in detail in different studies (Sakaguchi and Bray 1987, Erlanson-Albertsson and Larsson 1988).

Overall, a single, but semi-repetitive meal plan, as seen in the average population, is thought to engage BAT activation, maintain brown fat recruitment, and subsequently decrease metabolic efficiency (Glick, Teague et al. 1983).

Chronic Low Nutrient Density Food Intake and Obesity

Much interest has fallen on the topic of chronic, nutritionally lacking diets, their thermogenic effects and their relation to obesity (Rothwell, Stock et al. 1983). Most experiments have been performed on animals other than humans and various diets have been implemented to simulate nutritional similarities to that of junk food, i.e., food items high in energy but low in nutrient content (Cannon and Nedergaard 2004). In hopes of simulating obesity in humans due to chronic overeating, high energy with low nutrient content diets have been employed in rodent models with the forethought of discovering linkage between obesity, thermic effects of chronic eating, and BAT recruitment and activation (Shimizu, Aprahamian et al. 2014, Dodd, Decherf et al. 2015).

Several studies using these “protein diluting”, or diets that decrease protein energy percentage from around 20% to as low as 5%, have demonstrated an increase in food intake, some obesity, a decreased metabolic efficiency, yet an apparent proliferation of BAT (Rothwell, Stock et al. 1983). Little is known as to the signalling process between chronic food intake, its quality, and BAT recruitment, but it is apparent that a diet-induced thermogenesis exists. Some of these protein-diluting studies have shown significant increases in BAT activation after lower protein diets (Smith and Hock 1963, Rothwell, Stock et al. 1983) and while most believe these low protein diets initiate obesity as seen in humans, some consider it to be the subsequent development of obesity that triggers BAT recruitment (Llado, Proenza et al. 1991). Llado, Proenza et al. (1991) showed that BAT volume increase was only seen after removing rats from a low protein, nutrient low diet where obesity had been induced. They concluded that the increase in BAT volume was attributed to the obesity status of the rats rather than diet.

The answer to whether obesity could influence NST is of some debate. A number of studies have shown that in obese mice reintroduced to “normal” diets maintain their BAT volume and activity, suggesting that obesity does in fact trigger BAT activation (Llado, Proenza et al. 1991). Obese humans are hyperleptinemic and leptin,

whose blood concentration parallels the fraction of white adipose tissue (WAT) in an individual, has been postulated as the possible mediator in the effect of obesity on BAT thermogenesis. When treated with leptin, animals, but not humans, seem to have a decrease in body weight due to decreased food intake (Friedman 1998, Lee, Ho et al. 2011). Therefore, an expected result of BAT deactivation should be seen. This is not the case in mice, as the opposite effect has been documented (Collins, Kuhn et al. 1996); leptin treatment resulted in establishing signs of brown fat activation such as increased sympathetic nerve activity and increases in UCP-1 gene expression. The present underlying mechanisms for these responses is unknown.

The opposing hypothesis is that obesity is caused in part by a lack of diet-induced NST. It is well documented that many genetic models of obesity are also characterised by diminished BAT response and UCP-1 concentrations (Goodbody and Trayhurn 1982). So the question remains: does this diminished brown adipose activity contribute to the obese individual? Or is the atrophied tissue simply concurrent and coincidental? To date, UCP-1-ablated mice do not seem to gain weight, whereas brown fat-deficient mice become obese (Trayhurn, Thurlby et al. 1977, Goodbody and Trayhurn 1982). This is interesting as UCP-1's importance in the thermogenic response is clear. Still, it is believed by many that a decreased recruitment of BAT may magnify a dietary- or genetically-induced obesity in an individual (Rothwell and Stock 1979). Simply put, it is unclear, particularly in rodent models, whether BAT recruitment and activation is causal or consequential from chronic elevated food intake.

Cold-Induced Thermogenesis

Another physiological response of BAT NST is in the presence of mild cold exposure. As discussed above, ST contributes the greatest amount of heat gain in acute more intense cold environments but the contributions of BAT to cold-induced thermogenesis are apparent and extensive.

When an animal is exposed to a low ambient temperature, extra heat is needed to maintain ideal core temperatures. This extra heat needed to defend the body's core temperature is smaller in relative magnitude the larger the animal gets (Cannon and Nedergaard 2004). This means that smaller mammals have adapted to provide this

extra heat to a greater extent than larger animals, such as humans. This may be due to still unresolved topics relating to basal metabolism in relation to body weight (Cannon and Nedergaard 2004). For smaller animals chronically exposed to temperatures lower than that of their normal body temperatures, it is evident that there is a recruitment of non-shivering thermogenic tissues that account for this extra heat release. Although many experimental animals do this when exposed to acute and chronic cold exposure, evidence for these extra metabolic processes had not clearly been evident in humans exposed to mild cold (Trayhurn, Thurlby et al. 1977, Goodbody and Trayhurn 1982, Trayhurn and Wusteman 1987). While recent research on humans has almost conclusively put this debate to rest (Saito, Okamatsu-Ogura et al. 2009, Yoneshiro, Aita et al. 2011, Blondin, Labbe et al. 2014), most information on BAT activity during cold exposure comes from animal models.

BAT and Cold Exposure in Animal Models

Initial observations of BAT NST to cold exposure were seen in rodents (Carlson and Cottle 1956, Jansky 1973). Cold-acclimated rodents exposed to temperatures just below the thermo-neutral zone could withstand the effects of cold exposure longer than warm-acclimated rodents (Jansky and Hart 1963). These acclimated mice were able to suppress the need to shiver and relied almost exclusively on NST (Jansky 1973).

More recently, UCP-1-ablated mice, once exposed to $ß_3$-agonists or FFAs, demonstrated had no ability to utilise NST in response to cold (Himms-Hagen, Cui et al. 1994, Enerback, Jacobsson et al. 1997). This was paired with UCP-1-ablated mice that were shown to shiver with a constant intensity, even after chronic exposure to the cold (Golozoubova, Hohtola et al. 2001). This supports that these mice were unable to recruit any other means to release heat, as well as any other form of NST other than that found in BAT. Therefore, a fully functioning BAT appears to be an integral adaptation to repeated exposure to the cold and it is quite clear that, based on animal models, UCP-1 is necessary for NST in cold environments (Matthias, Ohlson et al. 2000, Golozoubova, Hohtola et al. 2001).

Hibernation and Postnatal Thermogenesis

Hibernation and Arousal Utilising BAT

Although many recent studies on BAT have involved humans (Hilliges, Wang et al. 1995, Cannon and Nedergaard 2004, Cypess, Lehman et al. 2009, Saito, Okamatsu-Ogura et al. 2009, van Marken Lichtenbelt 2012, Blondin, Labbe et al. 2014), most early findings of BAT's function were in hibernating mammals (Gessner 1551., Smith and Hock 1963). As early as the 1920's BAT was referred to as the hibernating gland (Rasmussen 1923) with little knowledge of it's physiology. Since then, studies have looked at the function and use of BAT in these hibernators.

A hibernating animal's body temperature set point decreases to around 5°C for most of the winter (Smith and Hock 1963). If the surrounding environment continues to drop, BAT is then activated to aid in the defence of this reduced core temperature set-point. Periodically throughout the winter, hibernators move through an arousal stage whereby BAT is able to contribute large amounts of energy to raise core temperatures back to around 37°C (Smith and Hock 1963, Hindle and Martin 2014).

Brown adipose tissue is relevant in all four stages of hibernation: pre-hibernation fattening, entry into hibernation, each hibernation bout, and during arousal from hibernation (Cannon and Nedergaard 2004, Hindle and Martin 2014). During pre-hibernation fattening, animals induce obesity with hyperphagic-style eating habits. As mentioned previously, some studies have observed increases in BAT recruitment from obesity (Llado, Proenza et al. 1991) and this pre-hibernation hyperphagia may be what contributes to the increase in BAT. An opposing argument suggests that this BAT recruitment could then diminish lipid stores in the body, counteracting the fattening stage for hibernation (Collins, Kuhn et al. 1996). Coupled with decreasing ambient temperatures and shorter days, however, BAT activation is apparent during this pre-hibernation phase. These environmental factors may be enough to produce BAT recruitment, although studies to isolate the physiological from environmental factors have not been performed (Cannon and Nedergaard 2004) and it is unsure whether the pre-hibernation phase creates a metabolic problem in these animals as an increase in BAT could contribute to a counteractive increase in energy expenditure.

The entry into hibernation phase requires the lowering of metabolic rate resulting in the hibernators core temperature to decrease by ~5°C. This requires a sufficient deactivation of BAT through decreased sympathetic stimulation of the area. As observed in studies using BAT G-protein-binding masks (Horwitz, Hamilton et al. 1985), during deep hibernation, BAT is inactive. This evidence suggests that rather than switching the regulation of body temperature off completely, the animal's set-point has simply been shifted down to defend a new lower temperature (Cannon and Nedergaard 2004, Hindle and Martin 2014); this is known as anapyrexia (Cabanac and Brinnel 1987).

Brown adipose tissue plays its largest role during the arousal phase of hibernation, as these mammals are able to rewarm to their normal euthermic conditions in lieu of persisting low ambient temperatures. This has been shown through studies of unmasking, or activation, of latent G-protein binding sites (Horwitz, Hamilton et al. 1985), and by the large temperature increase of BAT sometime 14°C higher than core (Smith 1964). The process can be understood as a resetting of the set-point, or anapyrexia, and because the mammal is unable to shiver during hibernation, brown fat-derived heat is essential in the arousal of hibernators (Smith 1964, Cannon and Nedergaard 2004, Hindle and Martin 2014).

Postnatal Infants and BAT

In most studied mammals, including humans, the most commonly seen use of BAT NST is observed in the postnatal infant (Aherne and Hull 1964, Dawkins and Hull 1964, Dawkins and Scopes 1965, Bruck 1969). Immediately after birth, an infant is exposed to the cooler temperatures of the surrounding environment and large amounts of BAT are responsible for its early heat release as reviewed by Bruck (1969). Initial observations were made in newborn rabbits where subcutaneous thermocouples presented increased temperatures in the scapular region after exposure to ~25°C (Dawkins and Hull 1964). Tissue samples determined that this was due to the large presence of BAT in the newborn rabbits.

While apparent in animal models, there were conflicting reports on the presence of BAT in newborn humans as investigators displayed trouble in its exact quantification

(Aherne and Hull 1964). Literature in this area therefore, has been fairly limited. Thermographic techniques have been used to quantify BAT heat release in infants, however this method is limited as it provides information on BAT function as opposed to the volume of BAT (Rylander, Pribylova et al. 1972, Rasmussen, Entringer et al. 2013). More modern methods of estimating BAT NST prevalence in newborns have come in the form of multi-echo water-fat MRI scans, usually done in post mortem infants (Hu and Gilsanz 2011, Hu, Tovar et al. 2012, Lidell, Betz et al. 2013). These studies are non-invasive and have been some of the first to quantify the volume and composition of BAT in newborns (Rasmussen, Entringer et al. 2013). During natural sleep, neonates' torsos were assessed and were shown to have large amounts of BAT volume in the supraclavicular, axillary, and spinal regions of the body (Rasmussen, Entringer et al. 2013). These were identified as both classical brown adipocytes as well as those relating to a more beige adipocyte lineage (Lidell, Betz et al. 2013).

Methods for BAT NST Estimation in Adult Humans

While methods for quantifying BAT are well established and considered mainly, yet not completely, a resolved science in animal models, less is known in adult humans as effectual methods for estimating BAT NST have arisen only in the past decades. Early studies using post-mortem tissue biopsies and histology showed that outdoor workers, such as lumberjacks and skid-row alcoholics, had more BAT than people who worked indoors (Huttunen, Hirvonen et al. 1981). This knowledge was obtained using histochemical enzyme reactions from these tissue samples and was one of the early observed, however, less practical methods for estimating BAT in adult humans (Huttunen, Hirvonen et al. 1981). Interesting theories arose based on a lack of applicable methods for estimating human adult BAT NST; for example, the hypothesis that most cold-induced NST came from an increased basal metabolism in skeletal muscle (Block 1994). The past decade has introduced one of the most intriguing methods to date with that includes employment of 2-[F^{18}] fluoro-2-desoxy-glucose (^{18}FDG) markers coupled with positron emission tomography (PET) and X-ray computed tomography (CT) scanning.

^{18}FDG and PET/CT Scanning

Discovery and Mechanism

To locate tumours, radioactive markers are often used to monitor cellular activity in nuclear medicine (Nedergaard, Bengtsson et al. 2007). As tumours are often glycolytic, ^{18}FDG is administer and acting like glucose, is taken up by various glycolytically active areas such as the heart, moving muscles, the brain, and tumours. First reported observations of "unusually symmetrical" masses in the shoulder and clavicular regions came in the early 1990's (Barrington and Maisey 1996, Engel, Steinert et al. 1996). As only PET scans were initially used, having a lower resolution, initial studies attributed these shapes to tense skeletal muscle and improper patient positioning. Linked PET and CT scanning eventually gave the resolution needed to conclusively determine that these areas of ^{18}FDG uptake were in fact BAT rather than skeletal muscle (Hany, Gharehpapagh et al. 2002, Minotti, Shah et al. 2004). Since then, dozens of studies have arisen and have applied various cooling protocols in estimating BAT activation, as will be discussed below (van der Lans, Wierts et al. 2014).

Cold Exposure Protocols and Results

Since 2009, there has been an eruption of studies applying ^{18}FDG and PET/CT scans to monitor BAT activation during cold exposure (Saito, Okamatsu-Ogura et al. 2009, Virtanen, Lidell et al. 2009, Yoneshiro, Aita et al. 2011, Ouellet, Labbe et al. 2012). Almost unanimously, these studies have demonstrated that when compared to uptake at normal room temperatures, mild cold exposure evokes increased ^{18}FDG uptake in the acromial-clavicular, supraclavicular, para-aortic, axillary, paravertebral and peri-renal regions of the body (Basu 2008, Sacks and Symonds 2013, van der Lans, Wierts et al. 2014). Studies dedicated to this acute mild cold exposure have revealed active BAT depots in 46 to 100% of their young healthy participants compared to 20 to 31% in the morbidly obese (Nedergaard, Bengtsson et al. 2007, van Marken Lichtenbelt, Vanhommerig et al. 2009). The large variations have been attributed to the large range of methodologies employed and current procedures cannot distinguish between the

previously discussed “classical” brown cells and the “inducible” beige cells seen in WAT (Seale, Bjork et al. 2008, Sharp, Shinoda et al. 2012). Beige adipocytes are white adipocytes that after extended cold exposure have been shown to undergo a “browning” effect, increasing their UCP-1 activity and begin acting like the metabolically active BAT (van der Lans, Hoeks et al. 2013, Dodd, Decherf et al. 2015). An in depth discussion on beige adipocytes is beyond the scope of this thesis but has been review extensively elsewhere (Lidell, Betz et al. 2013, Nedergaard and Cannon 2014).

Individual Variations of Human BAT Activity

There has been a high degree of inter-individual differences within PET/CT scan studies which have resulted in a vast array of estimates of BAT activation in adult humans (van der Lans, Wierts et al. 2014). They concluded that there are a number of factors that may influence the presence of BAT, one of which is body composition. Studies done with obese participants have yielded diminished BAT activation and have suggested that the cause lay with more insulation due to the thicker subcutaneous fat layers, blunting the afferent cold receptors (Wijers, Saris et al. 2010, Vijgen, Bouvy et al. 2011). Gender may also play a role, as males tend to require lower skin temperatures to induce shivering than females and some retrospective studies have demonstrated higher BAT prevalence in females (Au-Yong, Thorn et al. 2009, Cypess, Lehman et al. 2009). There have been conflicting reports recently as some studies demonstrated a similar BAT activation between sexes (van der Lans, Hoeks et al. 2013) while others showed females having a greater prevalence (Muzik, Mangner et al. 2012, Orava, Nuutila et al. 2013).

Further variation may result from the feeding status of individuals. As discussed earlier, a diet-induced thermogenesis may occur within BAT after a bout of feeding. Usually, participants are studied while fasting, however, some have shown that cold-exposed healthy males’ BAT activity was lower in fed individuals when compared with fasted individuals (Vrieze, Schopman et al. 2012). The contributions of BAT on diet-induced NST are uncertain. Finally, cold-adaption may play a role in inter-individual variations as studies have shown increased BAT in individuals living outdoors for most of their life (Huttunen, Hirvonen et al. 1981).

Fixed Versus Individualised Cooling Protocols

Studies with fixed cooling protocols were first used when looking at BAT activation with PET/CT scanning. Participants were exposed to ambient temperatures of 16°C for 2 h (van Marken Lichtenbelt, Vanhommerig et al. 2009) or with slightly higher ambient temperatures of ~19°C with leg cooling from ice (Saito, Okamatsu-Ogura et al. 2009, Yoneshiro, Aita et al. 2011) or chilled water (Virtanen, Lidell et al. 2009). These studies reported BAT prevalence in 46 to 100% of participants while the use of a cooling vest resulted in 100% BAT detection (Cypess, Chen et al. 2012).

Since then, some studies have adopted an individualised cooling protocol (van der Lans, Wierts et al. 2014). This was brought on by diminished BAT presence when fixed cooling methods were employed on the obese. Subjects are cooled until shivering and then temperature is increased 1–2°C above the temperature where the onset of shivering was observed. It is thought that maximal NST is obtained through this route and some studies have found a BAT prevalence of 94 to 100% in their participants using this method (Vosselman, van der Lans et al. 2012, van der Lans, Hoeks et al. 2013) while others have demonstrated BAT prevalence as low as 20 to 50% in participants when using individualised cooling protocols (Vijgen, Bouvy et al. 2011, Vijgen, Bouvy et al. 2012).

Air Versus Water Cooling Protocols

Brown adipose tissue activation has been induced by both air cooling (Saito, Okamatsu-Ogura et al. 2009, Yoneshiro, Aita et al. 2011, Vosselman, van der Lans et al. 2012) and liquid-perfused suits (Ouellet, Labbe et al. 2012, Blondin, Labbe et al. 2014). The absolute temperatures experienced by an individual differ between methods and this is based on the difference in media by which the cooling is occurring. Although the thermoneutral temperature zone is different, both methods have yielded similar metabolic responses (van der Lans, Wierts et al. 2014). This includes BAT detection in 94 to 100% of participants when using individualised protocols (Vosselman, van der Lans et al. 2012, van der Lans, Hoeks et al. 2013). Some argue that the ability of the liquid-perfused suits to tightly regulate temperature input is beneficial (Orava, Nuutila et al. 2011).

Chronic Cold Exposure Results

As acute cold exposure has yielded promising results (Saito, Okamatsu-Ogura et al. 2009, Yoneshiro, Aita et al. 2011) in BAT NST in response to mild cold exposure, so too have studies based on chronic cold exposure protocols (Yoneshiro, Aita et al. 2013, Blondin, Labbe et al. 2014) and have perhaps added some of the most interesting recent developments in BAT NST research. Yoneshiro, Aita et al. (2013) exposed participants to 17°C for 2 h every day for 6 weeks which resulted in significant increases in BAT activation of most participants after FDG analysis. Interestingly, participants who had previously demonstrated undetectable BAT activation at week 0 presented with active BAT after week 6 (Yoneshiro, Aita et al. 2013). Energy expenditure increased while body fat mass decreased over the 6 weeks, suggesting that BAT can be recruited and may contribute to an overall energy balance.

Blondin, Labbe et al. (2014) similarly demonstrated that the oxidative capacity as well as the volume of BAT increases with daily cold exposure in humans. A daily 2 h cold exposure of 10^{o}C water was circulated through a liquid conditioned suit. This occurred 5 consecutive days a week, for 4 consecutive weeks. Metabolic, shivering intensity and pattern, as well as PET/CT measurements were made prior to and following the cold acclimation (Blondin, Labbe et al. 2014). PET/CT analysis of ^{18}FDG uptake by BAT demonstrated a 45% increase in BAT volume following the 4-week cold acclimation. Using an acetate tracer, oxidative metabolism of BAT was shown to almost double after cold acclimation by the adult subjects (Blondin, Labbe et al. 2014). These findings support the conclusion that BAT is recruited, and increases its NST after repeated cold exposure.

Forward Looking Infrared Imaging

The uptake of ^{18}FDG in BAT coupled with PET/CT scanning has dominated the analysis of estimating BAT activation in adult humans for the past six years, with minimal direct biopsy studies completed. Disadvantages in using these techniques include the administration of radiopharmaceuticals, direct tissue sampling, and lack of real-time

analysis (Symonds, Henderson et al. 2012). These techniques can only be applied to a small sampling of subjects based on cost and availability alone. Need of a non-invasive method for monitoring BAT activity in larger populations is needed (van der Lans, Wierts et al. 2014). Recently, another method for estimating BAT activity has arisen which looks into the thermoregulatory response of BAT to mild cold exposure.

Thermal imaging using Forward Looking Infrared (FLIR®) cameras have been implemented and they may provide a new, efficient, non-invasive way of tracking BAT activity (Lee, Ho et al. 2011, Symonds, Henderson et al. 2012). Based on microcalorimetry studies, human rate of heat transfer in BAT has been estimated at ~300 $W \cdot kg^{-1}$ of BAT (Nedergaard, Cannon et al. 1977, Power 1989, Symonds, Henderson et al. 2012). This is compared to ~1 $W \cdot kg^{-1}$ in most other tissues. As the main function of BAT is to produce heat, finding a suitable method for monitoring heat transfer from BAT in adult humans seems only logical.

Symonds *et al.* (2012) used such a system in normal body mass index (BMI) individuals to assess the changes in temperature at the supraclavicular region of children, adolescent, and healthy adult subjects. The camera uses sensors to pick up infrared radiation that is emitted from a heat source and produces a topographical image of temperature levels. Using the FLIR® thermal camera imaging technique, and when exposed to mild cold conditions (16 – 20°C) coupled with a cool water bucket for feet placement, increases in surface temperature overlying BAT were greatest in children when compared to adolescents and adults (Symonds, Henderson et al. 2012). They also demonstrated the ability of BAT to be activated and deactivated during acute, mild cold exposure within 5 min. This suggests a greater importance of glucose uptake for BAT NST than previously hypothesised (Symonds, Henderson et al. 2012). Recently, a FLIR® thermal camera was used to determine the effectiveness of thermography in individuals with higher BMI's (Robinson, Ojha et al. 2014). A negative relationship between supraclavicular temperatures and BMI were observed with the smallest increase in temperature seen in children found above the 90^{th} percentile for BMI (Robinson, Ojha et al. 2014).

It should be noted that this method measures skin temperature and not heat release from BAT directly. Heat release by BAT is purposed with maintaining core body temperature and some argue that most of this heat release will be diverted to the centre of the body (van der Lans, Wierts et al. 2014). Some heat, however, is most likely diverted to the skin directly above BAT depots. At thermoneutral environmental temperatures, no changes were seen in supraclavicular skin temperatures while cooler ambient temperatures elicit increased skin temperatures (Symonds, Henderson et al. 2012). This suggests that infrared thermography may be used to show BAT activity in a qualitative way (van der Lans, Wierts et al. 2014).

Surface Heat Flux

Surface heat flux sensors have been employed in a variety of physiological studies in the past (Bell, Padbury et al. 1985, Mittleman and Mekjavic 1988, Niedermann, Psikuta et al. 2014) and measure the rate of heat transfer across a given body surface. This is done by measuring a temperature difference over a material, in this case skin, with a known thermal conductivity to quantify the rate of heat transfer from one side of the material to the other (Mittleman and Mekjavic 1988). Similar to Ohm's Law (Voltage = Current x Resistance), heat flux may be expressed in $W \cdot m^{-2}$ and is computed as:

$$\dot{Q} = \frac{\text{thermal potential difference}}{\text{thermal resistance}}$$

Early physiological applications for heat flux sensors were used to monitor heat loss on the skin following immersion in water (Cannon and Keatinge 1960, Kuehn 1978, Bell, Padbury et al. 1985) while extensive research utilising heat flux has also been done in studies concerned with heat loss in clothing apparel (Niedermann, Psikuta et al. 2014). To date, no studies have employed heat flux sensors to estimate BAT NST.

1.2. Rationale

The possible ties between BAT and human obesity have been suggested for decades (Arch, Ainsworth et al. 1984, Del Mar Gonzalez-Barroso, Ricquier et al. 2000). Initially ignited from animal studies looking at UCP-1 activation and UCP-1 ablated mice, there are many questions unresolved in the brown fat-obesity discussion as it applies to human energy expenditure. Cautions must be taken when conferring knowledge from animal models onto humans and more studies are warranted for human participants as the control of BAT NST is incompletely understood in humans. Whole body scan research utilising PET/CT scanning with radioactive markers have contributed to the discussion on human BAT activation, however, how afferent skin receptors contribute to the signalling of BAT activation during mild cold exposure are not well understood (Virtanen, Lidell et al. 2009, van Marken Lichtenbelt 2012, van der Lans, Wierts et al. 2014).

The results of Symonds, Henderson et al. (2012) and others (Lee, Ho et al. 2011, Robinson, Ojha et al. 2014) using FLIR® imaging cameras has opened up a new, non-invasive and easily available method of assessing BAT activity and NST responses to cold exposure. While infrared thermography has been employed on children of varying BMI's (Robinson, Ojha et al. 2014) little work has been done using this technique on adults of normal vs. larger BMI's and fat percentages and this may help in distinguishing differences in BAT activation between obese and non-obese individuals (van der Lans, Wierts et al. 2014). While infrared thermography will help to quantify temperatures over proposed BAT sites, heat flux measurements will aid in the estimation of BAT activity as well, giving a rate of heat transfer directly over BAT depots in the supraclavicular region. Electromyography permits one to assess the relative contributions of skeletal muscle activation during acute mild cold exposure, and when coupled with whole body indirect calorimetry, allows one to deduce any extra metabolic activity to BAT and NST.

Protocol exposure times in this study were chosen as prior pilot data displayed a stabilization of skin temperature at ~70 minutes after exposure (White and LeBlanc 1993). As well, acute BAT heat release at the supraclavicular area, as monitored by FLIR® thermal images, has been shown to reach maximum temperature change after 5

min in ambient temperatures of 19-20°C (Symonds, Henderson et al. 2012, Robinson, Ojha et al. 2014) and with a longer exposure, a time course of supraclavicular BAT temperatures in response to mild cold exposure in the obese and non-obese could be determined. Exposure to cooler temperatures would initiate the use of ST primarily. The current study's temperatures were chosen to introduce a primarily brown adipose derived thermogenic response in the absence of shivering as also described in other studies utilising FLIR® cameras (Symonds, Henderson et al. 2012, Robinson, Ojha et al. 2014).

To conclude, obese have demonstrated blunted metabolic responses to cold exposure, despite having lower skin and the same core temperatures as leaner individuals (Young 1988, White and LeBlanc 1993). In the absence of ST, it is unknown how this blunted metabolic response influences energy expenditure and substrate oxidation in the obese during cold exposure. Preliminary evidence suggests this may be due to a lower capacity to initiate NST, however, the physiology behind these differences in the obese and non-obese is incompletely understood.

1.3. Hypotheses

1.3.1. Study 1: Effect of Acute Mild Cold Exposure on Metabolic Responses and Substrate Oxidation in Obese Males

It was hypothesised that during acute mild cold exposure at 19°C, the obese relative to the non-obese would demonstrate a blunted NST metabolic response and lower mean heat flux despite having lower mean skin temperatures and the same core temperatures. It was also hypothesised that this response would be coupled with no difference in substrate oxidation rates.

1.3.2. Study 2: Effect of Acute Mild Cold Exposure on Non-Shivering Thermogenesis in Obese Males

Due to the paradoxical cooler skin temperatures seen in the obese in previous studies, it was hypothesised that relative to the non-obese, the obese would

demonstrate a reduced BAT NST at the supraclavicular fossae including a blunted metabolic response when normalised for lean body mass. This would correspond to, it was hypothesised, lower mean skin temperatures and heat flux over these supraclavicular fossae in the obese when exposed to mild cold. It was also hypothesised that this would be in concert with similar and minimal skeletal muscle activation as assessed by surface EMG.

Chapter 2.

Effect of Acute Mild Cold Exposure on Metabolic Responses and Substrate Oxidation Rates in Obese Males

2.1. Introduction

The fundamental requirements in order for humans to function in the cold are based on a delicate balance between rates of heat gain and heat loss (Buskirk 1963). Morphologically, humans possess a high capacity for heat loss and while this is advantageous in warmer conditions, they require additional metabolic responses to be activated in the cold to stave off potential lowering of core temperatures and hypothermia (Girling 1964).

Heat gain is a by-product of oxidation of substrates through exothermic reactions in cells throughout the body (Blondin, Tingelstad et al. 2014). When exercise or leaving the cold is not possible, the oxidation of these substrates is essential in maintaining sufficient thermogenesis to regulate core temperature. To sustain what is now thought to be a combined effect of ST and NST during cold exposure (Blondin, Tingelstad et al. 2014), each of protein, CHO, and FAT are oxidised to fuel thermogenesis (Haman 2006).

Over 30 years ago, Wang (1980, 1981) first hypothesised that the main physiological limitations to cold-induced thermogenesis in animals was related to the supply of metabolic fuels. It was later reasoned that humans would exhibit similar characteristics of limited heat gain due to substrate availability, as was shown to be evident for animals (Wang, Man et al. 1987). However, later studies demonstrated mixed results and the evidence supported that substrate availability may not alter overall

heat gain when differing amounts of CHO were consumed before cold exposure (Vallerand, Tikuisis et al. 1993). Subsequently, differences in fuel utilisation were examined, especially between CHO and FAT which have been shown to be the most prevalent substrates used for thermogenesis during cold exposure (Blondin, Tingelstad et al. 2014).

Carbohydrates, while only accounting for ~1% of total human energy stores, can contribute to ~20% to 80% of all heat gain in the cold (Haman 2006). Lipids, important in low-intensity exercise below ~50% to 60% of maximal power, have also been shown to play an important roll as an oxidisable fuel in mild cold exposure and lower rates of ST (Haman, Peronnet et al. 2005). While the contributions of FAT oxidation in mild cold temperatures and at low rates of ST seems to plateau at ~140 $mg \cdot kg^{-1} \cdot h^{-1}$, CHO oxidation rates in these conditions have an incredible variability that changes in response to exercise, feeding status and glycogen reserves (Haman, Legault et al. 2004, Haman, Peronnet et al. 2005). While little work has been done on the differences in obese and non-obese substrate oxidation, it is suggested that the main contribution to fuel selection is found in the relative availability of substrate reserves (Haman, Peronnet et al. 2002).

In addition to substrate oxidation during cold exposure, adiposity may contribute to changes in metabolic responses in the cold (Leblanc 1954). Initial observations found that women tended to have lower skin temperatures when exposed to the cold, possibly due to their increased levels of subcutaneous fat that insulates their skin from the heat generating core tissues (Hardy 1941). This was further confirmed with evidence that showed people with greater skinfolds, indicative of a greater subcutaneous fat, had lower mean skin temperatures (Leblanc 1954). Further testing in animals demonstrated the increase in metabolic responses to cooling of the skin while core temperatures remained steady (Iggo 1969, Hensel 1981, Kuhnen and Jessen 1988) and this suggested contributions control inputs from skin thermoreceptors and afferent cold sensitive neurons.

To thermoregulate in the cold there is the obvious need for increased substrate oxidation rates to fuel heat gain. In mild cold however, in the absence of ST, there

appears to be a paradoxical metabolic response based on body composition. Leaner individuals tend to have a greater metabolic response to the cold, including higher skin temperatures and the same core temperatures, relative to obese (White and LeBlanc 1993). This suggests those who tend to gain weight have a lower normalised rate of energy expenditure when exposed to cold than those who tend to be exempt from gaining weight or gain less weight (Tikuisis, Bell et al. 1991).

It was hypothesised that during acute mild cold exposure at 19°C, the obese relative to the non-obese would demonstrate a blunted NST metabolic response and lower mean heat flux despite having lower mean skin temperatures and the same core temperatures. It was also hypothesised that this response would be coupled with no difference in substrate oxidation rates between the non-obese and obese.

2.2. Methods

2.2.1. Ethics

Approval for this study was obtained through the Simon Fraser University Office of Research Ethics. All participants were provided the option of removing themselves from the study at any point without prejudice and without reason.

2.2.2. Participants

Each participant was brought into the lab for a detailed orientation session. This included familiarisation with the equipment, study protocol, informed consent and health screen questionnaire. Each participant was then given a minimum of a 24 h reflection period. Upon agreeing to participate in the study, the informed consent form and health screen questionnaire were reviewed and signed by the participant.

Sixteen male participants volunteered for the study. Participants were initially screened using BMI and skinfolds. Skinfolds, height and weight were collected according to the protocols outlined by Marfell-Jones (1991), and % body fat estimates

from skinfolds followed the 4-component model laid out by Peterson *et al.* (2003) and was applied to the equation:

$$\% \text{ Body Fat} = 20.95 + (\text{age} \times 0.12) - (\text{height} \times 0.12) + (\text{sum4} \times 0.43) - (\text{sum4}^2 \times 0.002)$$

where age is in yr, height is in cm, and sum4 is the sum of triceps, subscapular, suprailiac, and midthigh skinfold thicknesses in mm (Peterson, Czerwinski et al. 2003). Percent body fat was further assessed using Dual-energy X-ray absorptiometry (DEXA) scans (Hologic Discovery Ci/Wn 010 0575) (Figure A.1).

Participants were then separated into two groups (n = 8, each group) of comparison based on BMI, skinfold, and DEXA percent fat estimates: non-obese (BMI 20-25; % fat < 24) and obese (BMI > 30; % fat > 24.5). BMI was only used as an initial screening measure while % fat was used in the defining of groups. The non-obese had a mean age of 24 yr (0.9), a height of 1.80 m (0.11), a weight of 74.0 kg (10.6), a BMI of 22.9 $kg \cdot m^{-2}$ (1.4), and a % body fat of 16.3% (4.0). The obese had a mean (SD) age of 25 yr (3.3), a height of 1.82 m (0.08), a weight of 125.4 kg (16.4), a BMI of 38 $kg \cdot m^{-2}$ (6.9), and a % body fat of 32.2% (7.7) (Table 2.1).

A power calculation was used to determine the sample size required to have a power of 80% and a significance of 0.05. The sample size varied depending on the variable. The number of volunteers required was found to be a minimum of 8 per group in order to find a significant result, if it existed, in all variables of interest. The variables employed for this power calculation were mean skin temperature ($_{M}T_{SK}$), mean heat flux ($_{M}HF$), and mean VO_2.

Using pilot study data of $_{M}T_{SK}$, a sample size of 4 participants per group at 27°C and 6 participants per group at 19°C were required. This was found with differences to detect set at 3°C and a standard deviation between the two groups of 1.03°C at 27°C and 1.67°C at 19°C.

Using pilot study data of $_{M}HF$, a sample size of 4 participants per group at 27°C and 6 participants per group at 19°C were required. This was found with differences to

detect set at 20 $W \cdot m^{-2}$ and a standard deviation between the two groups of 5.94 $W \cdot m^{-2}$ at 27°C and 10.44 $W \cdot m^{-2}$ at 19°C.

Using pilot study data of VO_2, a sample size of 6 participants per group at 27°C and 7 participants per group at 19°C were required. This was found with differences to detect set at 0.1 $L \cdot min^{-1}$ and a standard deviation between the two groups of 0.06 $L \cdot min^{-1}$ at both 27°C and 19°C.

2.2.3. Instrumentation

Body Temperature and Heat Flux

Skin temperature (T_{SK}) and surface HF were measured at seven sites using thermocouples embedded in the surface of heat flux discs (Thermonetics, California, USA). These sites included the upper lateral arm (T_{UA}, HF_{UA}), posterior shoulder (T_{PS}, HF_{PS}), chest (T_{CH}, HF_{CH}), abdomen (T_{AB}, HF_{AB}), thigh (T_{TH}, HF_{TH}), and one on each of the supraclavicular fossa (T_{SC}, HF_{SC}) (Table A.1). Unweighted ${}_{M}HF$ and unweighted ${}_{M}T_{SK}$ were also calculated. Heat flux discs were attached to the skin using hypoallergenic tape (Tanspore, 3M, St. Paul, MN, USA). A water bath (VWR Int, Model 1196, West Chester, Penn, USA) monitored by a platinum thermometer (Fisher Scientific, Nepean, ON, Canada) was used to calibrate the thermocouples within the heat flux discs. The heat flux portion of the discs were calibrated using a copper encased water bath similar to that used by Nuckols and Piantadosi (1980) and Mittleman (1987).

Core temperature (T_{RE}) was monitored throughout the trial using flexible 30 cm rectal thermistors inserted 15 cm (DeRoyal TN, USA). Similar to the skin thermocouples, the rectal thermistors were calibrated using a water bath (VWR Int, Model 1196, West Chester, Penn, USA) monitored by a platinum thermometer (Fisher Scientific, Nepean, ON, Canada).

Metabolic and Ventilatory Variables

While seated comfortably, each participant was asked to breathe through a low resistance mouthpiece connected to a one-way valve allowing expired air to move through a 3.8 cm diameter tube. The respiratory tubing was attached to a two-way mass

flow sensor (Sensormedics, Yorba Linda, CA, USA). Each participant wore a nose clip to ensure all exhaled gas was collected through the mouthpiece and mass flow sensor.

The mass flow sensor was connected to a breath-by-breath metabolic cart (VMAX 229, Sensormedics, Yorba Linda, CA, USA), which was used to measure absolute rate of oxygen consumption (VO_{2ABS}), absolute rate of expired carbon dioxide (VCO_{2ABS}), normalised rate of oxygen consumption (VO_{2NORM}), normalised volume of consumed carbon dioxide (VCO_{2NORM}), and non-protein respiratory exchange ratio (RER).

The calibration of gas analysers in the metabolic cart were completed with room air and with compressed gas tanks with mixtures of 26% O_2, balance N_2; and 16% O_2, 4% CO_2, and balance N_2. The two-way mass flow sensor was calibrated with a 3 L syringe.

Electromyograms of Skeletal Muscles

Electromyograms (Bagnoli-8 Delsys®, Natick, MA, USA) were measured at 5 sites representing the trunk and limbs and were chosen to represent the largest possible fraction of total muscle mass of the body (>90%) (Bell, Tikuisis et al. 1992, Haman, Legault et al. 2004). These sites included the trapezius (TR), pectoralis major (PE), biceps brachii (BI), rectus femoris (RF), and gastrocnemius (GA) (Bell, Tikuisis et al. 1992).

Prior to the experiments, maximal EMG signals from each muscle group were determined from maximal voluntary contractions (MVC). Maximum voluntary contractions were obtained utilising isometric movements as described previously (Bell, Tikuisis et al. 1992, Peier, Moqrich et al. 2002, Haman, Legault et al. 2004). The following procedures were used to identify the maximal EMG signal for each muscle group: 1) for TR, participants sat upright with their arm straight against the body. Grasped in the hand participants raised their shoulders trying to elevate against the cord. 2) For PE, participants sat upright with their arm extended away from the body at 90^{o}. Participants performed a horizontal shoulder flexion against the cord. 3) For BI, participants started with their arm fully extended at their side. Participants held the cord

in a supinated hand and maximally flexed at the elbow joint. 4) For RF, MVC was determined while participants sat on a chair in an upright position. The cord was placed slightly above the ankle and the participant was asked to perform a maximal knee extension against the weight. 5) For GA, the participant laid down, the cord was placed on the foot and the participant then performed a maximal ankle flexion against the weight. All movements were completed as close to the seated experimental position as possible. Delsys® EMG systems are calibrated using standard calibration services at their main offices.

Thermal Imaging

Thermal imaging of the supraclavicular region ($FLIR_{Sc}$) was carried out using a Forward Looking Infrared (FLIR®) camera (FLIR T650sc, FLIR Systems Inc., Burlington, ON, CAN). The thermal imaging camera was set 1 m away from the seated participant and was stationed on a large tripod and raised to a height that gave an angle of 20° from the horizontal of the participant's supraclavicular fossae. This ensured that no reflective radiation from the skin would occur. The thermal imaging camera was selected based on the high resolution and accuracy when compared to other cameras used in various studies (Table A.2).

To ensure consistent and comparable measurements using the thermal imaging camera, all participants remained perfectly still throughout the protocol while seated comfortably with a straight back and neck, relaxed shoulders and adducted arms. FLIR® thermal imaging cameras are calibrated using standard calibration services located at their main offices (FLIR 2014).

2.2.4. Data Acquisition

Cardiorespiratory and Temperature Variables

Cardiorespiratory variables were sampled and recorded at 20 s intervals with a VMAX 229 metabolic cart (Sensormedics, Yorba Linda, CA, USA). Body temperature was assessed with thermocouples embedded in heat flux transducers and were sampled at a rate of 40 Hz using LabVIEW software (Ver. 7.1, National Instruments, Austin, TX, USA) and recorded every 20 s.

Electromyograms of Skeletal Muscle

Electromyograms were sampled at 1,000 Hz using the Bagnoli-8 Delsys Systems® amplifier. Measurements were made using parallel-bar EMG sensors (DE-2.1 Differential EMG Sensor) placed on the surface of the skin. The signals recorded to .txt files at a rate of 1,000 Hz. Referencing was done using a reusable reference electrode (Dermatode®, Nuland, BR, The Netherlands).

Using a custom LabVIEW software (Ver. 8.6, National Instruments, Austin, TX, USA), maximal RMS values from MVC's were compared to exposure data. EMG signals were filtered to remove 60 Hz noise (and associated harmonics).

Thermal Imaging

The thermal imaging camera was employed to capture sequential images in .jpeg format every 10 min during the exposure and these files were then processed and analysed using the FLIR® Quick Report 2.1 software system. Using the box area tool, a region of interest at the supraclavicular area for each participant was defined and temperature data were exported into Microsoft Excel 2010. The supraclavicular regions were bordered using the anatomical landmarks of the superior border of the clavicles and the sternocleidomastoid muscle inferiorly (Symonds, Henderson et al. 2012, Robinson, Ojha et al. 2014). 3-D plot graphs in Microsoft Excel 2010 were also employed to measure the thermal topography at the supraclavicular regions.

2.2.5. Protocol

Each participant participated in a single session during the testing period from 8 November to 11 December, and all sessions were conducted at least 6 hours fasted to remove any confounding, food-induced, thermogenic effects. The participant was asked to refrain from any consumption of caffeine, drugs, alcohol, and intense exercise in the 12 hours leading up to the study. All sessions began between 8 am and 10 am.

Following instrumentation, each volunteer sat comfortably in a chair placed in the centre of a climatic chamber (Tenney Engineering Inc., Union, NJ, USA). Each volunteer participated in one trial within the climatic chamber which included exposure to

90 min of baseline data collection at 27°C, followed by a cold exposure of 90 min at 19°C. Enclosure temperatures during the 27°C exposure remained at 27.1°C (0.07) and at 18.9°C (0.49) during the 19°C exposure (Figure 2.1).

2.2.6. Statistical Analysis

The main effect of Group (Non-obese, Obese), Ambient Temperature (27, 19°C) and their interaction (Group x Ambient Temperature) were examined employing a 2-Factor Mixed Model ANOVA using the SPSS software program (Version 22, Surrey, UK) across all 90 min of exposure. Group was set as a non-repeated between-subjects factor while Ambient Temperature was set as the repeated within-subjects factor. Factors analysed in this study were VO_{2NORM}, VO_{2ABS}, RER, ${}_{M}T_{SK}$, ${}_{M}HF$, T_{RE}, CHO and FAT and delta values for each.

A two-tailed, unpaired t-test was used to compare means if there was a significant interaction from the ANOVA model. The level of significance was set at 0.05.

Files were averaged using a custom LabVIEW program and exported into .txt files. Substrate oxidation variables CHO and FAT were calculated using proposed equations based on reviewed literature from (Jeukendrup and Wallis 2005). Delta values were calculated by subtracting the initial 27°C value of each participant from their mean value for each time point.

2.3. Results

Both ${}_{M}T_{SK}$ ($F = 17.33$, $p < 0.05$) and $\Delta_{M}T_{SK}$ ($F = 10.96$, $p < 0.05$) had a significant Group x Ambient Temperature interaction. Mean T_{SK} was different between the two groups at 27°C with obese averaging 33.02°C (1.11) and non-obese averaging 33.71°C (0.94) ($p < 0.05$). For the 19°C exposure, the difference between groups doubled with obese having a mean T_{SK} of 29.12°C (1.72) while the non-obese averaged 30.72°C (1.63) ($p < 0.05$). At 27°C the obese had a $\Delta_{M}T_{SK}$ of 0.28°C (0.37) while the non-obese had a $\Delta_{M}T_{SK}$ -0.09°C (0.30) ($p < 0.05$). The $\Delta_{M}T_{SK}$ remained significantly different at

19°C with obese having a greater change to -3.63°C (0.73) and non-obese decreasing to -3.09°C (0.77) ($p < 0.05$) (Table 2.2, Figure 2.2).

Both $_{M}$HF ($F = 11.34$, $p < 0.05$) and Δ_{M}HF ($F = 11.47$, $p < 0.05$) had a significant Group x Ambient Temperature interaction. Mean HF was different between the two groups at 27°C with obese averaging 58.84 $W \cdot m^{-2}$ (6.34) and non-obese averaging 66.96 $W \cdot m^{-2}$ (5.54) ($p < 0.05$) (Figure 2.3). For the 19°C exposure, the difference increased resulting in an obese $_{M}$HF of 80.46 $W \cdot m^{-2}$ (7.56) and a non-obese $_{M}$HF of 97.50 $W \cdot m^{-2}$ (13.32) ($p < 0.05$). At 27°C, the obese Δ_{M}HF was minimal at -0.66 $W \cdot m^{-2}$ (3.15) while the non-obese had a Δ_{M}HF of -4.24 $W \cdot m^{-2}$ (5.20) ($p < 0.05$). This significant difference grew at 19°C to a Δ_{M}HF 20.95 $W \cdot m^{-2}$ (7.56) in the obese compared to a greater Δ_{M}HF in the non-obese of 26.30 $W \cdot m^{-2}$ (7.21) ($p < 0.05$) (Table 2.2, Figure 2.3).

There was no significant Group x Ambient Temperature interaction for T_{RE} ($F = 0.44$, $p = 0.52$) or ΔT_{RE} ($F = 0.44$, $p = 0.54$) (Figure 2.4). Mean T_{RE} however, was different only at 27°C averaging 37.15°C (0.22) for the obese and 36.75°C (0.45) for the non-obese ($p < 0.05$) (Table 2.2, Figure 2.4).

Mean VO_{2ABS} ($F = 7.68$, $p < 0.05$), ΔVO_{2ABS} ($F = 7.68$, $p < 0.05$), VO_{2NORM} ($F = 17.56$, $p < 0.05$) and ΔVO_{2NORM} ($F = 17.57$, $p < 0.001$) all had significant Group x Ambient Temperature interactions (Table 2.2, Figure 2.5). Obese mean VO_{2ABS} increased from 0.30 $L \cdot min^{-1}$ (0.06) at 27°C to 0.32 $L \cdot min^{-1}$ (0.05) at 19°C compared to a significantly greater increase in the non-obese from 0.24 $L \cdot min^{-1}$ (0.05) at 27°C to 0.31 $L \cdot min^{-1}$ (0.07) at 19°C ($p < 0.05$). The ΔVO_{2ABS} values saw the obese increase slightly from -0.03 $L \cdot min^{-1}$ (0.06) at 27°C to -0.01 $L \cdot min^{-1}$ (0.08) at 19°C compared to a significantly greater increase in the non-obese from -0.03 $L \cdot min^{-1}$ (0.03) to 0.03 $L \cdot min^{-1}$ (0.05) ($p < 0.05$). The VO_{2NORM} in the obese remained relatively unchanged with a slight increase from 2.40 $mL \cdot min^{-1} \cdot kg^{-1}$ (0.05) at 27°C to 2.56 $mL \cdot min^{-1} kg^{-1}$ (0.05) at 19°C ($p < 0.05$) while the non-obese increased significantly from 3.22 $mL \cdot min^{-1} \cdot kg^{-1}$ (0.05) at 27°C to 4.18 $mL \cdot min^{-1} \cdot kg^{-1}$ (0.05) ($p < 0.001$) at 19°C. The ΔVO_{2NORM} increased from -0.22 $mL \cdot min^{-1} \cdot kg^{-1}$ (0.52) at 27°C in the obese to -0.05 $mL \cdot min^{-1} \cdot kg^{-1}$ (0.68) at 19°C compared to an increase from -0.48 $mL \cdot min^{-1} kg^{-1}$ (0.47) at 27°C to 0.47 $mL \cdot min^{-1} \cdot kg^{-1}$ (0.70) at 19°C ($p < 0.05$) in the non-obese (Table 2.2, Figure 2.6). Non-protein RER ($F = 0.36$, $p =$

0.56) did not have a significant interaction between the two groups at 27 and 19°C (Table 2.2, Figure 2.7).

The obese and non-obese saw no significant interaction in CHO ($F = 2.50$, $p = 0.14$) or FAT ($F = 0.57$, $p = 0.46$) (Figures 2.8, 2.9, 2.10). This was echoed by no significant Group x Ambient Temperature interaction for ΔCHO ($F = 2.68$, $p = 0.12$) or for ΔFAT ($F = 0.36$, $p = 0.36$) (Table 2.2, Figure 2.8, 2.9). Regression lines were fitted to ${}_{M}T_{SK}$ against all three physique variables including percent fat from DEXA, sum of 9 skinfolds (S9SF), and weight. All three showed a trend that larger individuals demonstrated lower ${}_{M}T_{SK}$ at 19°C: percent fat ($r^2 = 0.72$, $p < 0.001$), S9SF ($r^2 = 0.67$, $p < 0.05$), and weight ($r^2 = 0.73$, $p < 0.05$) (Figure 2.10).

2.4. Discussion

Novel Findings

Our results show that while having lower ${}_{M}T_{SK}$ and corresponding lower ${}_{M}HF$, the obese relative to non-obese demonstrate a paradoxical blunted metabolic response to mild cold exposure in absolute values and when normalised for body weight. This was seen in significant interactions of both VO_{2ABS} and VO_{2NORM} where a larger increase in the non-obese was seen at 19°C when compared to the obese. Demonstrated by regression equations as well, individuals with greater weight and the associated greater % body fat and S9SF had significantly lower skin temperatures at 19°C.

Substrate oxidation rates for both CHO and FAT were not statistically different between the two groups at 27 and 19°C. FAT remained at ~0.10 – 0.17 $g \cdot min^{-1}$ in both groups, increasing slightly during cold exposure. This was compared to CHO of around 0.05 – 0.09 $g \cdot min^{-1}$, which remained similar throughout the two exposures. This was further supported by non-protein RER rates that remained constant around 0.70, suggesting a primarily FAT based fuel source.

Comparison to Literature and Underlying Mechanisms

The lower skin temperatures exhibited by the obese seems to be accounted for by their additional adiposity as previous research suggests (Leblanc 1954, White and LeBlanc 1993). Body fat has been identified as a major insulating factor and acts to modify the impact of cold on the body (Buskirk 1963). Early studies in both cold air (Leblanc 1954, Buskirk 1963) and cold water (Cannon and Keatinge 1960, Keatinge 1960) confirmed that body composition is related to overall body cooling, presumably by buffering the stimulatory impact of cold through insulative protection once peripheral vasoconstriction has occurred in the overlying skin.

Studies done on animals (Kuhnen and Jessen 1988) and humans of normal weight (Cannon and Keatinge 1960) demonstrate the direct relationship of decreasing skin temperature with an increasing metabolic rate, all while keeping a steady core temperature. This is not seen in the obese subjects in this study, and others (White, Ross et al. 1992, White and LeBlanc 1993), and may be caused by some alteration in their peripheral cold receptors transduction of a cold environmental stimulus.

Cold induced vasoconstriction increases blood pressure, blood viscosity and decreases blood plasma volume and typically increases cardiac work by an individual (Rintamaki 2007). The paradoxical low metabolic response by the obese is intriguing. These results support previously hypothesised theories of calorie saving and reduced energy expenditure by obese individuals when exposed to the cold (Buskirk 1963). Although exposure to cold temperatures in daily life may be infrequent, obese subjects seem to have a built in insulation that may contribute to their conservation of energy rather than dissipate it. Failing to metabolically react to the cold air, or at a much lower rate than normal-weight individuals, could contribute to their net energy saving and positive energy balance.

To date, evidence suggests that adult humans are able to sustain increased whole body heat gain in response to varying cold exposures with a wide range of metabolic fuels (Blondin, Tingelstad et al. 2014). When one of the three fuel sources that supply cells with the capacity to aid in thermogenic processes is diminished or

depleted, others are able to compensate to maintain ATP production at a consistent thermogenic rate (Blondin, Tingelstad et al. 2014).

Carbohydrates and FAT are the most important fuel sources during cold exposure and have been shown to display a great deal of variability between individuals and studies (Vallerand and Jacobs 1990, Vallerand and Jacobs 1992, Vallerand, Tikuisis et al. 1993, Haman, Peronnet et al. 2005, Haman 2006). When exposed to mild (Haman, Legault et al. 2004) or moderate cold exposures (Martineau and Jacobs 1989), decreasing the size of glycogen reserves caused a large shift from CHO to FAT use. Despite large shifts in substrate oxidation, core and skin temperatures remained relatively unchanged. These studies demonstrate the extreme variability of CHO oxidation in particular, and could explain this studies insignificant differences in CHO rates. While an attempt was made to control for any dietary or post-exercise influences, the current literature demonstrates the tremendous adaptability of the human body to control heat gain based on differing CHO rates of oxidation (Martineau and Jacobs 1989, Haman, Legault et al. 2004, Haman 2006).

While this could explain the increased variability in CHO oxidation rates in our participants, the slow increase in FAT utilisation when exposed to the mild cold seems to be supported by the literature (Haman, Peronnet et al. 2005). Lipids are by far the largest and most complete energy stores in the human body and the size of the reserves and total energy used by FAT can be determined by a person's level of adiposity (Haman, Peronnet et al. 2004, Blondin, Tingelstad et al. 2014). Also, relative contributions of FAT can dominate oxidation rates at more moderate levels of cold and decreases in importance as ST is recruited (Haman, Peronnet et al. 2005). This could explain our participant's increased usage of FAT after 90 min exposure to 19°C. The selected research above demonstrates the influences of energy reserves and nutritional status on CHO and FAT oxidation rates during cold exposure. While some studies have looked at the differences between participants of differing adiposities, more research is needed on these two groups at more moderate levels of cold exposure, particularly FAT oxidation rates in the obese.

Future Directions and Limitations

Much work is still needed to fully understand the effects of various macronutrients needed for extended cold exposures, particularly in comparing obese to non-obese adults humans. This study was limited to estimates of CHO and FAT from metabolic responses in fasted participants, however, future studies looking at substrate oxidation rates in the obese versus non-obese may choose to identify the sources of CHO, whether from blood glucose or muscle glycogen, as well as account for the contribution of proteins (Blondin, Tingelstad et al. 2014).

Conclusion

It was hypothesised that the obese would demonstrate blunted NST metabolic responses and lower mean heat flux to the cold while having lower mean skin temperatures and the same core temperatures. Our data supported this hypothesis, with obese participants possibly adding to their positive energy balance when exposed to mild cold. It was hypothesised that when exposed to 19°C ambient temperatures, obese relative to non-obese participants would demonstrate no difference in oxidation of fuels. FAT and CHO oxidation rates were not different between groups in either the 27 or 19°C exposures.

2.5. Tables

Table 2.1. Summary of participants' age (y), height (m), weight (kg), BMI ($kg \cdot m^{-2}$), and percent body fat by DEXA (%).

Group	Volunteer Code	Age (y)	Height (m)	Weight (kg)	BMI ($kg \cdot m^{-2}$)	Percent Body Fat (%)
Non-obese	1	24	1.78	68.1	21.5	16.9
	2	24	1.70	72.6	25.1	18.0
	3	24	1.75	71.4	23.3	23.5
	4	25	1.84	74.8	22.1	16.2
	5	23	1.98	91.9	23.4	18.6
	6	22	1.85	80.7	23.6	11.5
	14	23	1.63	55.0	20.7	11.2
	16	23	1.83	77.8	23.4	14.2
Mean		24	1.80	74.0	22.9	16.3
(SD)		(0.9)	(0.11)	(10.6)	(1.4)	(4.0)
Obese	7	23	1.81	152.9	46.7	31.8
	8	25	1.65	130.8	48.0	46.3
	9	23	1.82	120.8	36.5	26.2
	10	31	1.79	109.0	34.0	32.3
	11	20	1.92	114.2	31.0	31.7
	12	23	1.85	146.1	42.7	40.3
	13	24	1.88	111.5	31.5	24.5
	15	27	1.88	117.9	33.4	24.6
Mean		25	1.82	125.4	38.0	32.2
(SD)		(3.3)	(0.08)	(16.4)	(6.9)	(7.7)

Table 2.2. Mean (SD) and corresponding delta (Δ) values for unweighted surface heat flux ($_{M}$HF, W•m^{-2}), unweighted surface skin temperature ($_{M}T_{SK}$, °C), rectal temperature (T_{RE}, °C), rate of oxygen consumption (VO_{2ABS}, L•min^{-1}), rate of oxygen consumption (VO_{2NORM}, mL•min^{-1}•kg^{-1}), non-protein respiratory exchange ratio (RER), carbohydrate oxidation rate (CHO, g•min^{-1}), and lipid oxidation rate (FAT, g•min^{-1}) during 90 min exposures at both 27 and 19°C in the obese and non-obese. t-test comparisons are between groups at each ambient temperature. Significance: ‡ = $p < 0.05$; ϕ = $p < 0.001$.

	Ambient Temperature			
	27°C		**19°C**	
	Obese	Non-obese	Obese	Non-obese
$_{M}$HF (W•m^{-2})	58.84 (6.34)‡	66.96 (5.54)	80.46 (7.56)‡	97.50 (13.32)
Δ_{M}HF (W•m^{-2})	-0.66 (3.15)‡	-4.24 (5.20)	20.95 (7.85)‡	26.30 (7.21)
$_{M}T_{SK}$ (°C)	33.02 (1.11)‡	33.71 (0.94)	29.12 (1.72)‡	30.72 (1.63)
$\Delta_{M}T_{SK}$ (°C)	0.28 (0.37)‡	-0.09 (0.30)	-3.63 (0.73)‡	-3.09 (0.77)
T_{RE} (°C)	37.15 (0.22)‡	36.75 (0.45)	37.03 (0.16)	36.53 (0.65)
ΔT_{RE} (°C)	-0.14 (0.16)	-0.19 (0.17)	-0.25 (0.23)	-0.41 (0.44)
VO_{2ABS} (L•min^{-1})	0.30 (0.06)‡	0.24 (0.05)	0.32 (0.05)‡	0.31 (0.07)
ΔVO_{2ABS} (L•min^{-1})	-0.03 (0.06)‡	-0.03 (0.05)	-0.01 (0.08)‡	0.03 (0.05)
VO_{2NORM} (mL•min^{-1}•kg^{-1})	2.40 (0.05)ϕ	3.22 (0.05)	2.56 (0.05)ϕ	4.18 (0.05)
ΔVO_{2NORM} (mL•min^{-1}•kg^{-1})	-0.22 (0.52)‡	-0.48 (0.47)	-0.05 (0.68)ϕ	0.47 (0.70)
RER	0.73 (0.05)	0.76 (0.05)	0.70 (0.05)	0.74 (0.05)
CHO (g•min^{-1})	0.06 (0.05)	0.09 (0.10)	0.05 (0.06)	0.09 (0.10)
ΔCHO (g•min^{-1})	0.00 (0.06)	-0.03 (0.05)	-0.01 (0.07)	-0.01 (0.10)
FAT (g•min^{-1})	0.14 (0.05)	0.10 (0.04)	0.17 (0.06)	0.14 (0.06)
ΔFAT (g•min^{-1})	-0.01 (0.04)	0.00 (0.03)	0.01 (0.05)	0.04 (0.05)

2.6. Figures

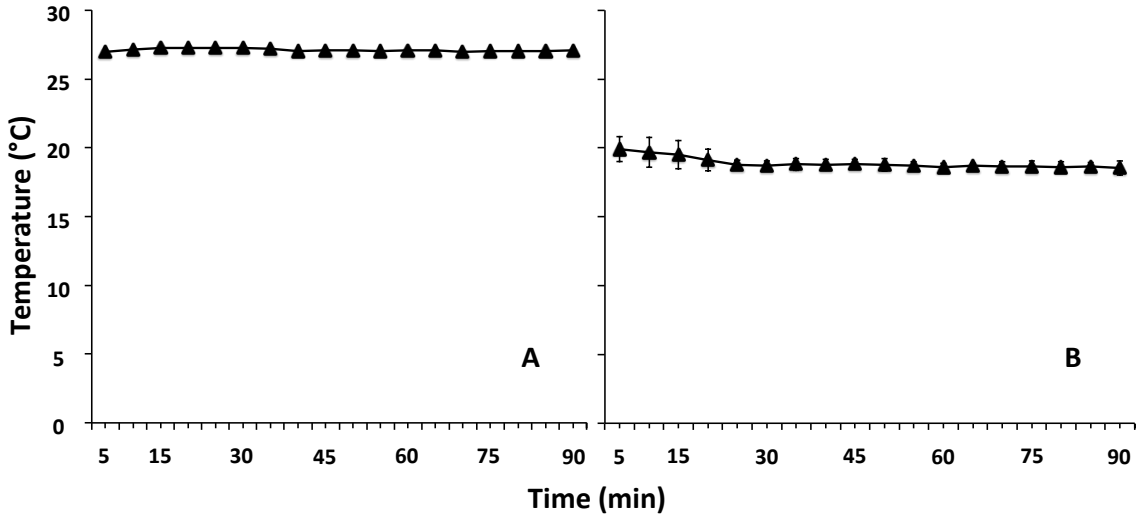

Figure 2.1. Climatic chamber temperatures (°C) during 90 min at A) 27°C followed by 90 min at B) 19°C. Values are mean ± SD.

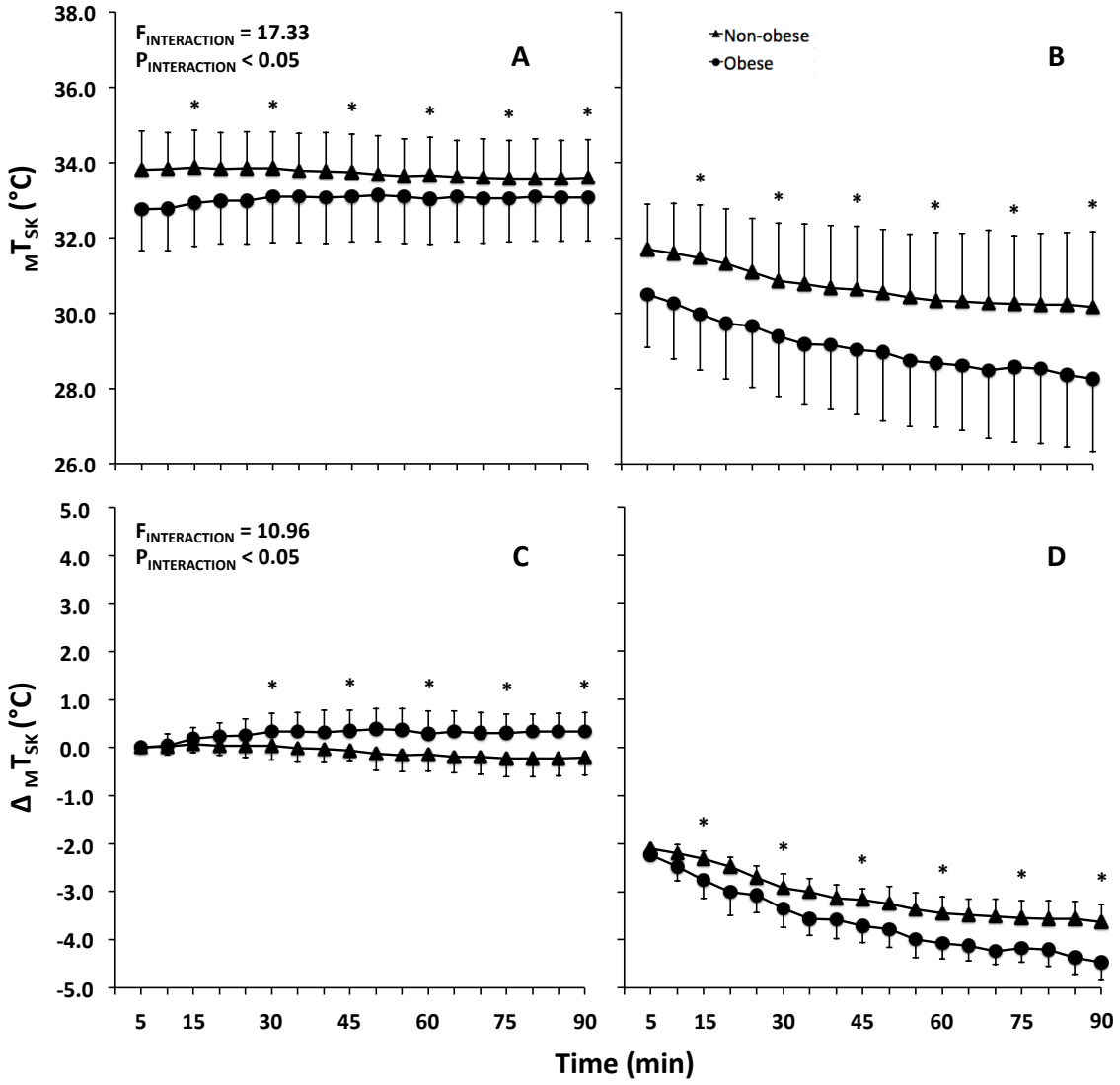

Figure 2.2. Obese and Non-obese mean skin temperatures ($_MT_{SK}$, °C) during A) 90 min exposure at 27°C, followed by B) 90 min at 19°C; and delta mean skin temperature ($\Delta\ _MT_{SK}$, °C) during C) 90 min exposure at 27°C, followed by B) 90 min at 19°C. Δ Values calculated by subtracting each time point value by initial 27°C value. Values are mean ± SD. Significance: * < 0.05.

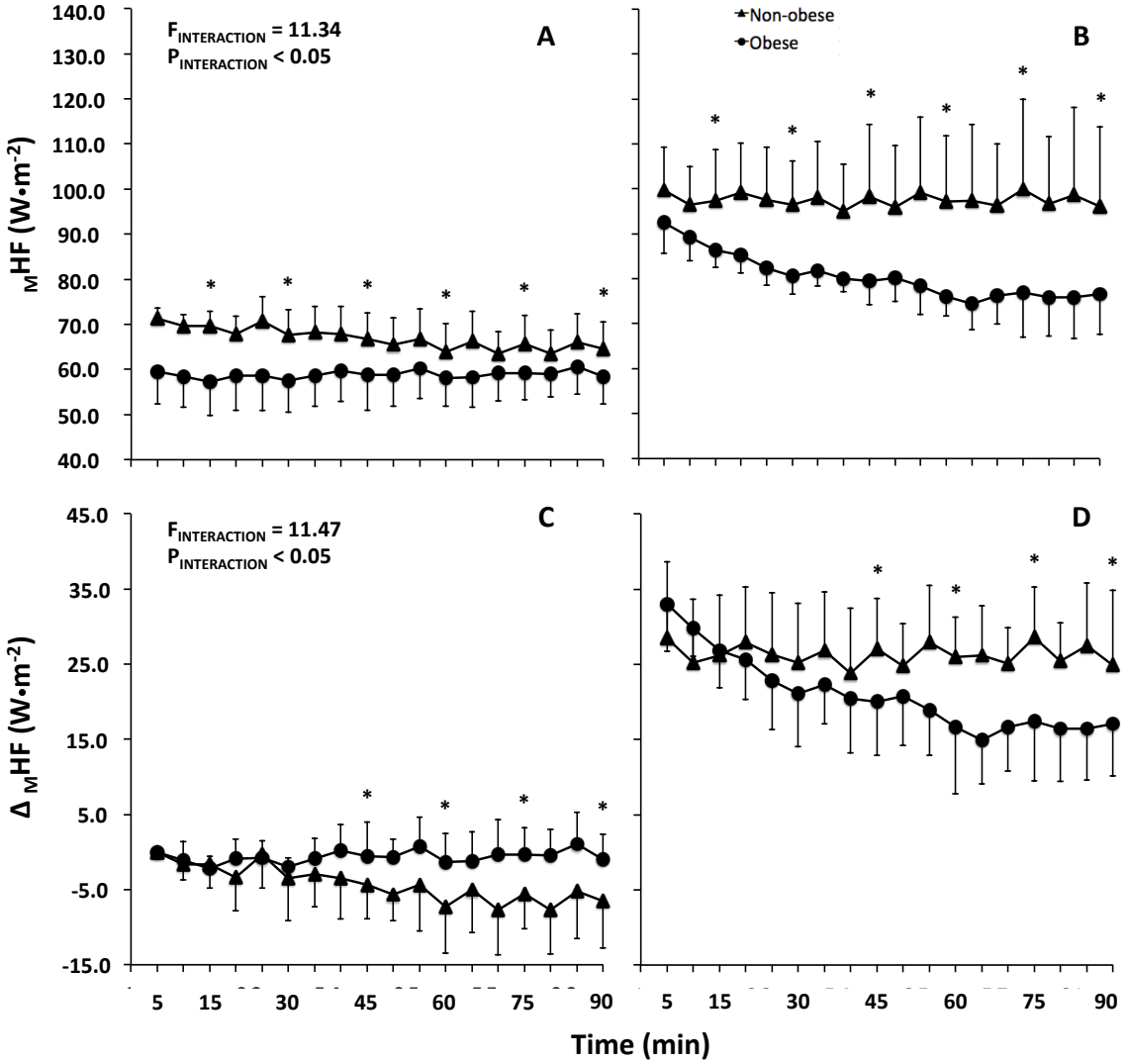

Figure 2.3 Obese and Non-obese mean heat flux ($_{M}$HF, W•m^{-2}) during A) 90 min exposure at 27°C, followed by B) 90 min at 19°C; and delta mean HF (Δ $_{M}$HF, W•m^{-2}) during C) 90 min exposure at 27°C, followed by B) 90 min at 19°C. See first figure for delta calculation. Values are mean ± SD. Significance: * < 0.05.

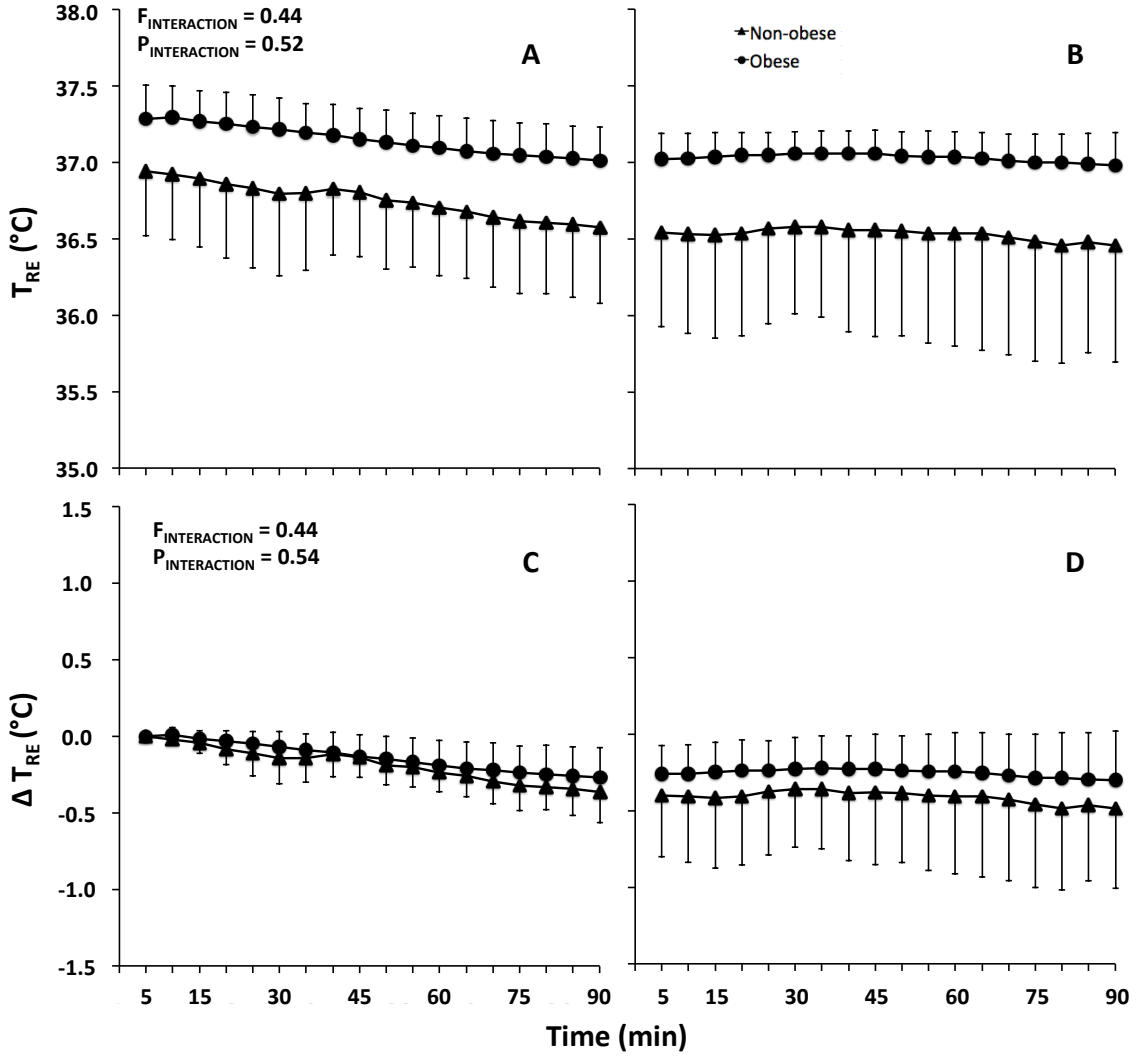

Figure 2.4 Obese and Non-obese rectal temperatures (T_{RE}, °C) during A) 90 min exposure at 27°C, followed by B) 90 min at 19°C; and delta rectal temperature (ΔT_{RE}, °C) during C) 90 min exposure at 27°C, followed by B) 90 min at 19°C. See first figure for delta calculation. Values are mean ± SD. Significance: * < 0.05.

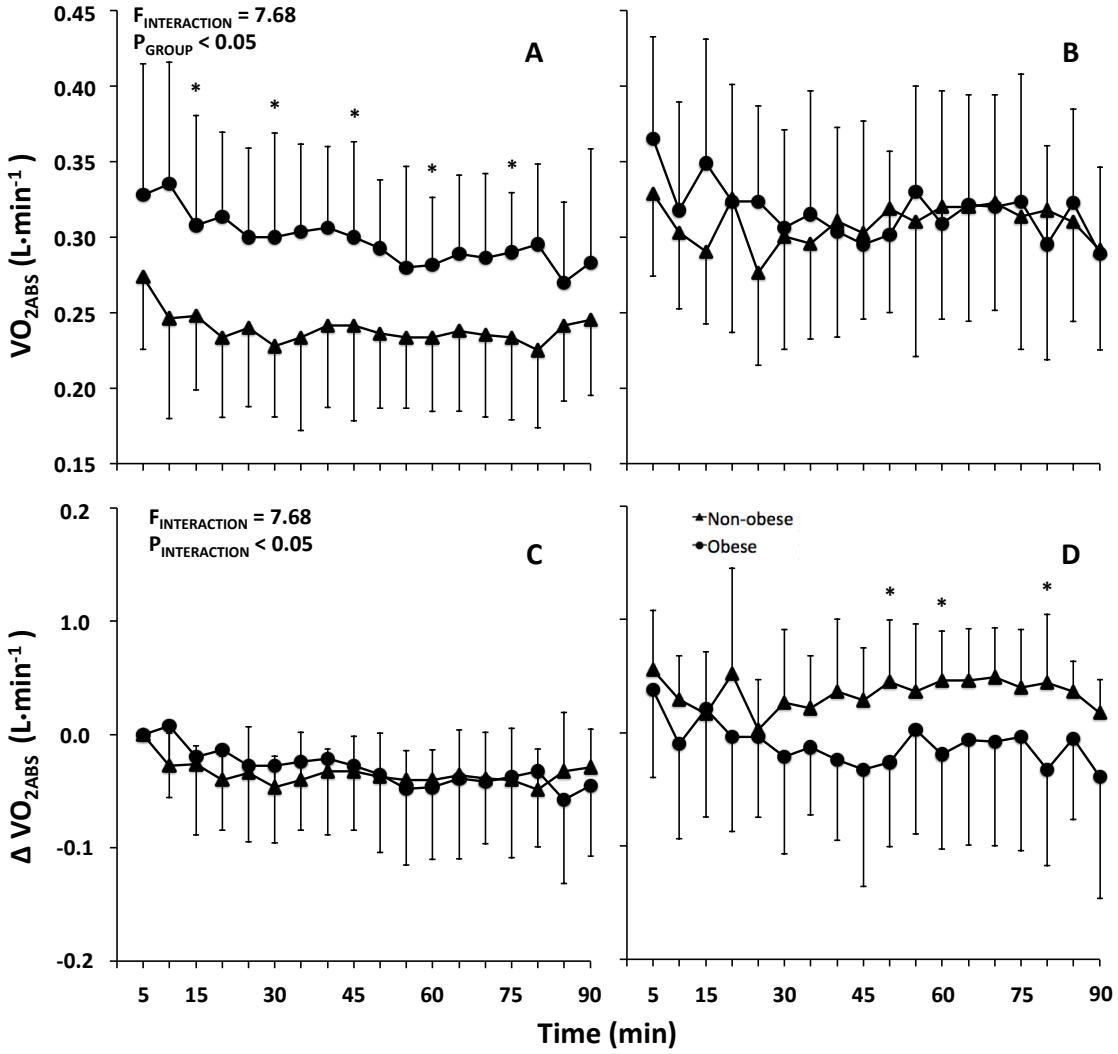

Figure 2.5. Obese and Non-obese absolute rate of oxygen consumption (VO_{2ABS}, L•min^{-1}) during A) 90 min exposure at 27°C, followed by B) 90 min at 19°C; and delta absolute rate of oxygen consumption (ΔVO_{2ABS}, L•min^{-1}) during C) 90 min exposure at 27°C, followed by B) 90 min at 19°C. See first figure for delta calculation. Values are mean ± SD.

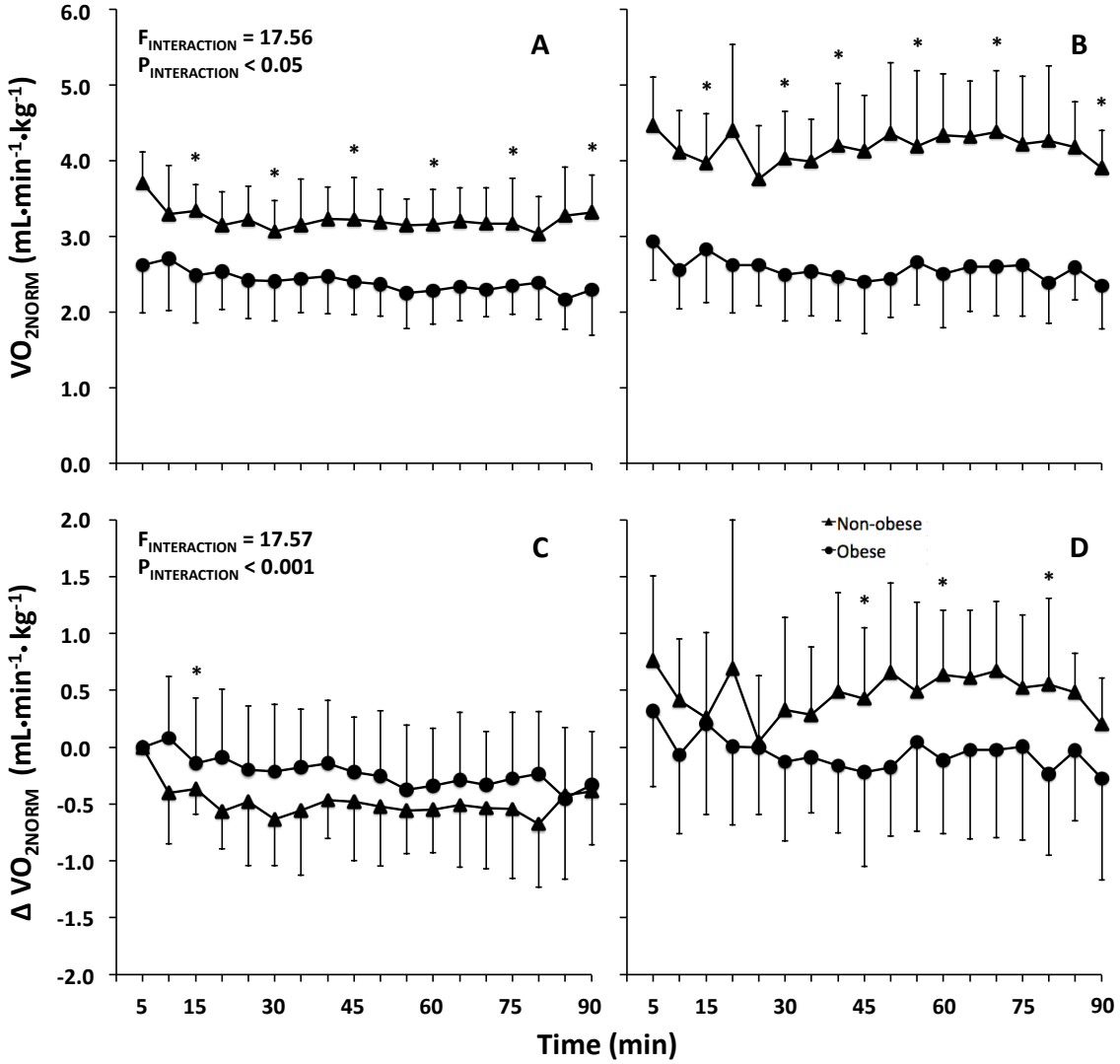

Figure 2.6. Obese and Non-obese normalised rate of oxygen consumption (VO_{2NORM}, mL•min^{-1}•kg^{-1}) during A) 90 min exposure at 27°C, followed by B) 90 min at 19°C; and delta normalised rate of oxygen consumption (ΔVO_{2NORM}, mL•min^{-1}•kg^{-1}) during C) 90 min exposure at 27°C, followed by B) 90 min at 19°. See first figure for delta calculation. Values are mean ± SD. Significance: * < 0.05.

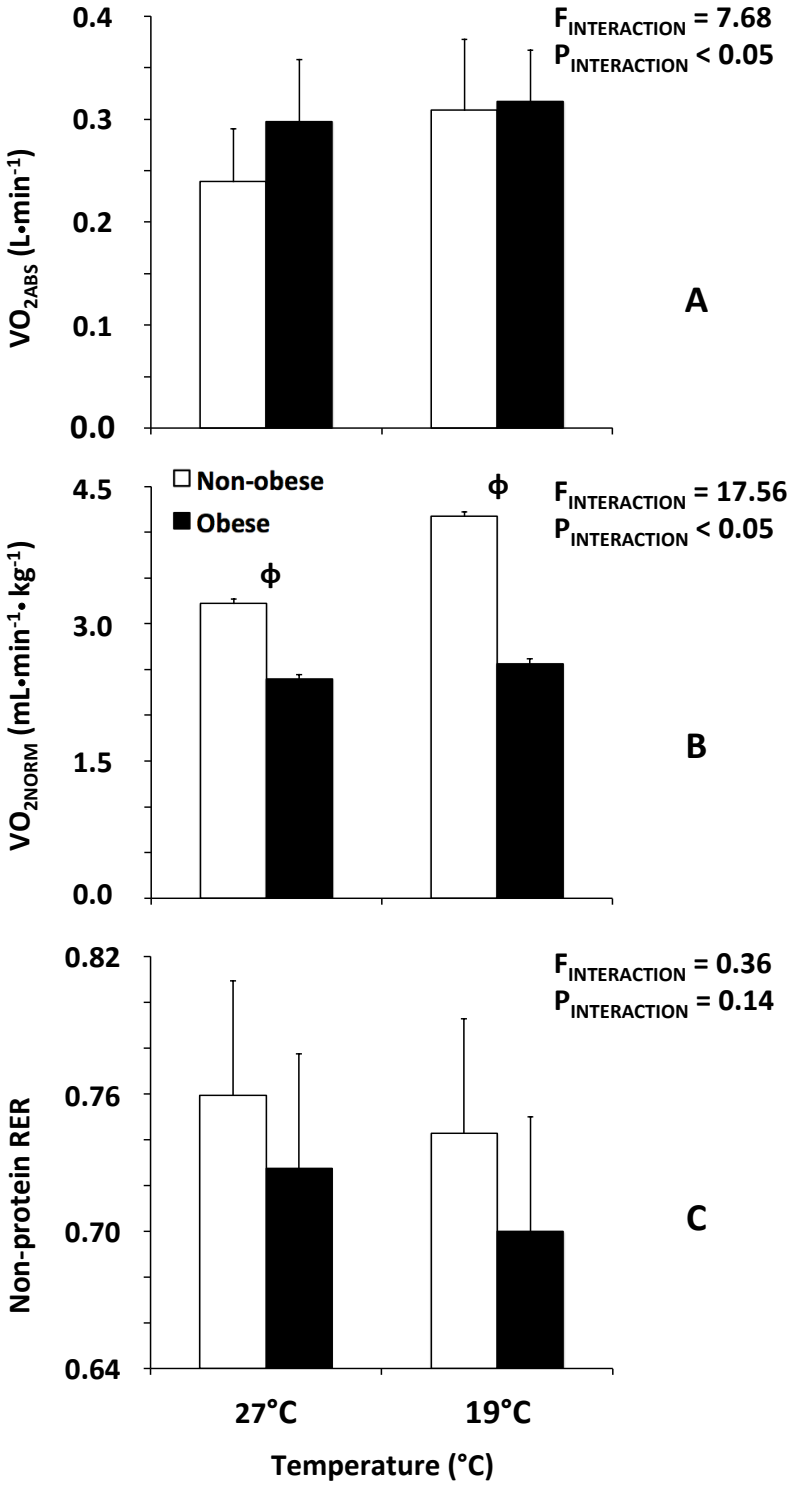

Figure 2.7 Obese and Non-obese A) absolute rate of oxygen consumption (VO_{2ABS}, L•min^{-1}), B) normalised rate of oxygen consumption (VO_{2NORM}, mL•min^{-1}•kg^{-1}), and C) non-protein respiratory exchange ratio (RER) during 27°C and 19°C exposures. Values are mean ± SD. Significance: ϕ = $p < 0.001$.

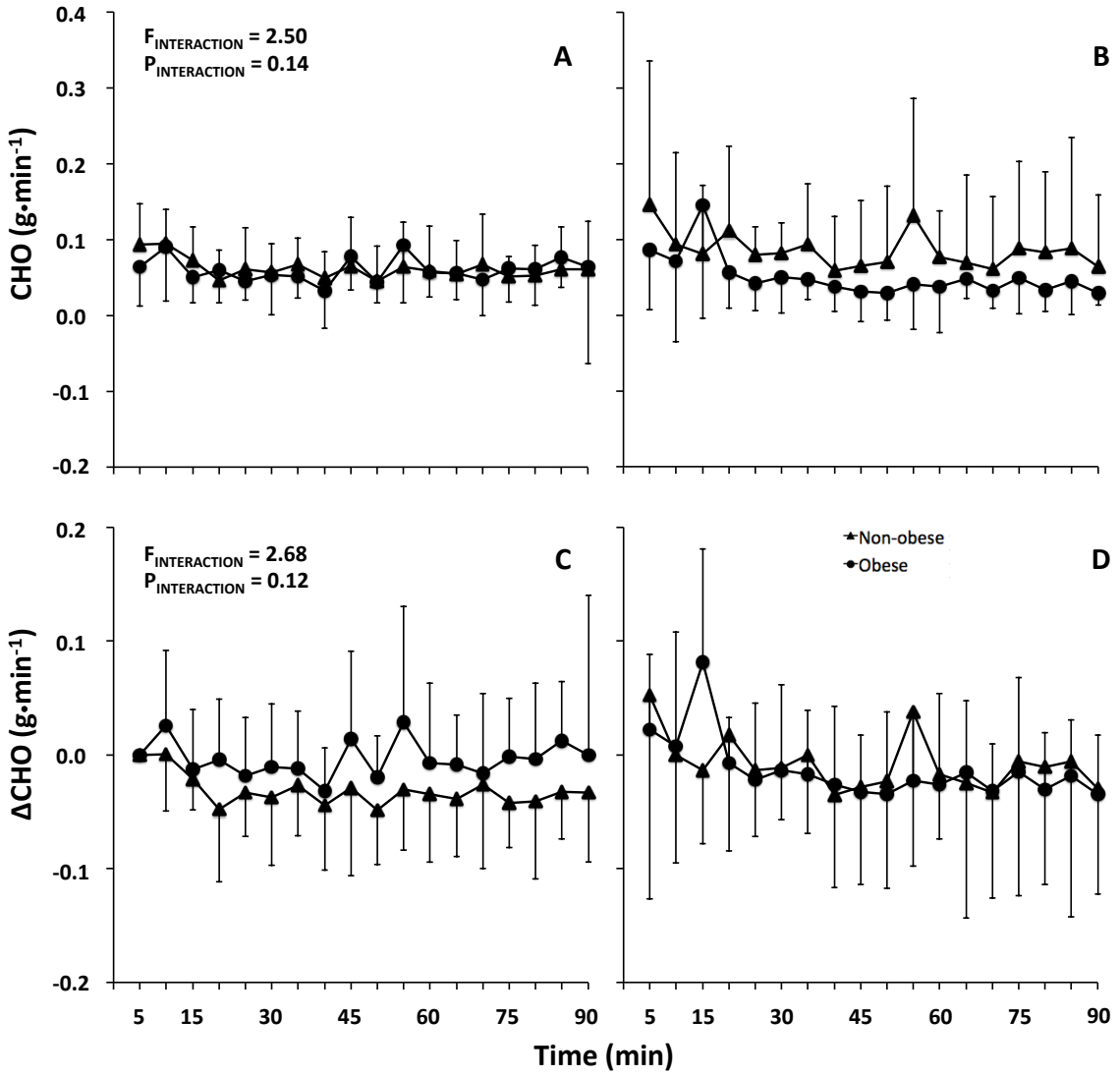

Figure 2.8 Obese and Non-obese carbohydrate (CHO) oxidation rate (g•min^{-1}) during A) 90 min exposure at 27°C, followed by B) 90 min at 19°C; and delta carbohydrate oxidation rate (ΔCHO, g•min^{-1}) during A) 90 min exposure at 27°C, followed by B) 90 min at 19°. See first figure for delta calculation. Values are mean ± SD.

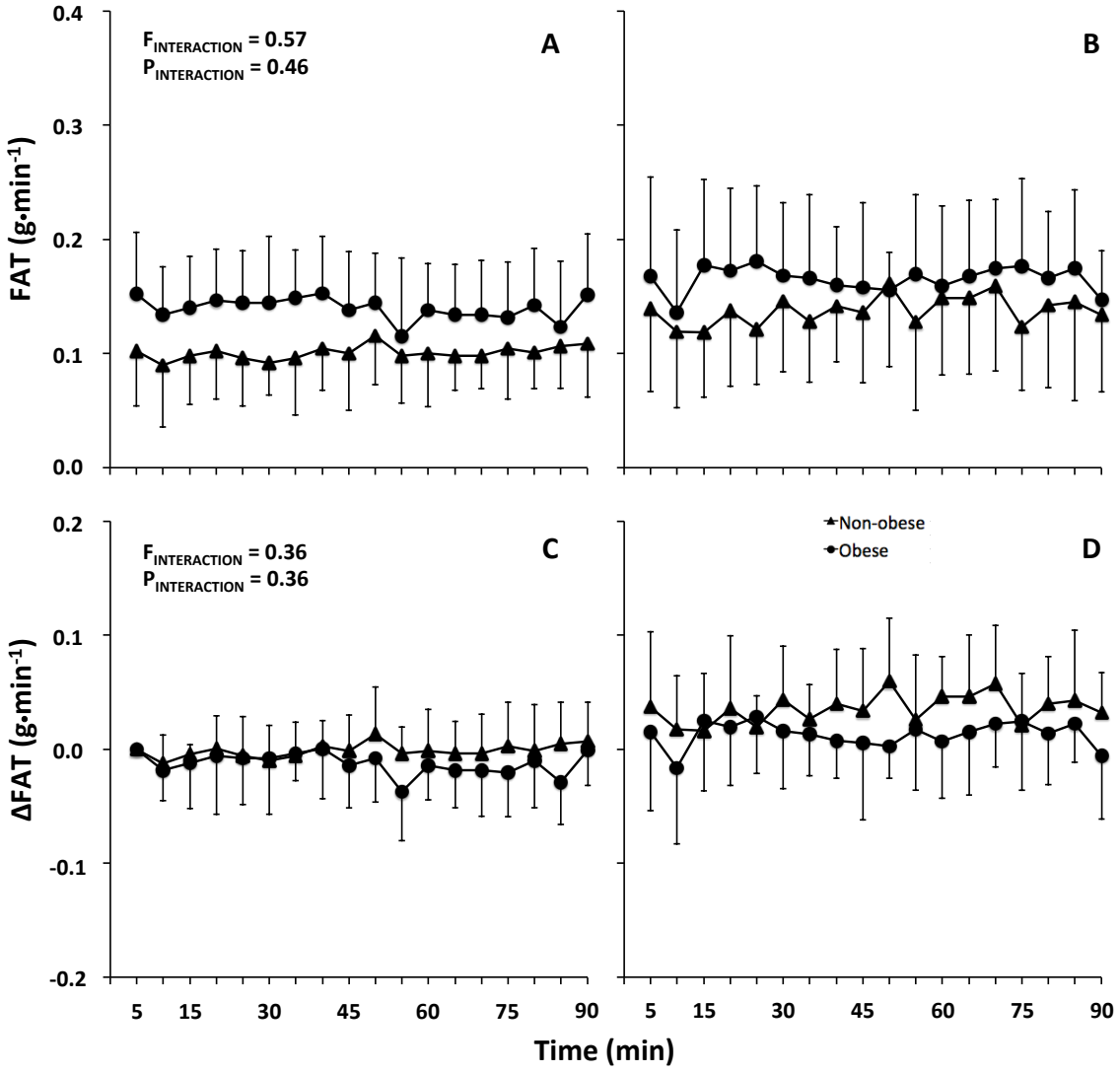

Figure 2.9 Obese and Non-obese lipid (FAT) oxidation rate (g•min^{-1}) during A) 90 min exposure at 27°C, followed by B) 90 min at 19°C; and delta FAT (ΔFAT, g•min^{-1}) during A) 90 min exposure at 27°C, followed by B) 90 min at 19°. See first figure for delta calculation. Values are mean ± SD.

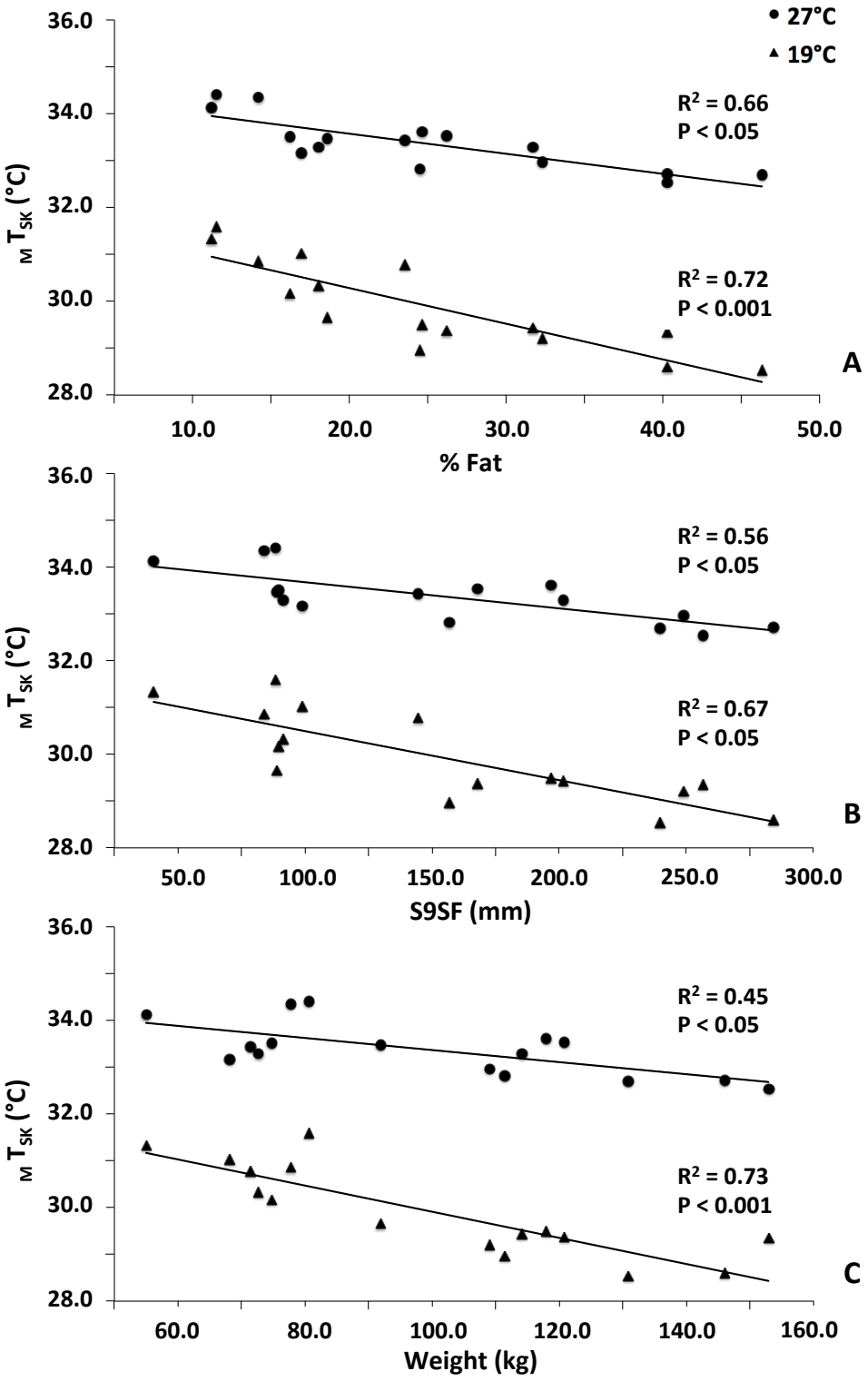

Figure 2.10 Regression lines of mean unweighted skin temperature ($_{M}T_{SK}$, °C) against, A) percent (%) fat from DEXA, B) sum of 9 skinfolds (S9SF), and C) weight (kg). n = 8 per group.

Chapter 3.

Effect of Acute Mild Cold Exposure on Non-Shivering Thermogenesis in the Obese Males

3.1. Introduction

Brown adipose tissue is a metabolically active tissue found most abundantly in mammalian species routinely exposed to cold environments (Smith and Hock 1963, Jansky 1973). In conjunction with skeletal muscle-activated shivering thermogenesis, mammals exposed to cold environments also have the capacity to initiate an involuntary NST fuelled by BAT (Blondin, Tingelstad et al. 2014).

Initial BAT NST observations (Carlson and Cottle 1956, Jansky 1973) of cold acclimated mice exposed to temperatures just below the thermo-neutral zone demonstrated they could withstand the effects of cold exposure much longer than warm acclimated rodents (Jansky and Hart 1963). These acclimated mice were able to suppress the need to shiver and relied almost exclusively on NST (Jansky 1973). Brown adipose tissue NST was also observed to be an important thermogenic tissue in hibernating animals during states of torpour (Smith and Hock 1963).

The cold exposure in mice evoked responses accounted for by BAT activation and UCP-1 in the mitochondria of the brown adipocyte (Himms-Hagen, Cui et al. 1994, Enerback, Jacobsson et al. 1997). UCP-1-ablated mice where shown to shiver at a constant intensity after chronic cold exposure, indicating they were unable to recruit any other form of heat gain (Golozoubova, Hohtola et al. 2001).

Although extensively observed in human infants to combat the initial cold stress of childbirth (Aherne and Hull 1964, Dawkins and Hull 1964, Dawkins and Scopes 1965, Bruck 1969), and in some histological examinations of adults exposed to the cold

(Heaton 1972, Huttunen, Hirvonen et al. 1981), the physiological importance of BAT in humans remained unclear and it was largely believed to be insignificant in the adult human (Blondin, Labbe et al. 2015). Nuclear medicine studies used PET/CT examinations coupled with ^{18}FDG administration showed an uptake in 4% of all patients in BAT (Cohade, Osman et al. 2003). Although physiological importance remained unclear, it did show a certain percentage of metabolically active glucose substrate uptake in BAT (van der Lans, Wierts et al. 2014).

The possible relevance of BAT in human adults was eventually demonstrated in 2009. Three independent studies using cold exposure revealed metabolically active BAT depots in 46 – 100% of young healthy subjects (Saito, Okamatsu-Ogura et al. 2009, van Marken Lichtenbelt, Vanhommerig et al. 2009, Virtanen, Lidell et al. 2009) showing that adult humans, similar to rodents and human infants, demonstrated a cold-induced metabolically active BAT response (van der Lans, Wierts et al. 2014). Since these initial papers, there has been over 20 dedicated studies that have confirmed cold-activated BAT depots and that it is usually in the supraclavicular, acromial-clavicular, para-aortic, axillary, paravertebral, and in peri-renal depots (Sacks and Symonds 2013).

These PET/CT studies have included varying cold-inducing protocols to stimulate BAT activity. Many have employed ambient temperatures just below thermo-neutral conditions of 16 – 20°C in hopes of initiating a NST without the stimulation of ST (van Marken Lichtenbelt, Vanhommerig et al. 2009, Muzik, Mangner et al. 2012, Vrieze, Schopman et al. 2012), some with the addition of periodical placement of feet in cold water or on ice (Virtanen, Lidell et al. 2009, Orava, Nuutila et al. 2011, Yoneshiro, Aita et al. 2011), and others with liquid-perfused suits (Ouellet, Labbe et al. 2012). Still, others have attempted a more personalised cooling protocol on a per-subject basis (Vosselman, van der Lans et al. 2012, van der Lans, Hoeks et al. 2013). This individualised cooling protocol included exposing participants to slowly decreasing temperatures. After the onset of shivering, the temperature was increased just above that minimum temperature in order to remove shivering but have the lowest temperature to activate the highest possible NST. Collectively these studies have shown a prevalence of BAT ranging between 20 –100% of the number of cold exposed humans (Vosselman, van der Lans et al. 2012, van der Lans, Hoeks et al. 2013).

The vast majority of cold-induced BAT activation in adult humans have been employed using radioactive tracers (van der Lans, Wierts et al. 2014). Because of the ionising radiation, as well as the cost associated with these scans, there is a need for an alternative technique that will aid in the investigation of BAT control. As the main function of BAT is heat release, a number of groups have begun testing this as a valid method of measurement (van der Lans, Wierts et al. 2014). Placement of temperature probes within BAT is not practical as seen in some mice studies (Christoffolete, Linardi et al. 2004, Masamoto, Kawabata et al. 2009)), therefore the use of forward looking infrared (FLIR) thermography has been employed to measure surface temperatures over known BAT depots (Lee, Ho et al. 2011, Symonds, Henderson et al. 2012, Robinson, Ojha et al. 2014). These studies have focused on individuals of healthy weight and children, and little work has been done on how the control of BAT in the obese may differ. Robinson, Ojha et al. (2014) demonstrated that an increase in BMI in children was coupled with a decrease in supraclavicular temperature, adding to the popular theory that BAT contributes to a balanced energy expenditure.

It was hypothesised that relative to the non-obese, the obese would demonstrate a reduced BAT NST at the supraclavicular fossae including a blunted metabolic response when normalised for lean body mass. This would correspond to, it was hypothesised, lower mean skin temperatures and heat flux over these supraclavicular fossae in the obese when exposed to mild cold. It was also hypothesised that this would be in concert with similar and minimal skeletal muscle activation as assessed by surface EMG.

3.2. Methods

3.2.1. Ethics

Approval for this study was obtained through the Simon Fraser University Office of Research Ethics. All participants were provided the option of removing themselves from the study at any point without prejudice and without reason.

3.2.2. Participants

Each participant was brought into the lab for a detailed orientation session. This included familiarisation with the equipment, study protocol, informed consent and health screen questionnaire. Each participant was then given a minimum of a 24 h reflection period. Upon agreeing to participate in the study, the informed consent form and health screen questionnaire were reviewed and signed by the participant.

Sixteen male participants volunteered for the study. Participants were initially screened using BMI and skinfolds. Skinfolds, height and weight were collected according to the protocols outlined by Marfell-Jones (1991), and % body fat estimates from skinfolds followed the 4-component model laid out by Peterson *et al.* (2003) and was applied to the equation:

$$\% \text{ Body Fat} = 20.95 + (\text{age} \times 0.17) - (\text{height} \times 0.17) + (\text{sum4} \times 0.43) - (\text{sum4}^2 \times 0.002)$$

where age is in yr, height is in cm, and sum4 is the sum of triceps, subscapular, suprailiac, and midthigh skinfold thicknesses in mm (Peterson, Czerwinski et al. 2003). Percent body fat was further assessed using Dual-energy X-ray absorptiometry (DEXA) scans (Hologic Discovery Ci/Wn 010 0575) (Figure A.1).

Participants were separated into two distinct groups (n = 8, each group) after taking part in a DEXA scan. Obese participants had a mean fat content of 39.38 kg (12.58) and a mean percent body fat of 32.2% (7.7) (Table 3.1). This was compared to the non-obese group who averaged 12.0 kg (3.57) of total fat and had a mean percent body fat of 16.4% (4.0) (Table 3.1). Fractionation of surface area by body region was also calculated to be an average of 2.51 m^2 (0.22) for the obese and 1.92^2 (0.21) for the non-obese (Table 3.2).

A power calculation was used to determine the sample size required to have a power of 80% and a significance of 0.05. The sample size varied depending on the variable. The number of volunteers required was found to be a minimum of 8 in order to find a significant result, if it existed, in all variables of interest. The variables employed

for this power calculation were mean skin temperature ($_{M}$TSK), mean heat flux ($_{M}$HF), and VO2.

A power calculation was used to determine the sample size required to have a power of 80% and a significance of 0.05. The sample size varied depending on the variable. The number of volunteers required was found to be a minimum of 8 per group in order to find a significant result, if it existed, in all variables of interest. The variables employed for this power calculation were mean skin temperature ($_{M}T_{SK}$), mean heat flux ($_{M}$HF), and mean VO_2.

Using pilot study data of $_{M}T_{SK}$, a sample size of 4 participants per group at 27°C and 6 participants per group at 19°C were required. This was found with differences to detect set at 3°C and a standard deviation between the two groups of 1.03°C at 27°C and 1.67°C at 19°C.

Using pilot study data of $_{M}$HF, a sample size of 4 participants per group at 27°C and 6 participants per group at 19°C were required. This was found with differences to detect set at 20 $W \cdot m^{-2}$ and a standard deviation between the two groups of 5.94 $W \cdot m^{-2}$ at 27°C and 10.44 $W \cdot m^{-2}$ at 19°C.

Using pilot study data of VO_2, a sample size of 6 participants per group at 27°C and 7 participants per group at 19°C were required. This was found with differences to detect set at 0.1 $L \cdot min^{-1}$ and a standard deviation between the two groups of 0.06 $L \cdot min^{-1}$ at both 27°C and 19°C.

3.2.3. Instrumentation

Body Temperature and Heat Flux

Skin temperature and surface HF were measured at seven sites using thermocouples embedded in the surface of heat flux discs (Thermonetics, California, USA). These sites included the upper lateral arm (T_{UA}, HF_{UA}), posterior shoulder (T_{PS}, HF_{PS}), chest (T_{CH}, HF_{CH}), abdomen (T_{AB}, HF_{AB}), thigh (T_{TH}, HF_{TH}), and one on each of the supraclavicular fossa (T_{SC}, HF_{SC}) (Table A.1). Unweighted $_{M}$HF and unweighted $_{M}T_{SK}$

were also calculated. Heat flux discs were attached to the skin using hypoallergenic tape (Tanspore, 3M, St. Paul, MN, USA). A water bath (VWR Int, Model 1196, West Chester, Penn, USA) monitored by a platinum thermometer (Fisher Scientific, Nepean, ON, Canada) was used to calibrate the thermocouples within the heat flux discs. The heat flux portion of the discs were calibrated using a copper encased water bath similar to that used by Nuckols and Piantadosi (1980) and Mittleman (1987).

Core temperature (T_{RE}) was monitored throughout the trial using flexible 30 cm rectal thermistors inserted 15 cm (DeRoyal TN, USA). Similar to the skin thermocouples, the rectal thermistors were calibrated using a water bath (VWR Int, Model 1196, West Chester, Penn, USA) monitored by a platinum thermometer (Fisher Scientific, Nepean, ON, Canada).

Metabolic and Ventilatory Variables

While seated comfortably, each participant was asked to breathe through a low resistance mouthpiece connected to a one-way valve allowing expired air to move through a 3.8 cm diameter tube. The respiratory tubing was attached to a two-way mass flow sensor (Sensormedics, Yorba Linda, CA, USA). Each participant wore a nose clip to ensure all exhaled gas was collected through the mouthpiece and mass flow sensor.

The mass flow sensor was connected to a breath-by-breath metabolic cart (VMAX 229, Sensormedics, Yorba Linda, CA, USA), which was used to measure absolute volume of consumed oxygen (VO_{2ABS}), which was then normalised to lean body mass (VO_{2LEAN}) from the DEXA results.

The calibration of gas analysers in the metabolic cart were completed with room air and with compressed gas tanks with mixtures of 26% O_2, balance N_2; and 16% O_2, 4% CO_2, and balance N_2. The two-way mass flow sensor was calibrated with a 3 L syringe.

Electromyograms of Skeletal Muscles

Electromyograms (Bagnoli-8 Delsys®, Natick, MA, USA) were measured at 5 sites representing the trunk and limbs and were chosen to represent the largest possible

fraction of total muscle mass of the body (>90%) (Bell, Tikuisis et al. 1992, Haman, Legault et al. 2004). These sites included the trapezius (TR), pectoralis major (PE), biceps brachii (BI), rectus femoris (RF), and gastrocnemius (GA) (Bell, Tikuisis et al. 1992).

Prior to the experiments, maximal EMG signals from each muscle group were determined from maximal voluntary contractions (MVC). Maximum voluntary contractions were obtained utilising isometric movements as described previously (Bell, Tikuisis et al. 1992, Peier, Moqrich et al. 2002, Haman, Legault et al. 2004). The following procedures were used to identify the maximal EMG signal for each muscle group: 1) for TR, participants sat upright with their arm straight against the body. Grasped in the hand participants raised their shoulders trying to elevate against the cord. 2) For PE, participants sat upright with their arm extended away from the body at 90^{o}. Participants performed a horizontal shoulder flexion against the cord. 3) For BI, participants started with their arm fully extended at their side. Participants held the cord in a supinated hand and maximally flexed at the elbow joint. 4) For RF, MVC was determined while participants sat on a chair in an upright position. The cord was placed slightly above the ankle and the participant was asked to perform a maximal knee extension against the weight. 5) For GA, the participant laid down, the cord was placed on the foot and the participant then performed a maximal ankle flexion against the weight. All movements were completed as close to the seated experimental position as possible. Delsys® EMG systems are calibrated using standard calibration services at their main offices.

Thermal Imaging

Thermal imaging of the supraclavicular region ($FLIR_{Sc}$) was carried out using a Forward Looking Infrared (FLIR®) camera (FLIR T650sc, FLIR Systems Inc., Burlington, ON, CAN). The thermal imaging camera was set 1 m away from the seated participant and was stationed on a large tripod and raised to a height that gave an angle of 20° from the horizontal of the participant's supraclavicular fossae. This ensured that no reflective radiation from the skin would occur. The thermal imaging camera was selected based on the high resolution and accuracy when compared to other cameras used in various studies (Table A.2).

To ensure consistent and comparable measurements using the thermal imaging camera, all participants remained perfectly still throughout the protocol while seated comfortably with a straight back and neck, relaxed shoulders and adducted arms. FLIR® thermal imaging cameras are calibrated using standard calibration services located at their main offices (FLIR 2014).

3.2.4. Data Acquisition

Cardiorespiratory and Temperature Variables

Cardiorespiratory variables were sampled and recorded at 20 s intervals with a VMAX 229 metabolic cart (Sensormedics, Yorba Linda, CA, USA). Body temperature was assessed with thermocouples embedded in heat flux transducers and were sampled at a rate of 40 Hz using LabVIEW software (Ver. 7.1, National Instruments, Austin, TX, USA) and recorded every 20 s.

Electromyograms of Skeletal Muscle

Electromyograms were sampled at 1,000 Hz using the Bagnoli-8 Delsys Systems® amplifier. Measurements were made using parallel-bar EMG sensors (DE-2.1 Differential EMG Sensor) placed on the surface of the skin. The signals recorded to .txt files at a rate of 1,000 Hz. Referencing was done using a reusable reference electrode (Dermatode®, Nuland, BR, The Netherlands).

Using a custom LabVIEW software (Ver. 8.6, National Instruments, Austin, TX, USA), maximal RMS values from MVC's were compared to exposure data. EMG signals were filtered to remove 60 Hz noise (and associated harmonics).

Thermal Imaging

The thermal imaging camera was employed to capture sequential images in .jpeg format every 10 min during the exposure and these files were then processed and analysed using the FLIR® Quick Report 2.1 software system. Using the box area tool, a region of interest at the supraclavicular area for each participant was defined and temperature data were exported into Microsoft Excel 2010. The supraclavicular regions were bordered using the anatomical landmarks of the superior border of the clavicles

and the sternocleidomastoid muscle inferiorly (Symonds, Henderson et al. 2012, Robinson, Ojha et al. 2014). 3-D plot graphs in Microsoft Excel 2010 were also employed to measure the thermal topography at the supraclavicular regions.

3.2.5. Protocol

Each participant participated in a single session during the testing period from 8 November to 11 December, and all sessions were conducted at least 6 hours fasted to remove any confounding, food-induced, thermogenic effects. The participant was asked to refrain from any consumption of caffeine, drugs, alcohol, and intense exercise in the 12 hours leading up to the study. All sessions began between 8 am and 10 am.

Following instrumentation, each volunteer sat comfortably in a chair placed in the centre of a climatic chamber (Tenney Engineering Inc., Union, NJ, USA). Each volunteer participated in one trial within the climatic chamber which included exposure to 90 min of baseline data collection at 27°C, followed by a cold exposure of 90 min at 19°C. Enclosure temperatures during the 27°C exposure remained at 27.1°C (0.07) and at 18.9°C (0.49) during the 19°C exposure (Figure 2.1).

3.2.6. Statistical Analysis

The main effect of Group (Non-obese, Obese), Ambient Temperature (27, 19°C) and their interaction (Group x Ambient Temperature) were examined in a 2-Factor Mixed Model ANOVA using the SPSS software program (Version 22, Surrey, UK) across all 90 min of exposure. Group was set as a non-repeated between-subjects factor while Ambient Temperature was set as the repeated within-subjects factor. Factors analysed in this study were TSK_{Sc}, HF_{Sc}, ΔTSK_{Sc}, ΔHF_{Sc}, $FLIR_{Sc}$, VO_{2LEAN} and EMG.

A two-tailed, unpaired t-test was used to compare means if there was a significant interaction from the ANOVA model. The level of significance was set at 0.05. Files were averaged using a custom LabVIEW program and exported into .txt files. Delta values were calculated by subtracting the initial 27°C value of each participant from their mean value for each time point.

Using the box area tool, a region of interest at the supraclavicular area for each participant was defined and temperature data were exported into Microsoft Excel 2010. The supraclavicular regions were bordered using the anatomical landmarks of the superior border of the clavicles and the sternocleidomastoid muscle inferiorly (Symonds, Henderson et al. 2012, Robinson, Ojha et al. 2014). 3-D plot graphs in Microsoft Excel 2010 were also employed to measure the thermal topography at the supraclavicular regions.

3.3. Results

Supraclavicular T_{SK} (TSK_{Sc}) ($F = 17.33$, $p < 0.001$) and HF_{Sc} ($F = 7.74$, $p < 0.05$) had significant Group x Ambient Temperature interactions (Table 3.3, Figure 3.2, 3.3). Supraclavicular T_{SK} showed differences at 27°C ($p < 0.05$) with obese TSK_{SC} at 33.67°C (0.15) and non-obese at 34.40°C (0.22) (Figure 3.3). At 19°C ($p < 0.001$), obese TSK_{SC} dropped almost 3°C to 30.70°C (0.29) while the non-obese TSK_{SC} remained higher, only dropping 1.74°C to 32.66°C (0.34) (Figure 3.3). At 19°C ($p < 0.05$), HF obese HF_{SC} increased only 25.50 $W \cdot m^{-2}$ from 58.51 (5.19) to 84.01 (4.93) $W \cdot m^2$, while the non-obese almost doubled that by increasing their HF_{SC} 44.33 $W \cdot m^{-2}$ from 69.90 (6.84) to 113.93 (9.54) $W \cdot m^{-2}$ (Figure 3.4). Both ΔTSK_{Sc} ($F = 27.01$, $p < 0.001$) and ΔHF_{Sc} ($F = 7.74$, $p < 0.05$) had significant interactions. The ΔTSK_{Sc} in the obese was 0.14°C (0.31) at 27°C and dropped to -2.83°C (0.58) at 19°C ($p < 0.05$). This was compared to the ΔTSK_{Sc} in the non-obese who had -0.28°C (0.58) at 27°C dropping to -2.02°C (0.89) at 19°C ($p < 0.05$). The ΔHF_{Sc} in the obese was -0.60 $W \cdot m^{-2}$ (6.27) at 27°C, increasing to 24.89 $W \cdot m^{-2}$ (17.36) at 19°C ($p < 0.05$). This was compared to the much greater increase seen in the non-obese from -2.07 $W \cdot m^{-2}$ (9.35) at 27°C to 41.96 $W \cdot m^{-2}$ (19.15) at 19°C ($p < 0.05$) (Table 3.3, Figure 3.2, 3.3).

Mean VO_{2LEAN} ($F = 12.93$, $p < 0.05$) demonstrated a significant Group x Ambient Temperature interaction (Figure 3.4). The obese increased minimally from 3.82 $mL \cdot min^{-1} \cdot kg^{-1}$ at 27°C to 4.10 $mL \cdot min^{-1} \cdot kg^{-1}$ at 19°C ($p < 0.05$). This was compared to the non-obese who increase ~1.2 $mL \cdot min^{-1} \cdot kg^{-1}$ from 4.07 $mL \cdot min^{-1} \cdot kg^{-1}$ at 27°C to 5.27 $mL \cdot min^{-1} \cdot kg^{-1}$ at 19°C ($p < 0.05$). Delta values were similarly significant as the obese showed a minimal change from -0.35 $mL \cdot min^{-1} \cdot kg^{-1}$ at 27°C to -0.08 $mL \cdot min^{-1} \cdot kg^{-1}$ at 19°C ($p <$

0.05) compared to the non-obese who increased from -0.60 $mL \cdot min^{-1} \cdot kg^{-1}$ at 27°C to 0.60 $mL \cdot min^{-1} \cdot kg^{-1}$ at 19°C ($p < 0.05$).

Electromyograms were employed to assess the contributions of skeletal muscle activation (Table 3.4). Maximum voluntary contractions in the obese averaged 0.24 V (0.08) while non-obese produced MVC's with a mean of 0.25 V (0.05) and were not significantly different ($F = 0.03$, $p = 0.86$). When expressed as a percentage of their MVC's ($F = 0.01$, $p = 0.94$), both obese at 1.58% (1.31) and non-obese at 1.64% (0.07) showed minimal movement at 19°C and were not significantly different (Table 3.4).

Infrared thermography demonstrated a statistically significant Group x Ambient Temperature interaction for $FLIR_{Sc}$ ($F = 13.93$, $p < 0.05$) (Table 3.3, Figure 3.1, 3.4). Differences were seen at both 27°C with obese having a mean $FLIR_{Sc}$ of 34.54°C (0.47) and the non-obese with a mean of 35.24°C (0.41) ($p < 0.05$). This difference of 0.7°C at 27°C grew to a difference of 1.76°C when exposed to 19°C (Table 3.3). Obese participants averaged 31.90°C (1.00) while non-obese averaged 33.66°C (0.71) ($p < 0.05$) (Table 3.3, Figure 3.1, 3.4).

3.4. Discussion

Novel Findings

The novel data collected in this study looked at the surface T_{SK} and HF over areas of known BAT depots in the supraclavicular fossa. An exhaustive literature review suggests this is the first study that has attempted to quantify these parameters in adult males, utilising both surface HF discs and FLIR thermography in the obese and non-obese. The results aligned with our hypotheses in that non-obese participants demonstrated a greater TSK_{Sc} and HF_{Sc} than the obese when exposed to acute mild cold. While this comparison was similar at 27°C as well as 19°C, it is important to note that the non-obese TSK_{SC} deceased less and their HF_{SC} increased more than the same sites in the obese. Supraclavicular T_{SK} in the non-obese decreased only 1.74°C at 19°C compared to almost 3°C in the obese, while non-obese HF_{SC} increased 44.33 $W \cdot m^{-2}$ at 19°C compared to only 25.50 $W \cdot m^{-2}$ in the obese. Coupled with minimal and similar

surface EMG quantified skeletal muscle activation, as well as a significantly higher VO_{2LEAN}, these results may suggest a greater capacity of non-obese individuals to initiate NST through BAT activation. While most studies employing HF sensors have looked at surface cooling in water (Bell, Padbury et al. 1985, Mittleman and Mekjavic 1988) and temperature changes across clothing apparel (Niedermann, Psikuta et al. 2014). Despite this, HF is a relatively new method of estimating energy expenditure above BAT sites and it helped demonstrate a greater BAT activation in the non-obese than in the obese.

To ensure all T_{SK}, HF, metabolic and FLIR variations from 27 to 19°C were attributed to NST, EMG was used to monitor any effects of skeletal muscle activation. This was close to being achieved in our study with both obese and non-obese participants demonstrating shivering between 2 – 6% of their MVC's, similar to previous studies looking at ST (Haman, Legault et al. 2004, Ouellet, Labbe et al. 2012, Blondin, Labbe et al. 2014). There was a considerable variation in signals between muscle groups however and although minimal, stating a complete absence of shivering during these exposures may be considered unlikely (Blondin, Labbe et al. 2015).

Comparison to Literature and Underlying Mechanisms

The purpose of this study was to produce thermogenic and metabolic changes that may be solely correlated to changes in NST. To achieve this, a steady ambient temperature of ~19°C was selected. This temperature was chosen based on previous BAT studies utilising PET/CT scanning done with both air conditioned rooms between 16 – 19°C (Muzik, Mangner et al. 2012, Orava, Nuutila et al. 2013, Yoneshiro, Aita et al. 2013) and liquid perfused suits (Ouellet, Labbe et al. 2012, Blondin, Labbe et al. 2014, Blondin, Labbe et al. 2015). This ambient temperature choice is further justified by similar ambient temperatures produced in BAT studies utilising FLIR imaging (Symonds, Henderson et al. 2012, Robinson, Ojha et al. 2014). As was demonstrated in the T_{SK}, HF, and FLIR data, the desired effect of having a just-below thermoneutral ambient temperature was achieved. All temperature variables of interest produced lowered values while HF values increased at 19°C as was expected.

Several studies in the past few years have begun adopting more individualised cooling protocols for their participants (Vijgen, Bouvy et al. 2011, Vijgen, Bouvy et al. 2012, Vosselman, van der Lans et al. 2012, van der Lans, Hoeks et al. 2013). Participants would be cooled to a temperature where ST was observed and then warmed back in 1°C intervals until shivering ceased. The goal of this methodology is to produce conditions where NST is maximised with no contributions from ST. With studies done in this manner, the obese showed minimal BAT activation at around 20 – 50% of participants (Vijgen, Bouvy et al. 2011, Vijgen, Bouvy et al. 2012) while studies using healthy subjects showed some of the most pronounced levels of BAT activation in any study utilising cooling protocols at around 94 – 100% of participants (Vosselman, van der Lans et al. 2012, van der Lans, Hoeks et al. 2013).

The employed HF sensors, which provided both HF and temperature readings, provide single point measurements over known BAT depots and only a few studies have attempted to employ thermal imaging to map out a more complete thermal topography of the area (Lee, Ho et al. 2011, Symonds, Henderson et al. 2012, Robinson, Ojha et al. 2014). While most have only looked at children and adults of normal BMI ranges, only one other study to date has attempted to use FLIR imaging in assessing NST in people of normal and larger weights (Robinson, Ojha et al. 2014). In that study, Robinson, Ojha et al. (2014) demonstrated a negative relationship between BMI and TSK_{SC} in children aged 6 -11. This study demonstrated similar results with FLIR imaging capturing a significant amount of heat release in the supraclavicular regions directly over sites known to house BAT as seen in PET/CT studies (Nedergaard, Bengtsson et al. 2007, Saito, Okamatsu-Ogura et al. 2009, Virtanen, Lidell et al. 2009). When compared to these studies utilising radiometric glucose markers, the non-obese demonstrated strikingly accurate pockets of increased heat as seen in the 3D graphs (Figure 3.5), while obese individuals produced little evidence of the same activation.

More recent studies have suggested that surface EMG may not be a suitable method of estimating skeletal muscle activity during studies geared towards assessing BAT activation and NST (Blondin, Tingelstad et al. 2014, Blondin, Labbe et al. 2015). While surface EMG may typically elucidate mean MVC's of around 2 – 3%, deeper muscles such as the longus colli or sternocleidomastoid may be contributing to overall

metabolism and shivering more so than typically goes detection (Ouellet, Labbe et al. 2012, Blondin, Labbe et al. 2015). These findings, coupled with earlier studies showing reduced surface EMG signals with increased adiposity, suggest a possible need to use more advanced methods of monitoring skeletal muscle activation, particularly in the obese.

Just like electrical signals impeded in the human body when moving through different tissues, a similar difference in infrared absorption can be detected between areas of high fat and areas of low fat (Yang 2005, Yang 2009). This has been documented in a number of studies including biology and physics (Yang 2005, Yang 2009, Buniyamin 2011). When fat thickness increases, the detected diffuse reflectance increases. This may be be explained by fat giving a high scattering of infrared radiation and low absorption, while muscle has high absorption (Yang 2005). When fat thickness increases, less light is going to pass through the muscle. This causes less light to be absorbed and the reflectance to increase (Yang 2005).

Future Directions and Limitations

Employing FLIR imaging to assess BAT activation during acute mild cold has its limitations. While heat gain and NST activation can be inferred from our results, at its most basic application, FLIR imaging is limited to heat release at the surface of the skin. As ST is used to stave off a reduction in core temperature at more extreme cold exposures, BAT NST is thought to be activated for the same purpose, to help regulate core temperatures. Because of this, it has been suggested that the majority of heat being dissipated by BAT may be directed to the core of the body (van der Lans, Wierts et al. 2014). The question that remained is if some BAT heat may leak towards the surface of the skin and this study's non-obese results demonstrate that this is the case. Coupled with this, there were no significant differences between $FLIR_{SC}$ and T_{SK} at other sites of the body at 27°C in this study, as well, Symonds, Henderson et al. (2012) saw no increases in supraclavicular T_{SK} at higher ambient temperatures. This may suggest that infrared thermography may be used as a qualitative way of assessing BAT activation (van der Lans, Wierts et al. 2014).

Another limiting factor of using FLIR imaging to access BAT activation may be seen when employing this method in obese individuals. With lower mean T_{SK}, increased adiposity may be blunting their responses to the cold and surface $FLIR_{SC}$ may be dissipated before being picked up by the thermal imaging camera. In that sense, the lower skin temperatures may be attributed to their added adiposity more so than their inability to activate BAT. Future studies could employ this method in conjunction with other previously used methods such as PET/CT scans. Utilising PET/CT scanning with FLIR imaging may be an interesting route to take. Employing both these methods in more individualised cooling protocols, particularly in the obese, may help to provide more accurate knowledge of the thermogenic properties of BAT. Both methods synchronised will also allow studies to compare FLIR imaging temperatures with BAT presence in individuals using PET/CT scanning, as many studies have demonstrated high variability of BAT presence between individuals. With these studies in mind, future directions using FLIR imaging may need to adopt a more individualised cooling protocol. With thicker subcutaneous fat layers, insulation from ambient temperatures can delay the onset of shivering in the obese (Vijgen, Bouvy et al. 2011) and may contribute to blunted NST if the ambient temperature is not low enough (Wijers, Saris et al. 2010).

A potential limitation is obese participants % MVC values may be influenced by their greater levels of subcutaneous fat found between the muscle and surface electrode as a number of studies have attributed greater adiposity with lower EMG signals (Lowery, Stoykov et al. 2002, Kuiken, Lowery et al. 2003) and greater crosstalk between muscles (Solomonow, Baratta et al. 1994). One study showed that the addition of 3, 9, and 18 mm of subcutaneous fat layers caused a reduction in surface EMG RMS value directly above the centre of the active muscle, of 31.3%, 80.2%, and 90.0% respectively (Kuiken, Lowery et al. 2003). This is supported by our results as obese participants demonstrated the lowest MVC values, especially in the abdominal area where some skinfolds reached over 20 mm

Whether due to increased insulation from greater adiposity and therefore a resistance to cold, or a lessened ability to activate BAT NST, the obese may contribute to a positive energy expenditure in this application of cold ambient temperatures. One of the lingering questions is whether obesity is causal or consequential of diminished BAT

activity and more research with standardised protocols, utilising both thermal and metabolic techniques is needed.

Conclusion

It was hypothesised that obese individuals would demonstrate a lower capacity to initiate NST through BAT activation during acute mild cold exposure. This hypothesis was supported since TSK_{Sc}, HF_{Sc}, and $FLIR_{Sc}$ were lower in obese vs. non obese volunteers during mild cold exposure. This was seen with similar and minimal contributions of skeletal muscle activation between the two groups and a greater VO_{2LEAN} in the non-obese.

3.5. Tables

Table 3.1. Summary of mean participants' DEXA (mean ± SD) fractionation values including bone marrow content (BMC), fat mass, lean mass, total mass, and percent body fat.

Group	Region	BMC (kg)	Fat (kg)	Lean (kg)	Total Mass (kg)	Percent Body Fat (%)
Non-obese	Left Arm	0.19	0.64	3.49	4.32	14.9
	Right Arm	0.21	0.49	3.88	4.58	10.9
	Trunk	0.70	5.76	27.15	33.60	16.9
	Left Leg	0.52	2.17	9.85	12.54	17.2
	Right Leg	0.53	2.00	10.49	13.02	15.2
	Subtotal	2.15	11.06	54.85	68.07	16.1
	Head	0.54	0.94	3.64	5.12	18.3
	Full body	2.69	12.00	58.50	73.19	16.3
Obese	Left Arm	0.19	2.04	3.32	5.56	36.5
	Right Arm	0.20	1.84	3.84	5.88	31.0
	Trunk	0.92	20.32	39.61	60.85	32.9
	Left Leg	0.68	7.08	13.17	20.93	33.4
	Right Leg	0.68	6.88	13.71	21.28	31.9
	Subtotal	2.66	38.17	73.66	114.49	32.9
	Head	0.57	1.21	4.39	6.17	19.6
	Full body	3.23	39.38	78.05	120.66	32.2

Table 3.2. Mean body (SD) surface area (m^2) and surface area to mass ratio ($m^2 \cdot kg^{-1}$) of participants' fractionated body region. s

	Surface Area (m^2)		Surface Area to Mass ($m^2 \cdot kg^{-1}$)	
	Non-obese	Obese	Non-obese	Obese
Left Arm	0.22 (0.03)	0.18 (0.07)	0.0030 (0.0001)	0.0015 (0.0007)
Right Arm	0.24 (0.03)	0.19 (0.06)	0.0032 (0.0001)	0.0016 (0.0007)
Left Ribs	0.13 (0.02)	0.18 (0.03)	0.0017 (0.0002)	0.0014 (0.0003)
Right Ribs	0.14 (0.03)	0.18 (0.04)	0.0018 (0.0003)	0.0014 (0.0003)
Thoracic Spine	0.13 (0.04)	0.12 (0.05)	0.0017 (0.0004)	0.0009 (0.0004)
Lumbar Spine	0.07 (0.02)	0.07 (0.03)	0.0010 (0.0003)	0.0006 (0.0003)
Pelvis	0.24 (0.03)	0.26 (0.02)	0.0033 (0.0004)	0.0021 (0.0003)
Left Leg	0.39 (0.04)	0.47 (0.04)	0.0053 (0.0004)	0.0038 (0.0005)
Right Leg	0.40 (0.04)	0.48 (0.02)	0.0054 (0.0004)	0.0039 (0.0006)
Head	0.26 (0.02)	0.25 (0.02)	0.0036 (0.0007)	0.0020 (0.0003)
Total	1.92 (0.21)	2.51 (0.22)	0.0301 (0.0017)	0.0192 (0.0034)

Table 3.3. Mean (SD) values and corresponding delta (Δ) values for mean unweighted supraclavicular heat flux (HF_{Sc}, $W \cdot m^{-2}$), mean unweighted supraclavicular skin temperature (TSK_{Sc}, °C), and mean FLIR skin temperature ($FLIR_{Sc}$, °C) during 90 min exposures at both 27 and 19°C in the obese and non-obese. t-test comparisons are between groups at each ambient temperature. Significance: ‡ = $p < 0.05$; ϕ = $p < 0.001$.

	Ambient Temperature			
	27°C		**19°C**	
	Obese	Non-obese	Obese	Non-obese
HF_{Sc} ($W \cdot m^{-2}$)	58.51 (5.19)‡	69.90 (6.84)	84.01 (4.93)‡	113.93 (9.54)
ΔHF_{Sc} ($W \cdot m^{-2}$)	-0.60 (6.27)‡	-2.07 (9.35)	24.89 (17.36)‡	41.96 (19.15)
TSK_{Sc} (°C)	33.67 (0.15)‡	34.40 (0.22)	30.70 (0.29)‡	32.66 (0.34)
ΔTSK_{Sc} (°C)	0.14 (0.31)‡	-0.28 (0.58)	-2.83 (0.58)‡	-2.02 (0.89)
$FLIR_{Sc}$ (°C)	34.54 (0.47)‡	35.24 (0.41)	31.90 (1.00)‡	33.66 (0.71)

Table 3.4. Electromyogram (EMG) maximum voluntary contractions (MVC) and percent MVC's (%MVC) at 27°C and 19°C in the obese and non-obese groups. Mean unweighted EMG was taken from measured were: trapezius (TR), pectoralis major (PE), rectus abdominus (AB), biceps brachii (BI), rectus femoris (RF), gastrocnemius (GA). *Abdominals were omitted due to increased adiposity and unusable signal. Significance: ‡ = $p < 0.05$; ϕ = $p < 0.001$.

	MVC (V)		19°C (%MVC)	
	Obese	Non-obese	Obese	Non-obese
TR	0.24 (0.07)‡	0.32 (0.09)	1.22 (2.47)	1.75 (0.44)
PE	0.24 (0.03)	0.26 (0.07)	3.86 (1.21)	2.32 (1.66)
AB	--	--	--	--
BI	0.13 (0.15)	0.25 (0.28)	1.24 (1.72)	2.28 (1.22)
RF	0.36 (0.08)‡	0.25 (0.11)	1.09 (1.23)	0.82 (0.56)
GA	0.24 (0.08)	0.17 (0.06)	0.50 (0.88)	1.01 (0.79)
Mean (SD)	0.24 (0.08)	0.25 (0.05)	1.58 (1.31)	1.64 (0.07)

3.6. Figures

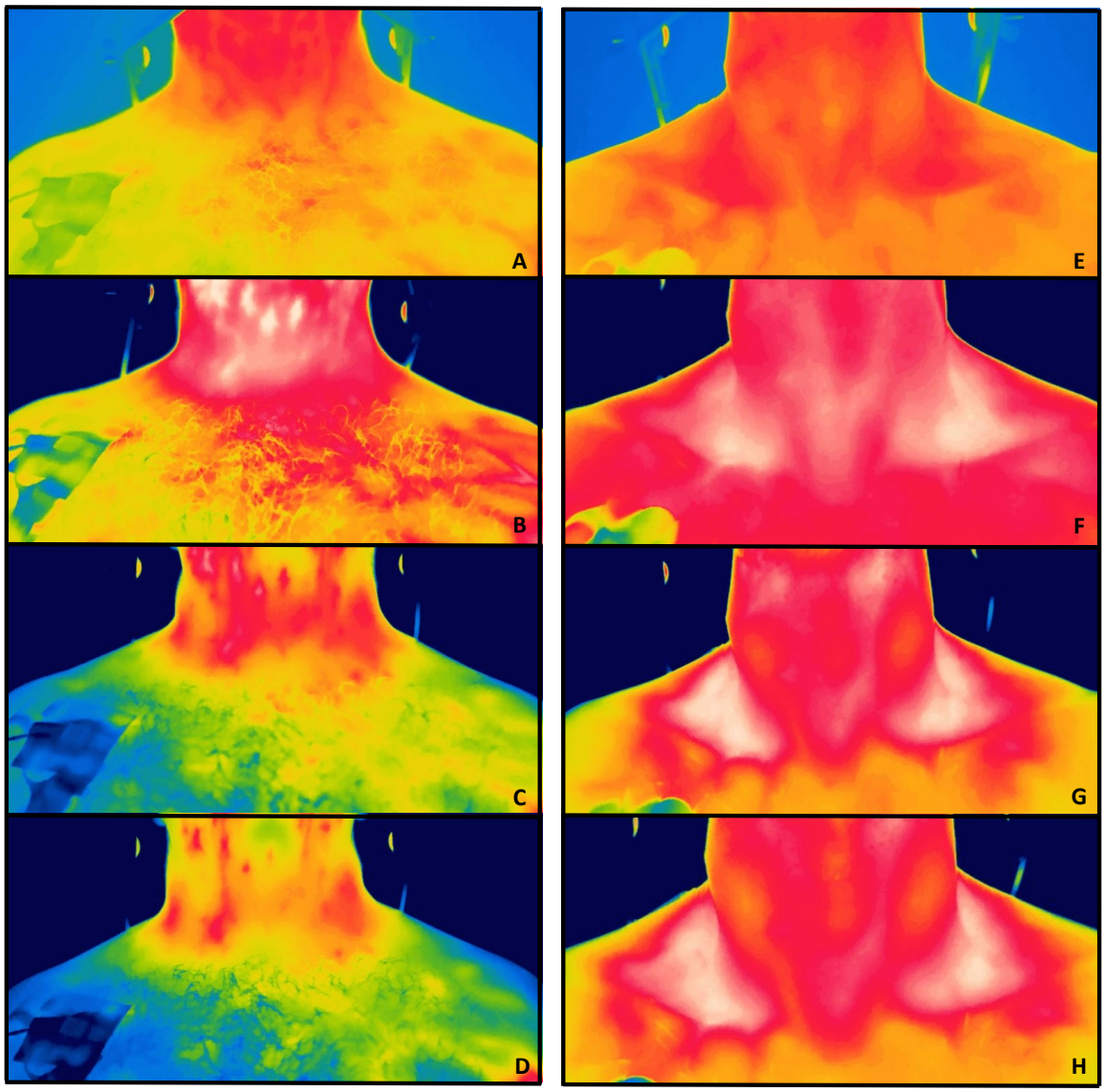

Figure 3.1. Typical thermal imaging of supraclavicular regions using a Forward Looking Infrared (FLIR) camera. Obese volunteer in 27°C at 90 min (A), and in 19°C at 10 min (B), at 40 min (C), and at 90 min (D). Non-obese volunteer in 27°C at 90 min (E), and in 19°C at 10 min (F), at 40 min (G), and at 90 min (H).

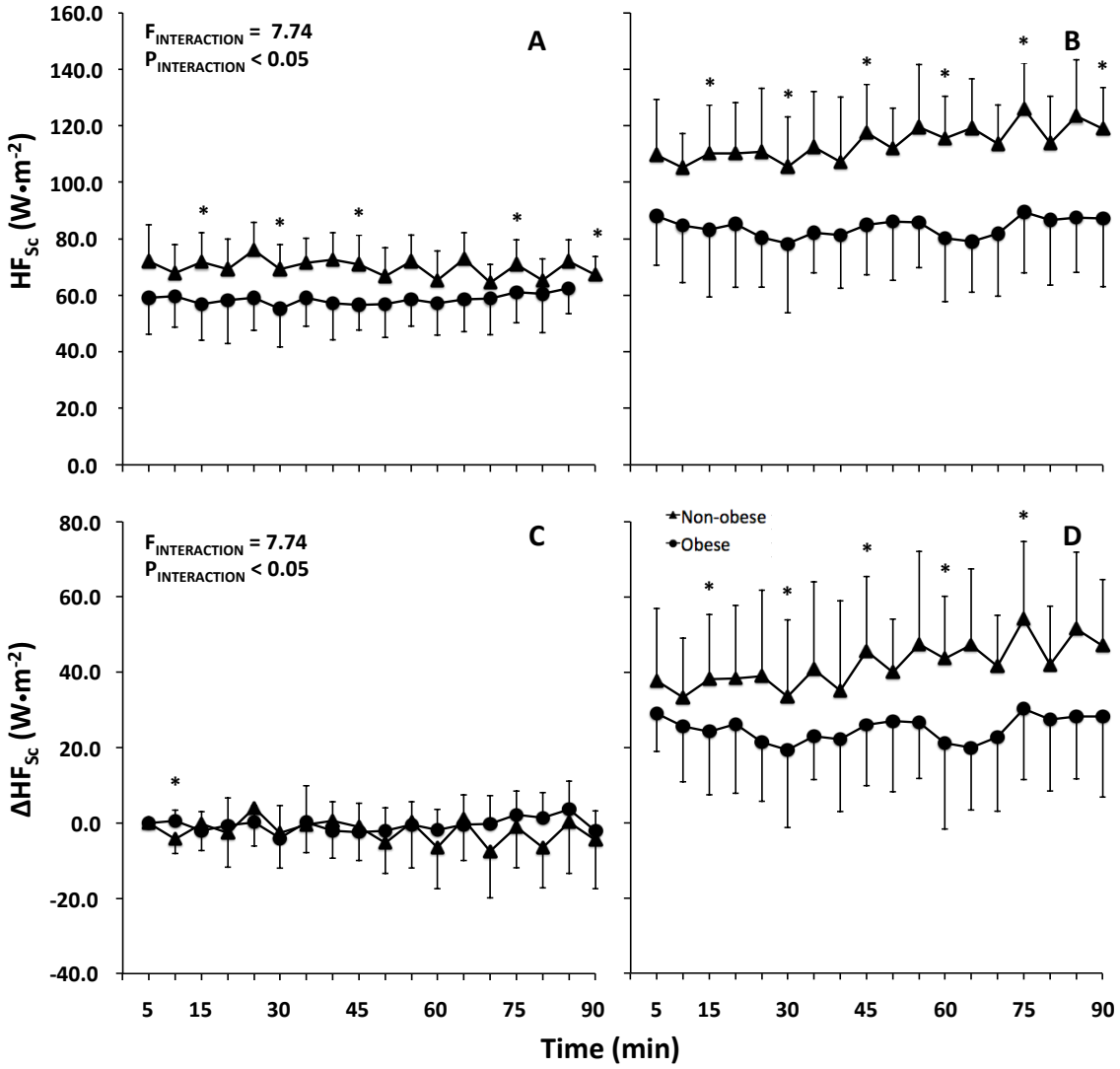

Figure 3.2. Obese and Non-obese supraclavicular heat flux (HF_{Sc}, W•m^{-2}) during A) 90 min exposure at 27°C, followed by B) 90 min at 19°C; and delta supraclavicular (ΔHF_{Sc}, W•m^{-2}) during C) 90 min exposure at 27°C, followed by B) 90 min at 19°C. Δ Values calculated by subtracting each time point value by initial 27°C value. Values are mean ± SD. Significance: * < 0.05.

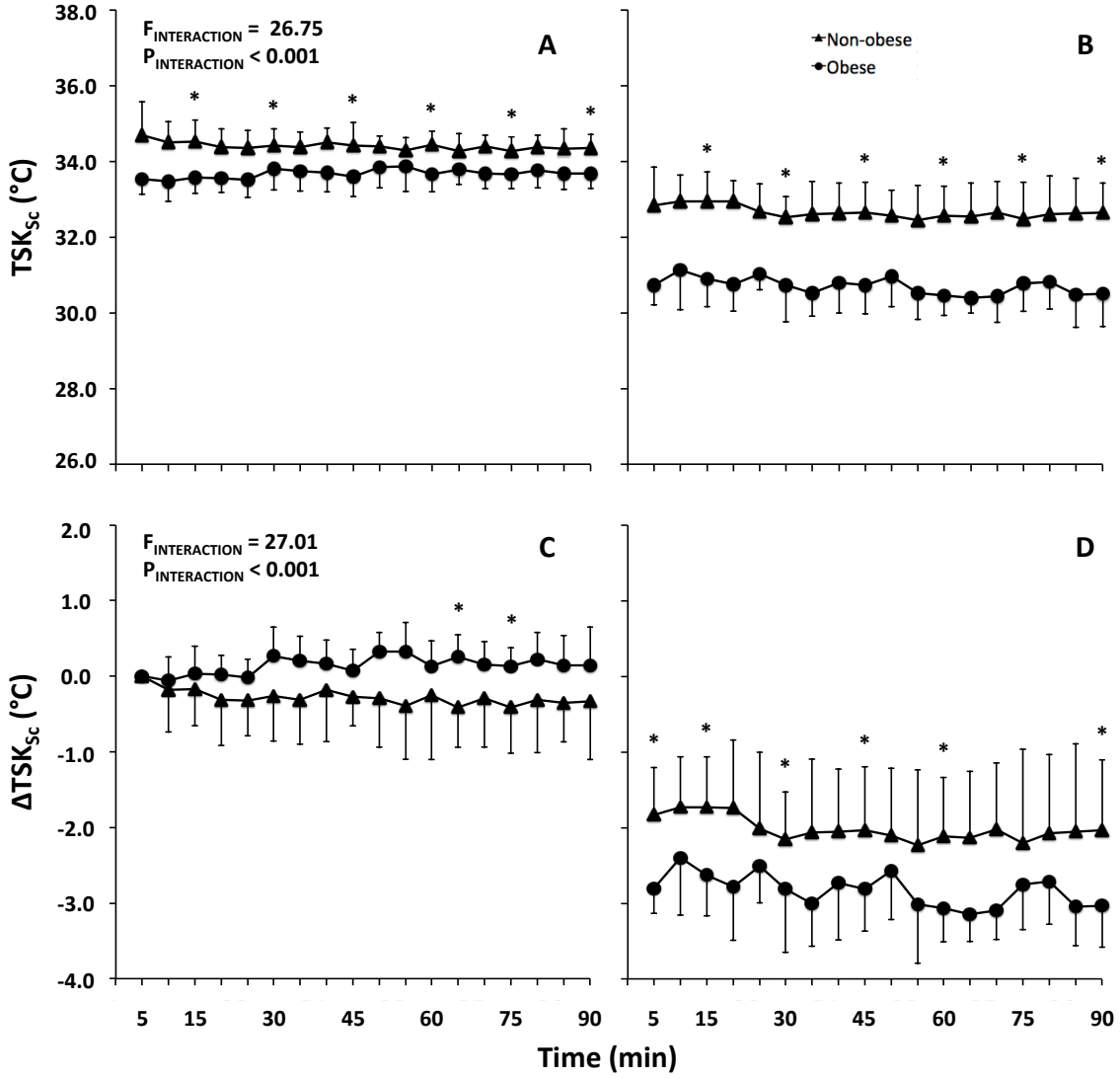

Figure 3.3. Obese and Non-obese mean supraclavicular temperatures (TSK_{Sc}, °C) during A) 90 min exposure at 27°C, followed by B) 90 min at 19°C; and delta TSK_{Sc} (ΔTSK_{Sc},°C) during C) 90 min exposure at 27°C, followed by B) 90 min at 19°C. See first figure for delta calculation. Values are mean ± SD. Significance: * < 0.05.

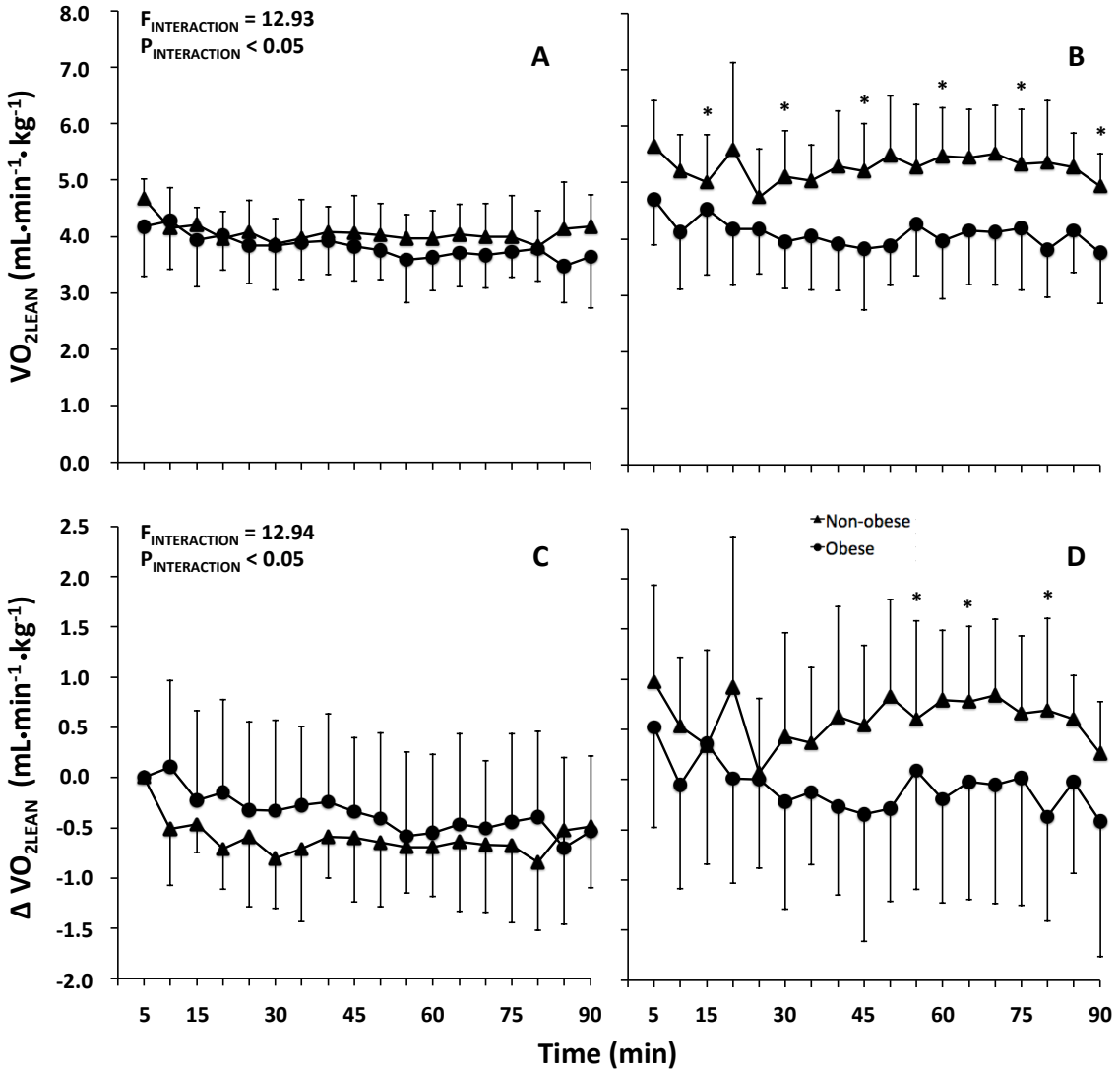

Figure 3.4 Obese and Non-obese mean rate of oxygen consumption normalised to DEXA lean body mass (VO_{2LEAN}, $mL \cdot min^{-1} \cdot kg^{-1}$) during A) 90 min exposure at 27°C, followed by B) 90 min at 19°C; and delta VO_{2LEAN} (ΔVO_{2LEAN}, $mL \cdot min^{-1} \cdot kg^{-1}$) during C) 90 min exposure at 27°C, followed by D) 90 min at 19°C. See first figure for delta calculation. Values are mean ± SD. Significance: * < 0.05.

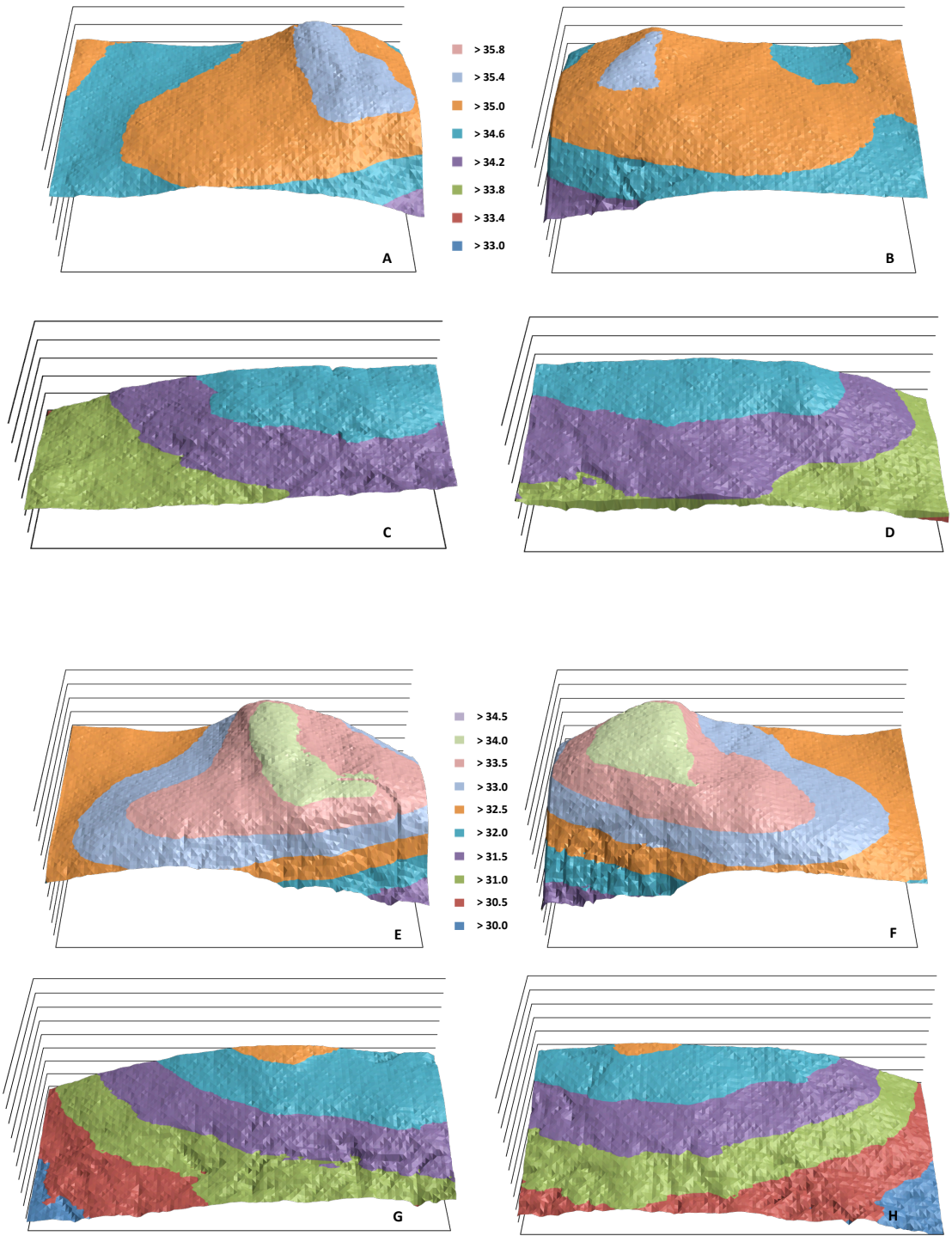

Figure 3.5. Mean $FLIR_{Sc}$ for left and right side after 90 min of exposure at 27°C (top four), and 19°C (bottom four). Non-obese right (A) and left (B) at 27°C and right (E) and left (F) at 19°C. Obese right (C) and left (D) at 27°C and right (G) and left (H) at 19°C.

References

Aherne, W. and D. Hull (1964). "The Site of Heat Production in the Newborn Infant." Proc R Soc Med **57**: 1172-1173.

Arch, J. R., A. T. Ainsworth, M. A. Cawthorne, V. Piercy, M. V. Sennitt, V. E. Thody, C. Wilson and S. Wilson (1984). "Atypical beta-adrenoceptor on brown adipocytes as target for anti-obesity drugs." Nature **309**(5964): 163-165.

Au-Yong, I. T., N. Thorn, R. Ganatra, A. C. Perkins and M. E. Symonds (2009). "Brown adipose tissue and seasonal variation in humans." Diabetes **58**(11): 2583-2587.

Barrington, S. F. and M. N. Maisey (1996). "Skeletal muscle uptake of fluorine-18-FDG: effect of oral diazepam." J Nucl Med **37**(7): 1127-1129.

Bartelt, A., O. T. Bruns, R. Reimer, H. Hohenberg, H. Ittrich, K. Peldschus, M. G. Kaul, U. I. Tromsdorf, H. Weller, C. Waurisch, A. Eychmuller, P. L. Gordts, F. Rinninger, K. Bruegelmann, B. Freund, P. Nielsen, M. Merkel and J. Heeren (2011). "Brown adipose tissue activity controls triglyceride clearance." Nat Med **17**(2): 200-205.

Basu, S. (2008). "Functional imaging of brown adipose tissue with PET: can this provide new insights into the pathophysiology of obesity and thereby direct antiobesity strategies?" Nucl Med Commun **29**(11): 931-933.

Bell, D. G., P. Tikuisis and I. Jacobs (1992). "Relative intensity of muscular contraction during shivering." J Appl Physiol (1985) **72**(6): 2336-2342.

Bell, P. Y., E. H. Padbury and P. A. Hayes (1985). "Optimal siting of heat flux transducers for the assessment of body heat loss when immersed in water." Undersea Biomed Res **12**(4): 465-483.

Bengtsson, T., B. Cannon and J. Nedergaard (2000). "Differential adrenergic regulation of the gene expression of the beta-adrenoceptor subtypes beta1, beta2 and beta3 in brown adipocytes." Biochem J **347 Pt 3**: 643-651.

Benzinger, T. H., A. W. Pratt and C. Kitzinger (1961). "The Thermostatic Control of Human Metabolic Heat Production." Proc Natl Acad Sci U S A **47**(5): 730-739.

Bligh, J. (2006). "A theoretical consideration of the means whereby the mammalian core temperature is defended at a null zone." J Appl Physiol **100**(4): 1332-1337.

Block, B. A. (1994). "Thermogenesis in muscle." Annu Rev Physiol **56**: 535-577.

Blondin, D. P., S. M. Labbe, H. Christian Tingelstad, C. Noll, M. Kunach, S. Phoenix, B. Guerin, E. E. Turcotte, A. C. Carpentier, D. Richard and F. Haman (2014). "Increased brown adipose tissue oxidative capacity in cold-acclimated humans." J Clin Endocrinol Metab: jc20133901.

Blondin, D. P., S. M. Labbe, S. Phoenix, B. Guerin, E. E. Turcotte, D. Richard, A. C. Carpentier and F. Haman (2015). "Contributions of white and brown adipose tissues and skeletal muscles to acute cold-induced metabolic responses in healthy men." J Physiol **593**(3): 701-714.

Blondin, D. P., H. C. Tingelstad, O. L. Mantha, C. Gosselin and F. Haman (2014). "Maintaining thermogenesis in cold exposed humans: relying on multiple metabolic pathways." Compr Physiol **4**(4): 1383-1402.

Boeuf, S., M. Klingenspor, N. L. Van Hal, T. Schneider, J. Keijer and S. Klaus (2001). "Differential gene expression in white and brown preadipocytes." Physiol Genomics **7**(1): 15-25.

Boulant, J. A. (2006). "Neuronal basis of Hammel's model for set-point thermoregulation." J Appl Physiol **100**(4): 1347-1354.

Boulant, J. A. and J. B. Dean (1986). "Temperature receptors in the central nervous system." Annu Rev Physiol **48**: 639-654.

Bronnikov, G., T. Bengtsson, L. Kramarova, V. Golozoubova, B. Cannon and J. Nedergaard (1999). "beta1 to beta3 switch in control of cyclic adenosine monophosphate during brown adipocyte development explains distinct beta-adrenoceptor subtype mediation of proliferation and differentiation." Endocrinology **140**(9): 4185-4197.

Bruck, K. (1969). "Thermoregulatory heat production and brown adipose tissue in the neonate." Z Klin Chem Klin Biochem **7**(2): 204-205.

Buniyamin, N., Ringgau, D., Mohamad, Z., Murat, Z.H. (2011). "Non-destructive fish fat detection using infrared sensor." 2011 Internation Conference on Food Engineering and Biotechnology **9**: 33-37.

Buskirk, E. R. T., R. H.; Whedon, G. D. (1963). "1963 (Buskirk et al.) Metabolic response to cold air in men and women in relation to total body fat content copy.pdf>." J Appl Physiol **18**: 603-612.

Cabanac, M. (2006). "Adjustable set point: to honor Harold T. Hammel." J Appl Physiol **100**(4): 1338-1346.

Cabanac, M. and H. Brinnel (1987). "The pathology of human temperature regulation: thermiatrics." Experientia **43**(1): 19-27.

Cabanac, M. and B. Massonnet (1977). "Thermoregulatory responses as a function of core temperature in humans." J Physiol **265**(3): 587-596.

Cannon, B. and J. Nedergaard (2004). "Brown adipose tissue: function and physiological significance." Physiol Rev **84**(1): 277-359.

Cannon, P. and W. R. Keatinge (1960). "The metabolic rate and heat loss of fat and thin men in heat balance in cold and warm water." J Physiol **154**: 329-344.

Carlson, L. D. and W. H. Cottle (1956). "Regulation of heat production in cold-adapted rats." Proc Soc Exp Biol Med **92**(4): 845-849.

Caterina, M. J. (2007). "Transient receptor potential ion channels as participants in thermosensation and thermoregulation." Am J Physiol Regul Integr Comp Physiol **292**(1): R64-76.

Chaudhry, A., R. G. MacKenzie, L. M. Georgic and J. G. Granneman (1994). "Differential interaction of beta 1- and beta 3-adrenergic receptors with Gi in rat adipocytes." Cell Signal **6**(4): 457-465.

Christoffolete, M. A., C. C. Linardi, L. de Jesus, K. N. Ebina, S. D. Carvalho, M. O. Ribeiro, R. Rabelo, C. Curcio, L. Martins, E. T. Kimura and A. C. Bianco (2004). "Mice with targeted disruption of the Dio2 gene have cold-induced overexpression of the uncoupling protein 1 gene but fail to increase brown adipose tissue lipogenesis and adaptive thermogenesis." Diabetes **53**(3): 577-584.

Cohade, C., M. Osman, H. K. Pannu and R. L. Wahl (2003). "Uptake in supraclavicular area fat ("USA-Fat"): description on 18F-FDG PET/CT." J Nucl Med **44**(2): 170-176.

Collins, S., C. M. Kuhn, A. E. Petro, A. G. Swick, B. A. Chrunyk and R. S. Surwit (1996). "Role of leptin in fat regulation." Nature **380**(6576): 677.

Cypess, A. M., Y. C. Chen, C. Sze, K. Wang, J. English, O. Chan, A. R. Holman, I. Tal, M. R. Palmer, G. M. Kolodny and C. R. Kahn (2012). "Cold but not sympathomimetics activates human brown adipose tissue in vivo." Proc Natl Acad Sci U S A **109**(25): 10001-10005.

Cypess, A. M., S. Lehman, G. Williams, I. Tal, D. Rodman, A. B. Goldfine, F. C. Kuo, E. L. Palmer, Y. H. Tseng, A. Doria, G. M. Kolodny and C. R. Kahn (2009). "Identification and importance of brown adipose tissue in adult humans." N Engl J Med **360**(15): 1509-1517.

Dawkins, M. J. and D. Hull (1964). "Brown Adipose Tissue and the Response of New-Born Rabbits to Cold." J Physiol **172**: 216-238.

Dawkins, M. J. and J. W. Scopes (1965). "Non-shivering thermogenesis and brown adipose tissue in the human new-born infant." Nature **206**(980): 201-202.

Del Mar Gonzalez-Barroso, M., D. Ricquier and A. M. Cassard-Doulcier (2000). "The human uncoupling protein-1 gene (UCP1): present status and perspectives in obesity research." Obes Rev **1**(2): 61-72.

Dodd, G. T., S. Decherf, K. Loh, S. E. Simonds, F. Wiede, E. Balland, T. L. Merry, H. Munzberg, Z. Y. Zhang, B. B. Kahn, B. G. Neel, K. K. Bence, Z. B. Andrews, M. A. Cowley and T. Tiganis (2015). "Leptin and insulin act on POMC neurons to promote the browning of white fat." Cell **160**(1-2): 88-104.

Ducharme, M. a. F. J. (1991). Methodology for calibration and use of heat flux transducers. D. a. C. I. o. E. Medicine. North York, Ontario.

Enerback, S., A. Jacobsson, E. M. Simpson, C. Guerra, H. Yamashita, M. E. Harper and L. P. Kozak (1997). "Mice lacking mitochondrial uncoupling protein are cold-sensitive but not obese." Nature **387**(6628): 90-94.

Engel, H., H. Steinert, A. Buck, T. Berthold, R. A. Huch Boni and G. K. von Schulthess (1996). "Whole-body PET: physiological and artifactual fluorodeoxyglucose accumulations." J Nucl Med **37**(3): 441-446.

Erlanson-Albertsson, C. and A. Larsson (1988). "A possible physiological function of pancreatic pro-colipase activation peptide in appetite regulation." Biochimie **70**(9): 1245-1250.

FLIR, A. (2014). The Ultimate Infared Handbook for R&D Professionals. FLIR Systems, AB.

Friedman, J. M. (1998). "Leptin, leptin receptors, and the control of body weight." Nutr Rev **56**(2 Pt 2): s38-46; discussion s54-75.

Garlid, K. D., M. Jaburek, P. Jezek and M. Varecha (2000). "How do uncoupling proteins uncouple?" Biochim Biophys Acta **1459**(2-3): 383-389.

Geloen, A., A. J. Collet, G. Guay and L. J. Bukowiecki (1990). "In vivo differentiation of brown adipocytes in adult mice: an electron microscopic study." Am J Anat **188**(4): 366-372.

Gessner, K. (1551.). "Conradi Gesneri medici Tigurine Historiae Animalium: Lib I De Quadrupedibus viviparis."

Gin, A. R., M. G. Hayward and W. R. Keatinge (1980). "Method for measuring regional heat losses in man." J Appl Physiol Respir Environ Exerc Physiol **49**(3): 533-535.

Girling, F. (1964). "Metabolic Response to Nude Human Subjects to Acute Exposure at 10 Degrees C." Can J Physiol Pharmacol **42**: 319-327.

Glick, Z., R. J. Teague, G. A. Bray and M. Lee (1983). "Compositional and metabolic changes in brown adipose tissue following a single test meal." Metabolism **32**(12): 1146-1150.

Glick, Z., S. J. Wickler, J. S. Stern and B. A. Horwitz (1984). "Regional blood flow in rats after a single low-protein, high-carbohydrate test meal." Am J Physiol **247**(1 Pt 2): R160-166.

Golozoubova, V., E. Hohtola, A. Matthias, A. Jacobsson, B. Cannon and J. Nedergaard (2001). "Only UCP1 can mediate adaptive nonshivering thermogenesis in the cold." FASEB J **15**(11): 2048-2050.

Goodbody, A. E. and P. Trayhurn (1982). "Studies on the activity of brown adipose tissue in suckling, pre-obese, ob/ob mice." Biochim Biophys Acta **680**(2): 119-126.

Guyton, A. C. H., J. E. (2006). Textbook of Medical Physiology. Philadelphia, Pennsylvannia, Elsevier, Inc.**:** 886-888.

Haman, F. (2006). "Shivering in the cold: from mechanisms of fuel selection to survival." J Appl Physiol **100**(5): 1702-1708.

Haman, F., S. R. Legault, M. Rakobowchuk, M. B. Ducharme and J. M. Weber (2004). "Effects of carbohydrate availability on sustained shivering II. Relating muscle recruitment to fuel selection." J Appl Physiol (1985) **96**(1): 41-49.

Haman, F., S. R. Legault and J. M. Weber (2004). "Fuel selection during intense shivering in humans: EMG pattern reflects carbohydrate oxidation." J Physiol **556**(Pt 1): 305-313.

Haman, F., F. Peronnet, G. P. Kenny, E. Doucet, D. Massicotte, C. Lavoie and J. M. Weber (2004). "Effects of carbohydrate availability on sustained shivering I. Oxidation of plasma glucose, muscle glycogen, and proteins." J Appl Physiol **96**(1): 32-40.

Haman, F., F. Peronnet, G. P. Kenny, D. Massicotte, C. Lavoie, C. Scott and J. M. Weber (2002). "Effect of cold exposure on fuel utilization in humans: plasma glucose, muscle glycogen, and lipids." J Appl Physiol (1985) **93**(1): 77-84.

Haman, F., F. Peronnet, G. P. Kenny, D. Massicotte, C. Lavoie and J. M. Weber (2005). "Partitioning oxidative fuels during cold exposure in humans: muscle glycogen becomes dominant as shivering intensifies." J Physiol **566**(Pt 1): 247-256.

Hammel, H. T., J. D. Hardy and M. M. Fusco (1960). "Thermoregulatory responses to hypothalamic cooling in unanesthetized dogs." Am J Physiol **198**: 481-486.

Hammel, H. T., D. C. Jackson, J. A. Stolwijk, J. D. Hardy and S. B. Stromme (1963). "Temperature Regulation by Hypothalamic Proportional Control with an Adjustable Set Point." J Appl Physiol **18**: 1146-1154.

Hany, T. F., E. Gharehpapagh, E. M. Kamel, A. Buck, J. Himms-Hagen and G. K. von Schulthess (2002). "Brown adipose tissue: a factor to consider in symmetrical tracer uptake in the neck and upper chest region." Eur J Nucl Med Mol Imaging **29**(10): 1393-1398.

Hardy, J. D., Milhorat, A. T., DuBois, E. F. (1941). Temperature, its measurement and control in science and industry. New York, N.Y., Reinhold Publishing Corporation**:** 529.

Heaton, J. M. (1972). "The distribution of brown adipose tissue in the human." J Anat **112**(Pt 1): 35-39.

Hemingway, A. (1963). "Shivering." Physiol Rev **43**: 397-422.

Hensel, H. (1981). "Thermoreception and temperature regulation." Monogr Physiol Soc **38**: 1-321.

Hilliges, M., L. Wang and O. Johansson (1995). "Ultrastructural evidence for nerve fibers within all vital layers of the human epidermis." J Invest Dermatol **104**(1): 134-137.

Himms-Hagen, J., J. Cui, E. Danforth, Jr., D. J. Taatjes, S. S. Lang, B. L. Waters and T. H. Claus (1994). "Effect of CL-316,243, a thermogenic beta 3-agonist, on energy balance and brown and white adipose tissues in rats." Am J Physiol **266**(4 Pt 2): R1371-1382.

Hindle, A. G. and S. L. Martin (2014). "Intrinsic circannual regulation of brown adipose tissue form and function in tune with hibernation." Am J Physiol Endocrinol Metab **306**(3): E284-299.

Horwitz, B. A., J. S. Hamilton and K. S. Kott (1985). "GDP binding to hamster brown fat mitochondria is reduced during hibernation." Am J Physiol **249**(6 Pt 2): R689-693.

Hu, H. H. and V. Gilsanz (2011). "Developments in the imaging of brown adipose tissue and its associations with muscle, puberty, and health in children." Front Endocrinol (Lausanne) **2**: 33.

Hu, H. H., J. P. Tovar, Z. Pavlova, M. L. Smith and V. Gilsanz (2012). "Unequivocal identification of brown adipose tissue in a human infant." J Magn Reson Imaging **35**(4): 938-942.

Huttunen, P., J. Hirvonen and V. Kinnula (1981). "The occurrence of brown adipose tissue in outdoor workers." Eur J Appl Physiol Occup Physiol **46**(4): 339-345.

Iggo, A. (1969). "Cutaneous thermoreceptors in primates and sub-primates." J Physiol **200**(2): 403-430.

Israel, D. J. and R. S. Pozos (1989). "Synchronized slow-amplitude modulations in the electromyograms of shivering muscles." J Appl Physiol (1985) **66**(5): 2358-2363.

Jansky, L. (1973). "Non-shivering thermogenesis and its thermoregulatory significance." Biol Rev Camb Philos Soc **48**(1): 85-132.

Jansky, L. and J. S. Hart (1963). "Participation of skeletal muscle and kidney during nonshivering thermogenesisin cold-acclimated rats." Can J Biochem Physiol **41**: 953-964.

Jeukendrup, A. E. and G. A. Wallis (2005). "Measurement of substrate oxidation during exercise by means of gas exchange measurements." Int J Sports Med **26 Suppl 1**: S28-37.

Kajimura, S. and M. Saito (2014). "A new era in brown adipose tissue biology: molecular control of brown fat development and energy homeostasis." Annu Rev Physiol **76**: 225-249.

Keatinge, W. R. (1960). "The effects of subcutaneous fat and of previous exposure to cold on the body temperature, peripheral blood flow and metabolic rate of men in cold water." J Physiol **153**: 166-178.

Klingenberg, M. and S. G. Huang (1999). "Structure and function of the uncoupling protein from brown adipose tissue." Biochim Biophys Acta **1415**(2): 271-296.

Kuehn, L. A. (1978). "Assessment of convective heat loss from humans in cold water." Journal of Biomechanical Engineering **100**(1): 7-13.

Kuhnen, G. and C. Jessen (1988). "The metabolic response to skin temperature." Pflugers Arch **412**(4): 402-408.

Kuiken, T. A., M. M. Lowery and N. S. Stoykov (2003). "The effect of subcutaneous fat on myoelectric signal amplitude and cross-talk." Prosthet Orthot Int **27**(1): 48-54.

Leblanc, J. (1954). "Subcutaneous fat and skin temperature." Can J Biochem Physiol **32**(4): 354-358.

LeBlanc, J., S. Dulac, J. Cote and B. Girard (1975). "Autonomic nervous system and adaptation to cold in man." J Appl Physiol **39**(2): 181-186.

Lee, P., K. K. Ho, P. Lee, J. R. Greenfield, K. K. Ho and J. R. Greenfield (2011). "Hot fat in a cool man: infrared thermography and brown adipose tissue." Diabetes Obes Metab **13**(1): 92-93.

Lidell, M. E., M. J. Betz, O. Dahlqvist Leinhard, M. Heglind, L. Elander, M. Slawik, T. Mussack, D. Nilsson, T. Romu, P. Nuutila, K. A. Virtanen, F. Beuschlein, A. Persson, M. Borga and S. Enerback (2013). "Evidence for two types of brown adipose tissue in humans." Nat Med **19**(5): 631-634.

Lindberg, O., J. de Pierre, E. Rylander and B. A. Afzelius (1967). "Studies of the mitochondrial energy-transfer system of brown adipose tissue." J Cell Biol **34**(1): 293-310.

Llado, I., A. M. Proenza, F. Serra, A. Palou and A. Pons (1991). "Dietary-induced permanent changes in brown and white adipose tissue composition in rats." Int J Obes **15**(6): 415-419.

Lowery, M. M., N. S. Stoykov, A. Taflove and T. A. Kuiken (2002). "A multiple-layer finite-element model of the surface EMG signal." IEEE Trans Biomed Eng **49**(5): 446-454.

Martineau, L. and I. Jacobs (1989). "Muscle glycogen availability and temperature regulation in humans." J Appl Physiol (1985) **66**(1): 72-78.

Masamoto, Y., F. Kawabata and T. Fushiki (2009). "Intragastric administration of TRPV1, TRPV3, TRPM8, and TRPA1 agonists modulates autonomic thermoregulation in different manners in mice." Biosci Biotechnol Biochem **73**(5): 1021-1027.

Matthias, A., K. B. Ohlson, J. M. Fredriksson, A. Jacobsson, J. Nedergaard and B. Cannon (2000). "Thermogenic responses in brown fat cells are fully UCP1-dependent. UCP2 or UCP3 do not substitute for UCP1 in adrenergically or fatty scid-induced thermogenesis." J Biol Chem **275**(33): 25073-25081.

McCormack, J. G. (1982). "The regulation of fatty acid synthesis in brown adipose tissue by insulin." Prog Lipid Res **21**(3): 195-223.

Mekjavic, I. B., C. J. Sundberg and D. Linnarsson (1991). "Core temperature "null zone"." J Appl Physiol **71**(4): 1289-1295.

Minotti, A. J., L. Shah and K. Keller (2004). "Positron emission tomography/computed tomography fusion imaging in brown adipose tissue." Clin Nucl Med **29**(1): 5-11.

Mittleman, K. D. (1987). Central Thermosensitivity of Metabolic Heat Production During Cold Water Immersion. Doctor of Philosophy, Simon Fraser Univsersity.

Mittleman, K. D. and I. B. Mekjavic (1988). "Effect of occluded venous return on core temperature during cold water immersion." J Appl Physiol (1985) **65**(6): 2709-2713.

Morrison, S. F. (2011). "2010 Carl Ludwig Distinguished Lectureship of the APS Neural Control and Autonomic Regulation Section: Central neural pathways for thermoregulatory cold defense." J Appl Physiol **110**(5): 1137-1149.

Muzik, O., T. J. Mangner and J. G. Granneman (2012). "Assessment of oxidative metabolism in brown fat using PET imaging." Front Endocrinol (Lausanne) **3**: 15.

Nedergaard, J., T. Bengtsson and B. Cannon (2007). "Unexpected evidence for active brown adipose tissue in adult humans." Am J Physiol Endocrinol Metab **293**(2): E444-452.

Nedergaard, J. and B. Cannon (2014). "The browning of white adipose tissue: some burning issues." Cell Metab **20**(3): 396-407.

Nedergaard, J., B. Cannon and O. Lindberg (1977). "Microcalorimetry of isolated mammalian cells." Nature **267**(5611): 518-520.

Nedergaard, J., A. Matthias, V. Golozoubova, A. Jacobsson and B. Cannon (1999). "UCP1: the original uncoupling protein--and perhaps the only one? New perspectives on UCP1, UCP2, and UCP3 in the light of the bioenergetics of the UCP1-ablated mice." J Bioenerg Biomembr **31**(5): 475-491.

Neves, S. R., P. T. Ram and R. Iyengar (2002). "G protein pathways." Science **296**(5573): 1636-1639.

Niedermann, R., A. Psikuta and R. M. Rossi (2014). "Heat flux measurements for use in physiological and clothing research." Int J Biometeorol **58**(6): 1069-1075.

Nuckols, M. L. and C. A. Piantadosi (1980). "Calibration and characterization of heat flow transducers for use in hyperbaric helium." Undersea Biomed Res **7**(4): 249-256.

Orava, J., P. Nuutila, M. E. Lidell, V. Oikonen, T. Noponen, T. Viljanen, M. Scheinin, M. Taittonen, T. Niemi, S. Enerback and K. A. Virtanen (2011). "Different metabolic responses of human brown adipose tissue to activation by cold and insulin." Cell Metab **14**(2): 272-279.

Orava, J., P. Nuutila, T. Noponen, R. Parkkola, T. Viljanen, S. Enerback, A. Rissanen, K. H. Pietilainen and K. A. Virtanen (2013). "Blunted metabolic responses to cold and insulin stimulation in brown adipose tissue of obese humans." Obesity (Silver Spring) **21**(11): 2279-2287.

Ouellet, V., S. M. Labbe, D. P. Blondin, S. Phoenix, B. Guerin, F. Haman, E. E. Turcotte, D. Richard and A. C. Carpentier (2012). "Brown adipose tissue oxidative metabolism contributes to energy expenditure during acute cold exposure in humans." J Clin Invest **122**(2): 545-552.

Peier, A. M., A. Moqrich, A. C. Hergarden, A. J. Reeve, D. A. Andersson, G. M. Story, T. J. Earley, I. Dragoni, P. McIntyre, S. Bevan and A. Patapoutian (2002). "A TRP channel that senses cold stimuli and menthol." Cell **108**(5): 705-715.

Petajan, J. H. and D. D. Williams (1972). "Behavior of single motor units during pre-shivering tone and shivering tremor." Am J Phys Med **51**(1): 16-22.

Peterson, M. J., S. A. Czerwinski and R. M. Siervogel (2003). "Development and validation of skinfold-thickness prediction equations with a 4-compartment model." Am J Clin Nutr **77**(5): 1186-1191.

Poppendick, H. (1969). "Why not measure heat flow directly." Environ Q **15**: 1-2.

Power, G. G. (1989). "Biology of temperature: the mammalian fetus." J Dev Physiol **12**(6): 295-304.

Preitner, F., P. Muzzin, J. P. Revelli, J. Seydoux, J. Galitzky, M. Berlan, M. Lafontan and J. P. Giacobino (1998). "Metabolic response to various beta-adrenoceptor agonists in beta3-adrenoceptor knockout mice: evidence for a new beta-adrenergic receptor in brown adipose tissue." Br J Pharmacol **124**(8): 1684-1688.

Prusiner, S. B., B. Cannon and O. Lindberg (1968). "Oxidative metabolism in cells isolated from brown adipose tissue. 1. Catecholamine and fatty acid stimulation of respiration." Eur J Biochem **6**(1): 15-22.

Rasmussen, A. T. (1923). "The so-called hibernating gland." Journal of Morphology **38**(1): 147-205.

Rasmussen, J. M., S. Entringer, A. Nguyen, T. G. van Erp, A. Guijarro, F. Oveisi, J. M. Swanson, D. Piomelli, P. D. Wadhwa, C. Buss and S. G. Potkin (2013). "Brown adipose tissue quantification in human neonates using water-fat separated MRI." PLoS One **8**(10): e77907.

Rial, E. and M. M. Gonzalez-Barroso (2001). "Physiological regulation of the transport activity in the uncoupling proteins UCP1 and UCP2." Biochim Biophys Acta **1504**(1): 70-81.

Rintamaki, H. (2007). "Human responses to cold." Alaska Med **49**(2 Suppl): 29-31.

Robinson, L., S. Ojha, M. E. Symonds and H. Budge (2014). "Body mass index as a determinant of brown adipose tissue function in healthy children." J Pediatr **164**(2): 318-322 e311.

Rothwell, N. J. and M. J. Stock (1979). "A role for brown adipose tissue in diet-induced thermogenesis." Nature **281**(5726): 31-35.

Rothwell, N. J. and M. J. Stock (1997). "A role for brown adipose tissue in diet-induced thermogenesis." Obes Res **5**(6): 650-656.

Rothwell, N. J., M. J. Stock and R. S. Tyzbir (1983). "Mechanisms of thermogenesis induced by low protein diets." Metabolism **32**(3): 257-261.

Rylander, E., H. Pribylova and J. Lind (1972). "A thermographic study of infants exposed to cold." Acta Paediatr Scand **61**(1): 42-48.

Sacks, H. and M. E. Symonds (2013). "Anatomical locations of human brown adipose tissue: functional relevance and implications in obesity and type 2 diabetes." Diabetes **62**(6): 1783-1790.

Saito, M., Y. Okamatsu-Ogura, M. Matsushita, K. Watanabe, T. Yoneshiro, J. Nio-Kobayashi, T. Iwanaga, M. Miyagawa, T. Kameya, K. Nakada, Y. Kawai and M. Tsujisaki (2009). "High incidence of metabolically active brown adipose tissue in healthy adult humans: effects of cold exposure and adiposity." Diabetes **58**(7): 1526-1531.

Sakaguchi, T. and G. A. Bray (1987). "The effect of intrahypothalamic injections of glucose on sympathetic efferent firing rate." Brain Res Bull **18**(5): 591-595.

Seale, P., B. Bjork, W. Yang, S. Kajimura, S. Chin, S. Kuang, A. Scime, S. Devarakonda, H. M. Conroe, H. Erdjument-Bromage, P. Tempst, M. A. Rudnicki, D. R. Beier and B. M. Spiegelman (2008). "PRDM16 controls a brown fat/skeletal muscle switch." Nature **454**(7207): 961-967.

Sharp, L. Z., K. Shinoda, H. Ohno, D. W. Scheel, E. Tomoda, L. Ruiz, H. Hu, L. Wang, Z. Pavlova, V. Gilsanz and S. Kajimura (2012). "Human BAT possesses molecular signatures that resemble beige/brite cells." PLoS One **7**(11): e49452.

Shibasaki, M., T. E. Wilson and C. G. Crandall (2006). "Neural control and mechanisms of eccrine sweating during heat stress and exercise." J Appl Physiol **100**(5): 1692-1701.

Shimizu, I., T. Aprahamian, R. Kikuchi, A. Shimizu, K. N. Papanicolaou, S. MacLauchlan, S. Maruyama and K. Walsh (2014). "Vascular rarefaction mediates whitening of brown fat in obesity." J Clin Invest **124**(5): 2099-2112.

Smith, R. E. (1964). "Thermoregulatory and Adaptive Behavior of Brown Adipose Tissue." Science **146**(3652): 1686-1689.

Smith, R. E. and R. J. Hock (1963). "Brown fat: thermogenic effector of arousal in hibernators." Science **140**(3563): 199-200.

Solomonow, M., R. Baratta, M. Bernardi, B. Zhou, Y. Lu, M. Zhu and S. Acierno (1994). "Surface and wire EMG crosstalk in neighbouring muscles." J Electromyogr Kinesiol **4**(3): 131-142.

Sowood, P. (1986). Calibration of heat flux transduers. R. A. F. I. o. A. Medicine. Scientific memorandum.

Symonds, M. E., K. Henderson, L. Elvidge, C. Bosman, D. Sharkey, A. C. Perkins and H. Budge (2012). "Thermal imaging to assess age-related changes of skin temperature

within the supraclavicular region co-locating with brown adipose tissue in healthy children." J Pediatr **161**(5): 892-898.

Thonberg, H., J. M. Fredriksson, J. Nedergaard and B. Cannon (2002). "A novel pathway for adrenergic stimulation of cAMP-response-element-binding protein (CREB) phosphorylation: mediation via alpha1-adrenoceptors and protein kinase C activation." Biochem J **364**(Pt 1): 73-79.

Tikuisis, P., D. G. Bell and I. Jacobs (1991). "Shivering onset, metabolic response, and convective heat transfer during cold air exposure." J Appl Physiol **70**(5): 1996-2002.

Timbal, J., C. Boutelier, M. Loncle and L. Bougues (1976). "Comparison of shivering in man exposed to cold in water and in air." Pflugers Arch **365**(2-3): 243-248.

Trayhurn, P., P. L. Thurlby and W. P. James (1977). "Thermogenic defect in pre-obese ob/ob mice." Nature **266**(5597): 60-62.

Trayhurn, P. and M. C. Wusteman (1987). "Sympathetic activity in brown adipose tissue in lactating mice." Am J Physiol **253**(5 Pt 1): E515-520.

Vallerand, A. L. and I. Jacobs (1990). "Influence of cold exposure on plasma triglyceride clearance in humans." Metabolism **39**(11): 1211-1218.

Vallerand, A. L. and I. Jacobs (1992). "Energy metabolism during cold exposure." Int J Sports Med **13 Suppl 1**: S191-193.

Vallerand, A. L., P. Tikuisis, M. B. Ducharme and I. Jacobs (1993). "Is energy substrate mobilization a limiting factor for cold thermogenesis?" Eur J Appl Physiol Occup Physiol **67**(3): 239-244.

van der Lans, A. A., J. Hoeks, B. Brans, G. H. Vijgen, M. G. Visser, M. J. Vosselman, J. Hansen, J. A. Jorgensen, J. Wu, F. M. Mottaghy, P. Schrauwen and W. D. van Marken Lichtenbelt (2013). "Cold acclimation recruits human brown fat and increases nonshivering thermogenesis." J Clin Invest **123**(8): 3395-3403.

van der Lans, A. A., R. Wierts, M. J. Vosselman, P. Schrauwen, B. Brans and W. D. van Marken Lichtenbelt (2014). "Cold-Activated Brown Adipose Tissue in Human Adults - Methodological Issues." Am J Physiol Regul Integr Comp Physiol.

van Marken Lichtenbelt, W. (2012). "Brown adipose tissue and the regulation of nonshivering thermogenesis." Curr Opin Clin Nutr Metab Care **15**(6): 547-552.

van Marken Lichtenbelt, W. D., J. W. Vanhommerig, N. M. Smulders, J. M. Drossaerts, G. J. Kemerink, N. D. Bouvy, P. Schrauwen and G. J. Teule (2009). "Cold-activated brown adipose tissue in healthy men." N Engl J Med **360**(15): 1500-1508.

Vijgen, G. H., N. D. Bouvy, G. J. Teule, B. Brans, J. Hoeks, P. Schrauwen and W. D. van Marken Lichtenbelt (2012). "Increase in brown adipose tissue activity after weight loss in morbidly obese subjects." J Clin Endocrinol Metab **97**(7): E1229-1233.

Vijgen, G. H., N. D. Bouvy, G. J. Teule, B. Brans, P. Schrauwen and W. D. van Marken Lichtenbelt (2011). "Brown adipose tissue in morbidly obese subjects." PLoS One **6**(2): e17247.

Virtanen, K. A., M. E. Lidell, J. Orava, M. Heglind, R. Westergren, T. Niemi, M. Taittonen, J. Laine, N. J. Savisto, S. Enerback and P. Nuutila (2009). "Functional brown adipose tissue in healthy adults." N Engl J Med **360**(15): 1518-1525.

Vosselman, M. J., A. A. van der Lans, B. Brans, R. Wierts, M. A. van Baak, P. Schrauwen and W. D. van Marken Lichtenbelt (2012). "Systemic beta-adrenergic stimulation of thermogenesis is not accompanied by brown adipose tissue activity in humans." Diabetes **61**(12): 3106-3113.

Vrieze, A., J. E. Schopman, W. M. Admiraal, M. R. Soeters, M. Nieuwdorp, H. J. Verberne and F. Holleman (2012). "Fasting and postprandial activity of brown adipose tissue in healthy men." J Nucl Med **53**(9): 1407-1410.

Wang, L. C. (1980). "Modulation of maximum thermogenesis by feeding in the white rat." J Appl Physiol Respir Environ Exerc Physiol **49**(6): 975-978.

Wang, L. C. (1981). "Effects of feeding on aminophylline induced supra-maximal thermogenesis." Life Sci **29**(24): 2459-2466.

Wang, L. C., S. F. Man and A. N. Belcastro (1987). "Metabolic and hormonal responses in theophylline-increased cold resistance in males." J Appl Physiol (1985) **63**(2): 589-596.

White, M. D. and J. LeBlanc (1993). Paradoxical adsence of shivering in obese humans? (Proceedings). International Union of Physiological Sciences Meeting on Thermal Physiology, Aberdeen, Scotland.

White, M. D., W. D. Ross and I. B. Mekjavic (1992). "Relationship between physique and rectal temperature cooling rate." Undersea Biomed Res **19**(2): 121-130.

Wijers, S. L., W. H. Saris and W. D. van Marken Lichtenbelt (2010). "Cold-induced adaptive thermogenesis in lean and obese." Obesity (Silver Spring) **18**(6): 1092-1099.

Williams, J. A. and E. K. Matthews (1974). "Membrane depolarization, cyclic AMP, and glycerol release by brown adipose tissue." Am J Physiol **227**(4): 987-992.

Winkler, E. and M. Klingenberg (1994). "Effect of fatty acids on H+ transport activity of the reconstituted uncoupling protein." J Biol Chem **269**(4): 2508-2515.

Wissler, E. a. K. R. (1982). "Errors involved in using thermal flux transducers under various conditions." Undersea Biomed Res **9**(3): 213-231.

Wyndham, C. H., C. G. Williams and H. Loots (1968). "Reactions to cold." J Appl Physiol **24**(3): 282-287.

Xizhong, Z., Zizhu, D., and Genhong, Z. (1993). "Application of the heat flux meter in physiological studies." Journal of Thermal Biology **18**(5): 473-476.

Yang, Y., Wei, X.J., Liu, J. (2009). "Suitability of using far-infrared imaging system for noncontact evaluation on working state of implantable medical devices." Journal of Applied Physics **105**: 1-13.

Yang, Y. S., O.O., Landry, M.R. Soller, B.S (2005). "Influence of a fat layer on the near infrared spectra of human muscle: quantitative analysis based on two-layered Monte Carlo simulations and phantom experiments." Optical Society of America **13**(5): 1570-1579.

Yoneshiro, T., S. Aita, M. Matsushita, T. Kameya, K. Nakada, Y. Kawai and M. Saito (2011). "Brown adipose tissue, whole-body energy expenditure, and thermogenesis in healthy adult men." Obesity (Silver Spring) **19**(1): 13-16.

Yoneshiro, T., S. Aita, M. Matsushita, T. Kayahara, T. Kameya, Y. Kawai, T. Iwanaga and M. Saito (2013). "Recruited brown adipose tissue as an antiobesity agent in humans." J Clin Invest **123**(8): 3404-3408.

Young, A. J. (1988). "Human adaptation to cold." Human Performance Physiology: 401-434.

Young, A. J., M. N. Sawka, P. D. Neufer, S. R. Muza, E. W. Askew and K. B. Pandolf (1989). "Thermoregulation during cold water immersion is unimpaired by low muscle glycogen levels." J Appl Physiol **66**(4): 1809-1816.

Appendix A.

Tables

Table A.1. Measurement sites for surface heat flux and skin temperatures on the upper arm (T_{UA}), posterior shoulder (T_{PS}), chest (T_{CH}), abdomen (T_{AB}), lower back (T_{LB}), and thigh (T_{TH}) and supraclavicular region (T_{SC}).

Thermocouple	Placement
T_{UA}	Superior deltoid insertion, lateral right arm
T_{PS}	Midway along infraspinatus, inferior to right scapular spine
T_{CH}	Centre of right pectoralis major
T_{AB}	Right of navel, 4 cm
T_{TH}	Centre of rectus femoris
T_{SC}	Centre of supraclavicular fossa

Table A.2. Summary of thermal imaging camera use for quantifying surface temperatures over brown adipose tissue depots.

Year	Author	Subjects	Make	Model	IR Resolution	Accuracy
1998	Paulik *et al.*	Adipocyte cell cultures	Agema Infrared Systems	Agema Thermovision 900	-	± 0.08˚C
2009	Marks *et al.*	Wistar rats	FLIR Systems	ThermaCAM P45	320 x 240 pixels	± 2˚C or ± 2% of reading
2010	Lee *et al.*	Healthy 32 year old male	FLIR Systems	SC660	640 x 480 pixels	± 1˚C or ± 1% of reading
2012	Symonds *et al.*	Normal BMI; adolescence	FLIR Systems	b60	180 x 180 pixels	± 2˚C or ± 2% of reading
2013	Lee *et al.*	Adipocyte cell cultures	FLIR Systems	T440	320 x 240 pixels	<0.045˚C at 30°C
2014	Robinson *et al.*	Varied BMI; children	FLIR Systems	B425	320 x 240 pixels	± 2˚C or ± 2% of reading
2015	Andrew's Thesis	Normal and Obese Adults	FLIR Systems	T650sc	640 x 480 pixels	± 1˚C or ± 1% of reading

Appendix B.

Figures

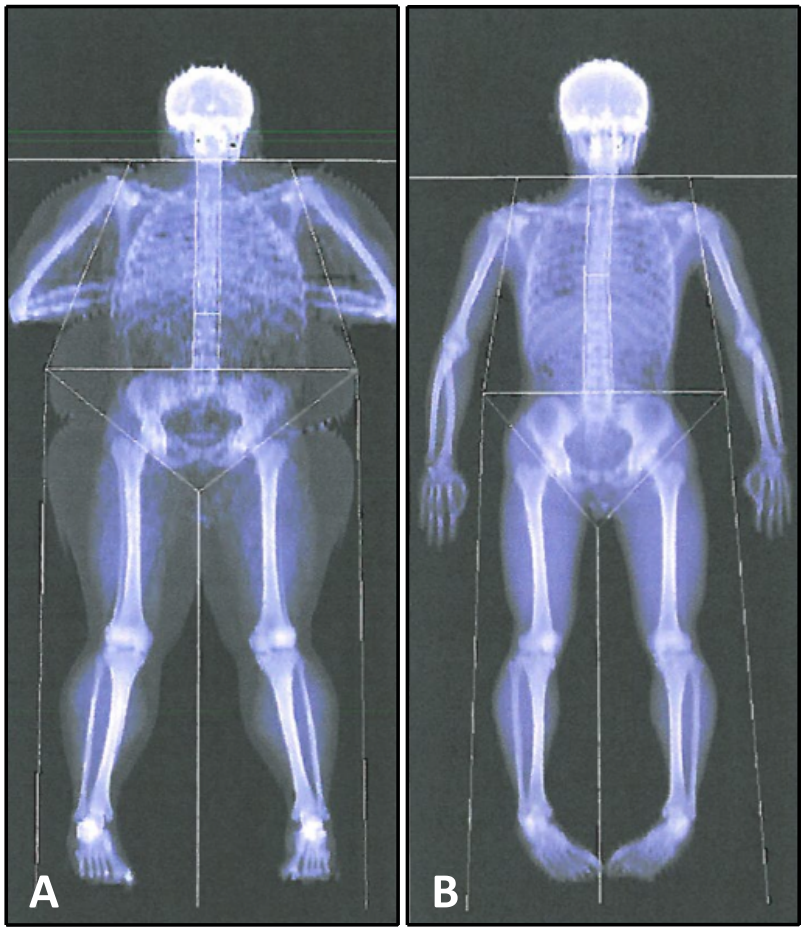

Figure B.1. **Typical Dual-energy X-ray absorptiometry (DEXA) scan of an A) Obese, and B) Non-obese participant.**

Appendix C.

Heat Flux Calibration Equations

Heat Flux Transducers

Heat flux (HF) transducers are used as a basic measurement in thermal physiology (Ducharme 1991). They are being used increasingly due to their reduced cost, their easy application, and their ability to be used in a variety of environmental conditions (Ducharme 1991).

The HF transducers contain many finite thermocouples arranged in series. Between these two series, a flat matrix is used to create a temperature difference (ΔT), which is the main factor in calculating the HF (Ducharme 1991). The thermocouple-matrix junction detects the temperature difference and the resultant voltage generated across this junction is proportional to the HF through the HF transducer (Ducharme 1991).

Despite its simplistic design, concerns have been raised regarding the reliability of the HF transducers and their manufacturers calibrations (Ducharme 1991). Nuckols and Piantadosi (1980) developed a calibration technique and found a significant difference of up to 20% between manufacturer-supplied calibrations and those found experimentally. Some however, have found that using a similar calibration method yielded negligible differences in the calibration constants (Sowood 1986). The HF transducer's design may also lead to an area of concern with the creation of a thermal resistance (R) (Poppendick 1969, Gin, Hayward et al. 1980, Wissler 1982). The contact of the HF transducer on the surface of the skin may modify the insulation of the area, consequently changing the skin temperature and heat flux.

Ducharme (1991) conducted a comprehensive study on various HF transducer models and calibration techniques and concluded that significant differences were seen in manufacturer's constants and recalibrated constants in one model (Thermonetics), but differences weren't as great in another common model (Concept Engineering). They concluded that recalibrations are necessary when using Thermonetics HF transducers only, however, when calibrated properly, both are equivalent.

Thermistors

Heat flux thermistors were calibrated using a water bath (Scientific Products, Model: 014937). Temperatures of 10, 20, 30, and 40°C were chosen to encompass the range of expected values. These were based on temperatures used by Mittleman (1987). The set temperatures were checked against a standard platinum thermometer.

Heat Flux Cylinder Apparatus

Manufacturer's calibration constants were checked using a copper encased water bath similar to those used by Nuckols and Piantadosi (1980) and Mittleman (1987). Water was continuously circulated in the copper cylinder (D: 0.21, H: 0.18 m) from a supply chiller-heater system through six tubes (D: 1 cm). Two hoses supplied water to inlet tubes located at opposite ends of the cylinder, 3 cm from the bottom. Four outlet tubes, situated at equidistant points around the cylinder, 5 cm from the material-cylinder interface, were connected by hoses to the water supply for recirculation. Six incremental bath temperatures (10, 20, 30, 40, 50, 60°C) were selected to provide a wide range of calibration HF values.

Three slabs of insulating Zote's Foam LTA (D: 0.15 m) were placed on top of the copper cylinder with fine gauge thermocouples placed centrally between each interface. Heat flux discs were

then individually placed adjacent to the middle thermistor. To ensure equilibrium was reached at each temperature, recording took place for 90 mins.

Heat Flux Calculations

Heat flux across a surface is influenced by a number of factors including thermal conductivity, thickness and area of the surface by which the heat is being transferred over. Using previously known measurements of the Zote's Foam LTA, the below calculations were completed to find the theoretical HF:

1) Known properties of **Zote's Foam LTA:**

- Thickness of the material (Δx) = **0.003 m** (given by the manufacturer)
- Thermal conductivity (k) = **0.0364 W/(m·K)** (given by the manufacturer)
- Thermal resistance (R) = **0.0824 (m^2·K)/W** (given by the manufacturer)*

* Thermal resistance (R) can also be calculated from the thickness (Δx) and thermal conductivity (k) of the material to get the same value:

$R = \Delta x \div k$

$= (0.003m) \div (0.0364W/(m\cdot K))$

$= 0.0824(m^2\cdot K)/W$

- Thermal contact resistance ($1/h_c$) = **0.0066 (m^2·K)/W** (given from Appendix A) (Mittleman 1987)**

**Can confirm the units of h_c through the following derivation calculation:

$Q = (T_{2A}-T_{2B}) \div (h_c\cdot A)^{-1}$

$[W] = \Delta[k] \times h_c \times [m^2]$

$h_c = [W/(m^2\cdot K)]$

2) Simplify the theoretical heat flux equation to:

$Q = [T_1-T_3] \div [\Delta x_A/(k_A\cdot A) + 1/(h_c\cdot A) + \Delta x_B/(k_B\cdot A)]$

$Q = A \times [T_1-T_3] \div [(1/A) \times (\Delta x_A/k_A + 1/h_c + \Delta x_B/k_B)]$

$Q = A \times [T_1-T_3] \div [2(\Delta x/k)+ 1/h_c]$

$Q = A \times [T_1-T_3] \div [2R+ 1/h_c]$

Hence, **$Q = [T_1-T_3] \div [2R+ 1/h_c]$** to get the heat flux in units of [W•m^{-2}].

3) Plug in the values we know into the simplified equation to get:

$$Q = [T_1\text{-}T_3] \div [2\times 0.0824(m^2\cdot K)/W + 0.0066(m^2\cdot K)/W]$$

$$Q = [T_1\text{-}T_3] \div 0.1714(m^2\cdot K)/W$$

Theoretical heat flux (units in [$\mathbf{W\cdot m^{-2}}$]):

$$\mathbf{Q = [T_1\text{-}T_3] \div [0.1714(m^2\cdot K)/W]}$$

Heat flux calculations were derived from Mittleman (1987). Below are definitions of the above calculation terms in order of appearance:

Thickness of the material (Δx): thickness of one individual foam pad between the top and bottom surface; units, m

Thermal conductivity (k): the property of a material to conduct heat. Materials with low thermal conductivity are used as thermal insulation; units, W/(m·K)

Thermal resistance (R): the property of a material to resist heat flow. It is the reciprocal of thermal conductance; units, $(m^2\cdot K)/W$

Thermal contact resistance ($1/h_c$): the property indicating the thermal resistance, or ability to resist heat flow, between two bodies in contact; units, $(m^2\cdot K)/W$

Thermal contact conductance (h_c): the property indicating the thermal conductivity, or ability to conduct heat, between two bodies in contact; units, $W/(m^2\cdot K)$

Heat Flux (Q): the rate of heat transferred through a given surface, per unit surface; units, $W\cdot m^{-2}$

Surface Area (A): surface area of the contact material, in this case, the Zote Foam LTR; units, m^2

Temperature (T): measured at four different points in the calibration device. T_1, top of outer foam; T_{2A}, top of middle foam; T_{2B}, bottom of middle foam; T_3, bottom of inner foam

Watt (W): the S.I. unit of power, equivalent to one joule per second.

Table C.1. Regression equations for calibration of heat flux discs.

	Temperature Factors			Heat Flux Factors		
	Slope	**Intercept**	**r^2**	**Slope**	**Intercept**	**r^2**
1872 (LSc)	1.014	-0.356	0.999	2.976	-65.529	0.987
1873 (RSc)	1.019	-0.309	0.999	2.506	-60.216	0.992
1874 (C)	1.012	-0.204	0.999	2.503	-49.821	0.999
1880 (A)	1.017	-0.267	0.999	2.738	-75.467	0.999
1876 (T)	1.013	0.103	0.999	2.555	-62.169	0.999
1877 (PS)	1.020	-0.043	0.999	2.098	-53.898	0.992
1878 (UA)	1.021	0.048	0.999	2.850	-80.909	0.997